**Title**
Rearrangements of the microtubule array in growth ones during axon elongation and growth cone guidance



**Author**
Tanaka, Elly,

**Publication Date**
1993

Peer reviewed|Thesis/dissertation

# Rearrangements Of The Microtubule Array In Growth Cones During Axon Elongation And Growth Cone Guidance

by

Elly Tanaka

**DISSERTATION**

**Submitted in partial satisfaction of the requirements for the degree of**

**DOCTOR OF PHILOSOPHY**

**in**

Biochemistry

**in the**

**GRADUATE DIVISION**

**of the**

**UNIVERSITY OF CALIFORNIA**

**San Francisco**

To David Drechsel who in so many ways has contributed to this thesis

## ACKNOWLEDGMENTS

I will cherish my years at UCSF both for my scientific training as well as for an education in life experiences, and so I have many people to thank. First and foremost, I would like to thank my advisor Marc Kirschner for early on giving me the encouragement as well as the freedom to pursue an unusual project which entailed using techniques and ways of thinking that were completely new to me. In working with Marc I learned his zest for experiments and I hope that I have acquired to some small extent his propensity towards finding unusual, creative means of solving problems. Personally, I have appreciated Marc's warmth and sympathy, and even his cutting sense of humor. I would like to thank Tim Mitchison, who over the years has given great support and advice. It is from him that I learned the hands-on approach to microscopy. Furthermore, "Friends of Microtubules" meeting has been one the most stimulating groups, largely through Tim's initiation and continued interest. Marc Tessier-Lavigne, the third member of my thesis committee has always provided keen insight and level-headed advice throughout our interactions. I will fondly remember the Growth Cone Collective--James Sabry and Sigrid Reinsch--as we explored and struggled together through the problems of the neuronal cytoskeleton and video-microscopy. Special thanks to James for all the trans-continental thesis and equipment transactions.

I owe tremendous gratitude to John Sedat and David Agard as it was their CCD-microscope system that was a crucial part of my thesis. I have learned not only from their expertise, but from their generosity in sharing their time, knowledge and facilities. The people in their group, Jason Swedlow, Hans Chen, Mel Jones, Angus McDonald, Bill Stock, all showed the

same generosity on a daily basis. Much thanks to Lou Reichardt who, over a period of several years, allowed me to use his microscope to do the bulk of my thesis work. Finally, I would like to acknowledge Doug McVey and Bob Shadel who took many of our wild ideas for contraptions and transformed them into practical designs and actual objects.

Outside of the lab, I would like to thank all the people with whom I explored music in various forms. There is, of course, Sex Lethal and the Shaven Babies--Ken Sawin, Sean Burgess, and Steve Salser. Quartets were always a good way of waking up on Sundays, with Sean, Dan Doherty, David Drechsel and Lauri Smith. Jazz with Tina Lee and Eliot Dresselhaus was a new world for me. And, opera-going with Andrew Murray was always a highlight of my Falls here.

The text of Chapter 2 is a reprint of the material as it appears in The Journal of Cell Biology, Volume 115, Number 2, October 1991

## ABSTRACT

Cell polarization, including changes in cell shape and the re-distribution of organelles, is an important aspect of cellular differentiation. Neuronal cells are the most remarkable example of cell polarization as they extend long processes which take complex paths to reach their targets. During neurite outgrowth, the movement of the growth cone away from the cell body generates the new axonal structure. The growth cone integrates diverse extracellular cues and transduces them into morphological changes to determine its orientation.

Crucial to elucidating the cellular mechanisms of neurite outgrowth and growth cone guidance will be understanding how the cytoskeleton reorganizes during these processes since the cytoskeleton ultimately determines the shape and the dynamic properties of the growth cone and must be a major target of extracellular signaling cues. Although microtubules are major structural elements of the developing axon, it is not clear how microtubule polymerization and distribution is controlled to generate the highly organized array in neurons and whether microtubules play any role in the pathfinding decisions in the growth cone. To address these issues I developed a system to uniformly label microtubules in neurons with rhodamine-tagged tubulin by injecting Xenopus eggs with labeled tubulin, and subsequently culturing the neural tubes from these embryos. Using anoxic culture conditions and a CCD imaging system, I acquired time-lapse sequences of living neurons at high temporal and spatial resolution.

I observed microtubule dynamic instability in growth cones but could not determine whether modulation of microtubule dynamics contributes to

the elongation of the microtubule array and the rearrangements of growth cone microtubules occur in large part by the forward and lateral translocation of microtubule polymer through the cytoplasm 2) microtubule polymerization into peripheral lamellae may coordinate actin-based growth cone motility with microtubule elongation by guiding microtubule bundling. Growth cone microtubules may slide along the newly assembled microtubules to generate bundles. 3) Microtubule bundling appears to be and essential step in axon formation and turning This bundling may in turn, elicit changes in actin organization.

Thesis advisor's signature.....

**TABLE OF CONTENTS**

# Chapter 1
# Introduction

**Neuronal morphogenesis**

During organogenesis, individual cells acquire polarized forms and elaborate complex structures in order to execute their specialized functions. Cell polarization includes changes in cell shape, as well as the re-distribution of organelles. One of the most remarkable examples of such specialization is the neuronal cell which transmits signals between distant regions of the body in milliseconds. This communication requires both extreme cell shape and segregation of cellular components. For example, motor neuron cell bodies reside in the spinal cord and extend thin processes called axons that can innervate muscles several meters away. Using vesicular transport these motor neurons deliver the neurotransmitters necessary for communication down the axon to the nerve terminal [1].

The mechanism by which neurons form these processes has long been controversial. In the late 19th century two hypotheses were dominant. One proposed that mature neurons derived their final form when multiple cells fused together, making a synticium in which only selective nuclei survived. The other asserted that a single cell extended a process out toward its target. Ramon y Cajal found evidence in support of the latter process in histological samples of embryos where he saw cells which appeared to be extending processes, with an enlarged, triangular form at their ends. He named this terminal structure "the growth cone" inferring that it guided the growing axonal process through the environment of the developing embryo [2]. Harrison definitively showed that neurons acquired their shape by elongating their axons. He isolated and cultured frog spinal cord cells, and followed individual cells over time. In this way, he found that the isolated neurons recapitulate their shape by extending processes with a dynamic growth cone at their end [3]. In addition to establishing that neurons generate their highly

polarized shape from single cells, Harrison initiated two techniques crucial to studying neuronal morphogenesis--cell culture and time lapse microscopic observation.

**Control of axonal outgrowth and guidance at the growth cone**

These initial discoveries stimulated great interest in understanding the mechanism of how neurons build the structure of the axon, and furthermore, how the neuron reads extracellular signals that guide the axon through its vast environment precisely to its target. These interests have focused largely on the growth cone, the terminal structure that moves in response to extracellular cues and that is the site where many new cell components are added. Using time-lapse observations of cultured neurons Bray found that small glass particles sprinkled onto the axon or growth cone would remain stationary with respect to the substrate while the growth cone moved away from the particle, leaving new axon between the growth cone and the particle [4]. These observations suggested that growth occurred at the end of the process. Other experiments implicated the growth cone as the primary sensor of environmental cues necessary to guide the axon to its target. As the growth cone moves over the substrate, it constantly extends and retracts long thin processes called filopodia or microspikes, and thin veils of membrane called lamellipodia. These structures transiently adhere to the substrate and appear to respond to extracellular cues to determine the direction of growth. The local perturbation of filopodial attachment altered the direction of the growth cone movement and consequently axon growth [5].

**The neuronal cytoskeleton**

To move beyond a phenomenological description of axonal outgrowth to a mechanistic understanding of the process requires the identification of molecules that mediate growth cone motility and generate axonal structure and that would be likely cellular targets for extracellular signaling molecules. In many cell types the actin and microtubule cytoskeleton are important structural determinants of cell shape and cell motility. In neurons, their organization and structure initially implicated their involvement in growth cone motility and axonal outgrowth while the use of specific cytoskeletal inhibitors have confirmed their importance in assembling the axon [6-8].

*Actin* The abundance of actin microfilaments in the dynamic structures of the growth cone immediately suggested their role in driving growth cone motility [8]. EM studies revealed that actin microfilaments permeate the lamella and the filopodia of the growth cone. In filopodia, actin forms dense, uni-oriented bundles, while in lamella the actin forms a relatively disorganized meshwork of filaments [9,10]. In the axon, the actin forms a thin cortical shell just beneath the cellular membrane, encasing other cytoplasmic components of the axon such as microtubules [11]. The apposition of actin with the membrane, and more recently the biochemical evidence of membrane-coupled actin nucleating sites strongly suggests that actin filaments constitute an immediate structural target for transduction of extracellular signals directing growth cone motility [12,13]. Inhibiting actin polymerization by treating with cytochalasin causes growth cone collapse and disoriented growth indicating a crucial role in motility and guidance [14].

*Microtubules* As with actin, early ultrastructural studies indicated an important function for microtubules in neurons. Microtubules extend down the axon in long bundles and become more sparsely distributed as individual

polymers in the growth cone [15-17]. This distribution inspired investigators to invoke two models for microtubule function; as tracks for polarized transport of components down to the growth cone and as structural elements for determining and maintaining axonal shape. Indeed, two large families of motor proteins, kinesin and dynein, which move along microtubules have been biochemically characterized and some of these motors likely transport vesicles to and from the growth cone [18,19]. The application of microtubule depolymerizing drugs bolstered the notion that microtubules are important structural elements of the neuron. These drugs inhibit the initiation of axonal outgrowth and cause existing neurites to retract [7,8,20,21].

More recent studies have refined our understanding of neuronal microtubule structure. Microtubules are arranged in parallel, polarized bundles[22]. Individual microtubules do not continuously extend from the cell body to the growth cone, rather, the axonal microtubule bundle consists of a staggered array of microtubules that are 100 μm-200 μm long [23-25]. Studies using the fluorescence recovery after photobleaching (FRAP) of fluorophores attached to tubulin showed that the microtubules in the axon turn over less frequently than the microtubules in the growth cone suggesting that microtubule bundling stabilizes axonal microtubules [26,27].

*The assembly properties of microtubules.* Both actin and microtubules are polar, non-equilibrium polymers that generate random arrays when assembled *in vitro* [28]. These arrays are highly dynamic in that individual polymers turn over very rapidly via polymerization and de-polymerization while the array as a whole maintain steady polymer levels. Both polymers exhibit polarity by the different assembly properties of the two ends[29]. The dynamics of individual microtubules, which have been particularly well-characterized, show unusual assembly properties when observed

microscopically. They stochastically alternate between sustained periods of growth via monomer addition at their ends, with bouts of rapid shrinkage through loss of subunits from their ends. These assembly characteristics termed "dynamic instability", are due to the hydrolysis of GTP by tubulin shortly after addition to the polymer lattice, and this nucleotide hydrolysis makes the growing state different from the shrinking state [29-31]. Current models for dynamic instability posit the existence of a poorly characterized GTP cap at the tip of growing microtubules, with loss of the cap leading to rapid disassembly [32].

In the cell, the dynamics and the spatial arrangement of these polymers must be controlled to generate the highly ordered structures found in neurons. Actin and microtubules both form multiple structures with different properties in a common cytoplasm. These structures must coordinately grow during axonal outgrowth. The static images of the neuronal cytoskeleton, while implicating function, are clearly insufficient for determining how the dynamic actin and microtubule cytoskeleton assembles during axon elongation. Three key questions about cytoskeletal assembly remain: 1) Where does new polymer assemble in the neuron and how is this assembly controlled? 2) How does the neuron coordinate assembly of actin with microtubules? 3) How do guidance molecules modulate assembly?

In my thesis, I my goal was to address these questions with respect to microtubules, and so the remainder of this chapter will focus on the assembly of microtubules during axonal elongation and guidance.

**Sites of microtubule assembly in neurons**

Although many biochemical activities from brain that stimulate microtubule assembly have been characterized, it is still unclear how these

activities are harnessed to yield organized arrays of microtubules. There has been much effort invested into locating the site of microtubule assembly in neurons as it is likely the region where microtubule assembly may be regulated. Indirect experiments from many investigators point to three different sites, the cell body, the axon, and the growth cone, as the major location of microtubule assembly in the growing neuron. As yet, a definitive conclusion has not been obtained.

*Assembly at the cell body*. Lasek proposed that microtubules assemble into a stable network that is extruded down the axon. By injecting radioactive amino acids into the retina and then slicing the optic nerve into sections at various time after injections, he found that labeled tubulin moved down the optic fiber at a slow, linear rate. Other observations of fixed cells using indirect markers for dynamic microtubules also suggest that microtubules are stabilized close to the cell body [33]. Both of these experiments are indirect and therefore inconclusive. The experiment by Lasek did not determine whether tubulin was transported down the axon as monomer or polymer. The second experiment, while looking at individual polymer, inferred the dynamic properties of individual microtubules in fixed specimens using indirect immunohistochemical markers. It was not independently verified if these markers accurately reflected the stabilization state of the microtubules.

The model of microtubule assembly at the cell body places the site of polymer assembly close to the site of tubulin biosynthesis allowing for tight coupling of the two processes and eliminating the need to transport tubulin to an assembly site. A weakness of this model is how tubulin assembly at the cell body is coordinated with the assembly of other components at distant sites in the growth cone.

*Assembly at the growth cone* If all new microtubule assembly occurred in the growth cone, then the axonal microtubule array would remain stationary and the tubulin subunits synthesized in the cell body would have to reach the growth cone. These subunits would add, presumably to plus ends of microtubules, and become stabilized and incorporated into the axonal array as the growth cone moved forward. FRAP studies of labeled microtubules in individual cultured neurons provide evidence for such a model since a photobleached mark does not move with respect to the substrate [26,27]. Photoactivation of fluorescence on labeled microtubules in mouse DRGs confirmed these results.

This model allows for tight coupling of microtubule assembly and growth cone advance but it is still unclear how tubulin would be transported down the axon in such a model. Photoactivation of a fluorescent signal on tubulin in mouse DRGs did not reveal a significant moving phase. Photobleaching studies detected a small pool of tubulin which rapidly diffused away from the mark. It is unlikely, however, that diffusion of monomer would be sufficient to supply subunits for growth when neurons become very long. While these marking experiments look at microtubules in living, growing neurons, they do not resolve single microtubules and can only examine characteristics of a bulk of microtubules in the marked spot so although it was inferred that polymer was not moving because the whole spot did not appear to translocate, it is possible that the asynchronous sliding of individual polymers would not be detected.

*Assembly along the axon* Microtubule ends are distributed along the length of the axon so unless these ends are blocked, they would provide sites for microtubule assembly. The microtubule lattice adjacent to these ends appears to be dynamic based on staining for markers of newly assembled

microtubules [23,25]. From these fixed sections it is, however, difficult to determine whether the addition of tubulin subunits to these ends can account for all the microtubule assembly required in an elongating axon or whether these ends are merely exhibiting the normal dynamics seen for microtubule arrays at steady state. If these ends constitute the major assembly sites of new microtubules, then these microtubules must slide forward during neurite outgrowth. Individual marks made on the axonal microtubules would be expected to broaden, and multiple marks made along an axon should move apart. Photoactivation of fluorescence in Xenopus neurons showed both of these behaviors suggesting that intercalary growth of microtubules occurs in the axon along with "telescoping" of microtubules [34]. Like the photobleaching experiments, the behavior of individual microtubules could not be observed and their behavior had to be inferred from bulk properties. Therefore, it was not directly shown that microtubules in the axon were growing. Furthermore, the source of the discrepancy between the photoactivation results in mouse DRGs versus the Xenopus motor neurons is still unknown.

Much of the uncertainty about the site of new microtubule assembly stems from the lack of direct information about how and where individual microtubules grow in neurons. Experiments which examine individual microtubules rely on fixed specimens, so the dynamic properties must be inferred rather than directly measured while experiments which directly examine microtubules in living neurons did not have sufficient resolution to examine individual polymers.

**How do microtubules and actin interact to give coordinate microtubule elongation and growth cone movement?**

During axonal elongation, growth of microtubules must match the growth of the rest of the axonal structure. In particular, the crawling forward of the actin-rich growth cone must match the growth of the microtubule array in the axon. Therefore, there has been much interest in understanding how the two cytoskeletal systems interact to give balanced growth.

*Growth cone pulling* Because of the abundance of actin in the growth cone seen in EM micrographs early models proposed that the growth cone crawled away from the cell body using the actin cytoskeleton, and microtubules "filled in" the space left free by this forward movement. Therefore the actin-rich growth cone "pulls" on the axon, and the microtubules buttress the new axonal structure[35,36]. In support of this model, Bray found that microtubules would fill the axon when the growth cone was mechanically pulled with a micropipette at a rate faster than normal axonal elongation (Bray). On a molecular level, it has been proposed that tension in the actin filament network could pull the microtubules forward. Direct measurements of growing PC12 cells indicate that actin mediates tension generated on the axon by the growth cone moving forward on the substrate [37,38].

*Axonal pushing* Other experiments suggested that the growth of the microtubule array determines the rate of growth cone advance, termed the "push" model. In particular, treatment with taxol, which stimulates microtubule polymerization, blocks neurite elongation unless cytochalasin was also added to disrupt actin, in which case, processes would extend. This was interpreted to mean that actin normally inhibited the pushing force of microtubules [39]. Furthermore, treatment of the grasshopper Ti1 neuron disrupted guidance of the neuron but did not inhibit outgrowth, suggesting that an intact actin network is not required for axonal elongation in situ [14].

*Actin-microtubule interactions in the growth cone* The most detailed work examining actin-microtubule interactions in the growth cone have come from studying cultured Aplysia neurons. Careful observation of growth cones using differential interference contrast (DIC) microscopy revealed that axons elongate when the organellar rich zones, that correlate with microtubule position, invade the actin-rich lamella. After invasion, the rest of the actin-rich growth cone collapsed around the organelles to form the new axon, and new lamellae extended ahead of the organelle -rich region, to form the new growth cone [40]. A similar sequence of events occurs when PC12 cells extend neurites on poly-lysine. These observations suggest that the growth cone does not crawl away from the microtubules, rather that the microtubules extend into actin-rich areas and cause the growth cone to coalesce around the microtubules to form the new axon.

Fluorescent localization of actin and microtubules in fixed Aplysia neurons indicates that in general, microtubules are excluded from lamella, which are densely populated by actin. When the neurons are treated with cytochalasin, microtubules surge forward into the distal regions of the lamella, suggesting that the actin normally blocks microtubule entry [41]. When these neurons, grown on poly-lysine, are stimulated to begin rapid growth by contact with another growth cone, organelles are observed to invade the site of contact. Prior to organelle invasion, high levels of actin accumulate at the contact site, but is depleted from the base lamella near the contact site [42]. Again, this localization data supports the notion that actin normally excludes microtubules from lamella, but a signal from the extracellular matrix can cause changes in the actin network that then allows microtubules to enter the lamella to form new axonal structure. Because organelle localization has been used as a marker for microtubule distribution

in these experiments, it is still unclear whether microtubules invade the lamella during axonogenesis by increased polymerization, or by sliding forward and whether microtubules follow the changes in the actin distribution directly, or whether there is a lag in the response of the microtubules. Microtubules could bind the actin in the lamella, and so the re-distribution of actin would "pull" the microtubules with it, or the re-distribution of actin may just provide a new space which microtubules fill via polymerization or sliding. It is also unclear to what extent the microtubules are necessary for directing the changes in actin distribution.

**How do microtubules respond to guidance signals?**

In order to reach their targets, neurons change their direction of growth in response to extracellular cues. In vitro and in vivo studies show that growth cones respond to patterns of both extracellular matrix molecules and membrane bound molecules as well as gradients of diffusible chemotactic factors [43-46]. These signals ultimately induce the reorganization of actin and microtubules to elicit growth in a new direction. The grasshopper neuron Ti1, which takes a stereotypical pathway from the limb to the central nervous system, has offered the most detailed picture thus far of microtubule reorganization during turning decisions. At segment boundaries where the neuron turns at border of membrane-bound molecules, actin-rich filopodia and branches extend in multiple directions and microtubules invade multiple branches, only one of which is eventually stabilized. In contrast, during turning at guidepost cells, microtubules only enter the filopodia that contacted the guidepost cell[47,48]. These observations indicated that during guidepost mediated turnings, microtubule reorientation is an early step in turning. However, due to the low spatial and temporal resolution of images

in the grasshopper it was not determined whether the microtubule rearrangements occurred through spatially-restricted modulation of microtubule dynamics, or through the movement of microtubules through the cytoplasm.

**The need for observing microtubules at high temporal and spatial resolution in neurons**

The microtubule array clearly grows and changes during axon outgrowth and growth cone turning, yet, the mechanism by which these changes occur is still unclear. Studies of microtubules in vitro and in living fibroblast cells demonstrated the necessity of following individual polymers over time to understand the mechanism of microtubule polymerization [29]. In neurons single microtubule resolution had only been achieved in fixed specimens, and bulk polymer could only be followed in living cells. My goal was to examine individual microtubule behavior in living neurons to determine 1) how dynamic instability was modulated to generate the stable axonal array 2) How microtubule elongation was coordinated with growth cone motility and 3) how microtubules responded to guidance cues during turning decisions. By characterizing the microtubule behaviors in growth cones, I hoped to understand what might be the important biochemical activities that modulate microtubule polymerization and organization so that ultimately, such activities and their regulation could be studied in vitro with purified tubulin.

To this end I developed a system to uniformly label microtubules in neurons with rhodamine-tagged tubulin by injecting Xenopus eggs with labeled tubulin, and subsequently culturing the neural tubes from these embryos. Using anoxic culture conditions and a CCD imaging system, I

acquired time-lapse sequences of living neurons at high temporal and spatial resolution.

I observed microtubule dynamic instability in growth cones but could not determine whether modulation of microtubule dynamics contributes to new axon formation. From my observations I could conclude that: 1)the elongation of the microtubule array and the rearrangements of growth cone microtubules occur in large part by the forward and lateral translocation of microtubule polymer through the cytoplasm. 2) Microtubule polymerization into peripheral lamellae may coordinate actin-based growth cone motility with microtubule elongation by guiding microtubule bundling. Growth cone microtubules may slide along the newly assembled microtubules to generate bundles. 3) Microtubule bundling appears to be and essential step in axon formation and turning This bundling may in turn, elicit changes in actin organization.

1.Peters, A., Palay, S. L. and Webster, H. 1991. The fine structure of the nervous system: neurons and their supporting cells.

2.Ramon y Cajal, S. 1890. Sur l'origine et les ramifications des fibres nerveuses de la moelle embyonaire. Anat Ang 5: 609-613.

3.Harrison, R. G. 1910. The outgrowth of the nerve fiber as a mode of protoplasmic movement. J Exp Zool 17: 521-544.

4.Shaw, G. and Bray, D. 1977. Movement and extension of isolated growth cones. . Exp Cell Res 104: 55-62.

5.Wessells, N. K. and Nuttall, R. P. 1978. Normal branching, induced branching, and steering of cultured parasympathetic motor neurons. Experimental Cell Research 115: 111-122.

6.Porter, M. E., Scholey, J. M., Stemple, D. L., Vigers, G. P., Vale, R. D., Sheetz, M. P. and McIntosh, J. R. 1987. Characterization of the microtubule movement produced by sea urchin egg kinesin. . J Biol Chem 262: 2794-802.

7.Daniels, M. P. 1973. Fine structural changes in neurons associated with colchicine inhibition of nerve fiber formation in vitro. J. Cell Biol. 58: 463-470.

8.Yamada, K. M., Spooner, B. S. and Wessells, N. K. 1970. Axon growth: role of microfilaments and microtubules. PNAS 66: 1206-1212.

9.Bridgman, P. C. and Dailey, M. E. 1989. The organization of myosin and actin in rapid frozen nerve growth cones. J Cell Biol 108: 95-109.

10.Lewis, A. K. and Bridgman, P. C. 1992. Nerve growth cone lamellipodia contain two populations of actin filaments that differ in organization and polarity. . J Cell Biol 119: 1219-43.

11.Letourneau, P. C. 1983. Differences in the organization of actin in the growth cones compared with the neurites of cultured neurons from chick embryos. J Cell Biol 97: 963-973.

12.Luna, E. J. 1991. Molecular links between the cytoskeleton and membranes. . Curr Opin Cell Biol 3: 120-6.

13.Hall, A. L., Warren, V., Dharmawardhane, S. and Condeelis, J. 1989. Identification of actin nucleation activity and polymerization inhibitor in ameboid cells: their regulation by chemotactic stimulation. . J Cell Biol 109: 2207-13.

14.Bentley, D. and Toroian-Raymond, A. 1986. Disoriented pathfinding by pioneer neuron growth cones deprived of filopodia by cytochalasin treatment. Nature 323: 712-715.

15.Porter, K. R. 1966. Cytoplasmic microtubules and their functions. Principles of Biomolecular Organization 308-356.

16.Yamada, K. M., Spooner, B. S. and Wessells, N. K. 1971. Ultrastructure and function of growth cones and axons of cultured nerve cells. J Cell Biol 49: 614-635.

17.Bunge, M. B. 1973. Fine structure of nerve fibers and growth cones of isolated sympathetic neurons in culture. J Cell Biol 56: 713-735.

18.Sheetz, M. P., Vale, R., Schnapp, B., Schroer, T. and Reese, T. 1986. Vesicle movements and microtubule-based motors. . J Cell Sci Suppl 5: 181-8.

19.Walker, R. A. and Sheetz, M. P. 1993. Cytoplasmic microtubule-associated motors. . Annu Rev Biochem 62: 429-51.

20.Daniels, M. P. 1972. Colchicine inhibition of nerve fiber formation *in vitro*. J.Cell Biol. 53: 164-176.

21.Bray, D. 1978. Growth cone formation in cultures of sensory neurons. Proc. Natl. Acad. Sci. USA 75: 5226-5229.

22.Heidemann, S. R., Landers, J. M. and Hamborg, M. A. 1981. Polarity orientation of axonal microtubules. J. Cell Biol. 91: 661-665.

23.Baas, P. W. and Black, M. M. 1990. Individual microtubules in the axon consist of domains that differ in both composition and stability. J. Cell Biol. 111: 495-509.

24.Bray, D. and Bunge, M. B. 1981. Serial analysis of microtubules of cultured rat sensory neurons. J. Neurocytol. 10: 589-605.

25.Okabe, S. and Hirokawa, N. 1988. Microtubule dynamics in nerve cells: analysis using microinjection of biotinylated tubulin into PC12 cells. 107: 651-664.

26.Lim, S., Sammack, P. J. and Borisy, G. G. 1989. Progressive and spatially differentiated stability of microtubules in developing neuronal cells. J. Cell Biol. 109: 253-264.

27.Okabe, S. and Hirokawa, N. 1990. Turnover of fluorescently labeled tubulin and actin in the axon. Nature 343: 479-482.

28.Kirschner, M. W. and Mitchison, T. J. 1986. Beyond sefl-assembly: from microtubules to morphogenesis. Cell 45: 329-342.

29.Mitchison, T. and Kirschner, M. W. 1984. Dynamic instability of microtubule growth. Nature 312: 237-242.

30.Horio, T. and Hotani, H. 1986. Visualization of dynamic instability of individual microtubules by dark field microscopy. Nature 321: 605-607.

31.Walker, R. A., O'Brien, E. T., Pryer, N. K., Soboeiro, M. F., Voter, W. A., Erickson, H. P. and Salmon, E. D. 1988. Dynamic instability of individual microtubules analyzed by video light microscopy: rate constants and transition frequencies. J. Cell Biol. 107: 1437-1448.

32.Mitchison, T. J. and Kirschner, M. W. 1987. Some thoughts on the partitioning of tubulin between monomer and polymer under conditions of dynamic instability. Cell Biophysics 11: 35-55.

33.Baas, P. W., Ahmad, F. J., Pienkowski, T. P., Brown, A. and Black, M. M. 1993. Sites of microtubule stabilization for the axon. . J Neurosci 13: 2177-85.

34.Reinsch, S. S., Mitchison, T. J. and Kirschner, M. W. 1991. Microtubule polymer assembly and transport during axonal elongation. J. Cell Biol. 115: 1364-1380.

35.Bray, D. 1979. Mechanical tension produced by nerve cells in tissue culture. J. Cell Sci. 37: 391-410.

36.Bray, D. and Chapman, K. 1985. Analysis of microspike movements on the neuronal growth cone. J Neurosci 5: 3204-3213.

37.Dennerell, T. J., Joshi, H. C., Steel, V. L., Buxbaum, R. E. and Heidemann, S. R. 1988. Tension and Compression in the Cytoskeleton of PC 12 Neurites II: quantitative measurments. J. Cell Biol. 107: 665-674.

38.Joshi, H. C., Chu, D., Buxbaum, R. E. and Heidemann, S. R. 1985. Tension and compression in the cytoskeleton of PC 12 neurites. J. Cell Biol. 101: 697-705.

39.Letourneau, P. C., Shattuck, T. A. and Ressler, A. H. 1987. Pull and push in neurite elongation: observations on the effects of different concentrations of cytochalasin B and taxol. Cell Motility and Cytoskel 8: 193-209.

40.Goldberg, D. J. and Burmeister, D. W. 1986. Stages in axon formation: observations of growth of *Aplysia* axons in culture using video-enhanced contrast-differential interference contrast microscopy. J Cell Biol 103: 1921-1931.

41.Forscher, P. and Smith, S. J. 1988. Actions of cytochalasins on the organization of actin filaments and microtubules in a neuronal growth cone. J Cell Biol 107: 1505-16.

42.Lin, C. H. and Forscher, P. 1993. Cytoskeletal remodeling during growth cone-target interactions. . J Cell Biol 121: 1369-83.

43.Tessier-Lavigne, M., Placzek, M., Lumsden, A. G., Dodd, J. and Jessell, T. M. 1988. Chemotropic guidance of developing axons in the mammalian central nervous system. Nature 336: 775-8.

44.Lumsden, A. G. and Davies, A. M. 1986. Chemotropic effect of specific target epithelium in the developing mammalian nervous system. . Nature 323: 538-9.

45.Walter, J., Henke, F. S. and Bonhoeffer, F. 1987. Avoidance of posterior tectal membranes by temporal retinal axons. . Development 101: 909-13.

46.Gundersen, R. W. and Barrett, J. N. 1979. Neuronal chemotaxis: chick dorsal-root axons turn toward high concentrations of nerve growth factor. Sci 206: 1079-1080.

47.O'Connor, T., Duerr, J. and Bentley, D. 1990. Pioneer growth cone steering decisions mediated by single filopodial contacts. J Neurosci 10: 3935-3946.

48.Sabry, J. H., O'Connor, T. P., Evans, L., Toroian-Raymond, A., Kirschner, M. W. and Bentley, D. 1991. Microtubule behavior during guidance of pioneer neurons growth cones *in situ*.. J. Cell Biol. 115:1381-1395

# Chapter 2
# Microtubule behavior in the growth cones of living neurons during axon elongation

# Microtubule Behavior in the Growth Cones of Living Neurons during Axon Elongation

**Elly M. Tanaka and Marc W. Kirschner**

Department of Biochemistry and Biophysics, University of California, San Francisco, California 94143

***Abstract.*** To understand how microtubules are generated in the growth cone, we have imaged fluorescently tagged microtubules in living frog embryonic neurons. The neurons were labeled by injecting rhodamine-labeled tubulin into the fertilized egg and explanting the neurons from the neural tube. Microtubules extend deep into the growth cone periphery and adopt three characteristic distributions: (*a*) dispersed and splayed throughout much of the growth cone; (*b*) looped and apparently contorted by compression; and (*c*) bundled into tight arrays. These distributions interconvert on a time scale of several minutes and these interconversions are correlated with the behavior of the growth cone. We observed microtubule growth and shrinkage in growth cones, but are unable to determine their contribution to net assembly. However, translocation of polymer from the axon appears to be a major mechanism of generating new polymer in the growth cone, while bundling of microtubules in the growth cone appears to be the critical step in generating new axon. Neurons that were about to turn spontaneously generated microtubules in the future direction of growth, suggesting that orientation of microtubules might be an important early step in neuronal pathfinding.

EARLY investigations of cytoplasmic structure using EM revealed organized arrays of microtubules in asymmetric cells. The arrangement of microtubules suggested that they may play a role in establishing or maintaining cell shape (Porter, 1966). In neurons, which are long asymmetric cells, parallel microtubules were found to run down the axon (Peters et al., 1991). Their importance in establishing and maintaining axonal structure was demonstrated when application of colchicine, a specific microtubule-disrupting agent, caused growing neurites to collapse, and inhibited new neurite outgrowth (Daniels, 1972; Yamada et al., 1971). Despite the acknowledged importance of microtubules in the structure of axons, their exact role in the growth of axons, their mechanism of assembly and transport in the axon, and the possible function of microtubules in the pathfinding decisions made at the growth cone are still unresolved.

Since the early morphological studies of Ramon y Cajal and Harrison (Ramon y Cajal, 1890; Harrison, 1910), the growth cone has been ascribed the major role for generating new axonal structure and for determining the orientation of that structure in pathfinding decisions. Even though microtubules are the major structural elements of the developing axon, it is not yet clear whether microtubules play any role in the pathfinding decisions in the growth cone. Some of the present uncertainty stems from an imprecise knowledge of where microtubules are located in the growth cone. Early studies found that they did not extend beyond the growth cone neck and appeared to be prevented from entering the lamella by a dense network of microfilaments (Bunge, 1973; Yamada et al., 1971). Among the cytoskeletal elements, actin was shown to be present in the growth cone, so it was proposed that the actin cytoskeleton and not the microtubules controls the motility and directionality of the growth cone and thus determines the direction and rate of axonal elongation. In this view, microtubules play a subordinate role: to fill in the axon structure generated by the advancing growth cone. The parallels between the motility of migrating cells, some of which can migrate without microtubules, and the motility of the growth cone, reinforce the idea that microtubules may play a minor role in growth cone guidance.

Other studies indicated that microtubules may play a more active role in the generation and orientation of the growing axon. More recent electron microscopic images show microtubules extending beyond the neck, deep into the growth cone lamella (Bridgman and Dailey, 1989; Cheng and Reese, 1985; Tsui et al., 1984). In time lapse recordings, organelles that presumably move along microtubules were seen to invade the peripheral lamellipodia, suggesting that as the axon grows, microtubules may sometimes populate the distal regions of the growth cone (Goldberg and Burmeister, 1986). In addition, although actin is undoubtedly important for growth cone structure, neurites continue to grow in the presence of cytochalasin B, an actin depolymerizing drug, suggesting that microtubule polymerization or extrusion may itself be able to drive axonal growth (Bentley and Toroian-Raymond, 1986; Marsh and Letourneau, 1984).

The heterogeneous morphology of growth cones has made

it difficult from static light or electron microscopic images to reconstruct the process of neurite outgrowth. Advancing growth cones actively remodel their cortex, continually forming and dissolving their filopodia, lamellipodia, and veils. These processes can be followed by phase or DIC microscopy, but they do not give any indication of the location or dynamics of the microtubules in the cell interior. So far, most studies of microtubules have been limited to the direct observation of fixed specimens by EM or immunofluorescence. In one study (Forscher and Smith, 1988), a limited number of microtubules could be seen in living growth cones after treatment with cytochalasin D and though this study showed that the actin network may restrict access of microtubules to the lamella, it did not examine the assembly of microtubules during normal growth.

It would be of particular interest to follow microtubules in living neurons to understand how they are assembled during neurite outgrowth and to define precisely their role in turning decisions. In other cell types, as well as in the studies of microtubule polymerization in vitro, it has been necessary to visualize and measure individual microtubules over time to appreciate their dynamic characteristics. In growth cones, direct observation can distinguish among several of the proposed models that predict different modes of microtubule stabilization and localization (Mitchison and Kirschner, 1988). We have developed a novel system to label and follow individual microtubules over time in the growth cones of rapidly growing neurons in culture. Here, we report our observations of microtubules in the growth cones of these neurons and discuss the implications of such observations on the mechanism of microtubule extension during axon elongation and turning.

## Materials and Methods

### Tubulin Labeling

Bovine brain tubulin was labeled with 5-(+6)-carboxytetramethylrhodamine succinimidyl ester (C-1171, Molecular Probes, Eugene, OR) essentially as described previously (Hyman et al., 1991). This resulted in a labeling of tubulin with 2 mol of rhodamine per mol of tubulin.

### Labeling and Culturing of Xenopus Neurons

*Xenopus* eggs were fertilized and dejellied in vitro as previously described (Newport and Kirschner, 1982). At the two-cell stage, the eggs were placed in 1× MMR (0.1 M NaCl, 2 mM KCl, 1.0 mM $MgSO_4$, 2.0 mM $CaCl_2$, 5.0 mM Hepes, 0.1 mM EDTA [pH 7.8]), 5.5% ficoll, 50 nl of 5 mg/ml rhodamine-tubulin was injected into one of the two blastomeres using an air pressure injector and calibrated needles. With an estimated content of tubulin in the egg of 1 μg (Gard and Kirschner, 1987), the initial ratio of labeled exogenous tubulin to endogenous tubulin was ~1:4. 1–3 h after injection, the normal eggs were transferred to 0.1× MMR, 5.5% ficoll to allow proper gastrulation, while the abnormally developing embryos (~20%, but highly dependent on egg batch) were discarded. Injected embryos that appeared normal at 3 h developed normally through tadpole stages and beyond. Half of the injected eggs were placed at 18°C, and the other half at 13°C to stagger development. The embryos were allowed to develop in the dark until ST 20–24 (Nieuwkoop and Faber, 1956) (~40 h at 18°C and 64 h at 13°C).

At the neurula stage, the neural tube was dissected as described previously (Hinkle et al., 1981). Briefly, the embryos were placed in Steinberg's solution (58 mM NaCl, 0.67 mM KCl, 0.44 mM $Ca(NO_3)_2$, 1.3 mM $MgSO_4$, 4.6 mM Tris, pH 7.8) for dissection, and using fine forceps, the entire dorsal portion of the embryo was removed and then incubated for 40 min at 19°C in 1 mg/ml collagenase (type 1A, Sigma C-9891; Sigma Chemical Co., St Louis, MO) dissolved in Steinberg's solution. The dorsal portions were then placed back into collagenase-free Steinberg's solution, and the neural tube was teased out using fine forceps. The neural tube was divided along its length into several pieces, and temporarily stored in a small tube containing Steinberg's solution. The neurons were cultured as explants in Steinberg's plating media (20% Leibovitz L-15, 58 mM NaCl, 0.67 mM KCl, 0.44 mM $Ca(NO_3)_2$, 1.3 mM $MgSO_4$, 4.6 mM Tris, pH 7.8, 10 mM $MgCl_2$, 0.1% Gentamycin) with no FCS, on 25-mm round glass coverslips (no. 1). The coverslips had first been acid washed with 1 N HCl for 6 h at 65°C, washed extensively with quartz distilled water, then immersed in 1 mg/ml poly-d-lysine (Sigma Chemical Co.) for 30 min at 25°C, rinsed with water, dried, then coated with Matrigel (Collaborative Research, Bedford, MA) for 30 min at 25°C, and thoroughly washed with $Ca^{++}$, $Mg^{++}$-free PBS. Generally, the coverslips were coated with Matrigel just before use. Neural tubes were plated at 19°C using a p200 Pipetteman pipetter by placing the tip just under the liquid surface before dispensing the neural tubes, and then allowing the neural tubes to settle by gravity. The cultures were ready for observation 5–8 h after plating. A few of the cultures were dissected using RTM dissecting media (12 mM NaCl, 4.0 mM KCl, 0.4 mM $Ca(NO_3)_2$, 0.05 mM $CaCl_2$, 0.8 mM Mg $SO_4$, 56 mM Nalsethionate, 4.0 mM $Na_2HPO_4$, 5.0 mM NaHEPES, pH 7.8, 0.1% Gentamycin) and plated in RTM media (20% Leibovitz L-15, 12 mM NaCl, 4.0 mM KCl, 0.4 mM $Ca(NO_3)_2$, 0.05 mM $CaCl_2$, 0.8 mM Mg $SO_4$, 56 mM Nalsethionate, 4.0 mM $Na_2HPO_4$, 5.0 mM NaHepes pH 7.8, 0.1% Gentamycin), supplemented with 1× embryo extract (Harris et al., 1985). The RTM media and the embryo extract increased the likelihood of finding flat neurons in the culture.

Just before observation, the cultures were placed in a custom-built chamber that was sealed under nitrogen. The chamber (illustrated in Fig. 1) consists of a thin (4 mm) metal base with a hole cut in the center to hold coverslips hinged to a thick (13 mm) top with a conically shaped well drilled into it. The coverslips are held between the bottom and the top using a silicone O-ring. A flat, plexiglass ring with a shallow well cut into it, was fitted to sit above the media, but within the well, as an open reservoir to hold oxygen scavenging solutions. In transferring the cultures from the petri dish to the cell chamber, the neurons would often lift off the coverslip from the surface tension of the liquid, which contained no serum. So, before transfer, a small amount of 5 mg/ml BSA in plating media was added directly over the explants to act as a surfactant. This was usually sufficient to prevent detachment of the neurons. Degassed media that had been bubbled with nitrogen was layered over the coverslip in the chamber, and the chamber was then placed in a nitrogen glove box. Under the nitrogen atmosphere, two separate oxygen-scavenging solutions, 1 M pyrogallol (Aldrich Chemical Co., Milwaukee, WI) in 1 N NaOH, and 0.4 M n-propylgallate (Sigma Chemical Co., St. Louis, MO) in 1 N NaOH were made fresh. 400 μl of each solution were placed in separate compartments of the open reservoirs described above. These oxygen scavengers helped to remove residual traces of oxygen in the chamber, and because they change color in response to oxygen, they indicated the presence of any leaks in the chamber. The chamber was then sealed air-tight using a clear plexiglass disc that covered the well and was held down by four thumbscrews.

### Microtubule Visualization and Data Acquisition

The neurons were visualized on an inverted microscope (Olympus IMT-2, Japan) equipped with epifluorescence optics, using the green filter set for rhodamine visualization and a 60×, 1.4 NA oil immersion objective. The light from the 100 W mercury lampsource was typically attenuated 4–10-fold with neutral density filters and constriction of an out of focus aperture. The excitation light was shuttered to 0.1 s per exposure. The frequency of image acquisition varied from 5 to 35 s, depending on the sequence. Images were collected using a Peltier cooled CCD camera (Photometrics Ltd., Tucson, AZ), equipped with a 900 × 900 pixel CCD chip (Texas Instruments, Dallas, TX). The final magnification onto the camera was 0.098 μm/pixel. For most experiments, only 512 × 512 pixels of information were collected. This allowed frequent image collection. Light shuttering and storage of digital data was controlled using a Microvax II workstation (Digital Equipment Corp., Marlboro, MA) coupled to a 32 Mgbyte Mercury Zip 3232+ array processor (Mercury Computer Systems Inc., Lowell, MA) and a display system (model 1280; Parallax Graphics Inc., Santa Clara, CA). The data was stored on a large format, 2 G-byte, optical disk (Emulex Corp./Optimem 1000, Costa Mesa, CA). This system was developed by Dr. David Agard and Dr. John Sedat. The images were photographed for publication using a Dunn digital camera system (Log E-Dunn) with Technical Pan 2415 film.

### Data Analysis

Microtubule growth and shrinkage measurements were performed on a Vax 8650 with an attached Parallax display station, using modelling and display software written in Fortran (Chen et al., 1989). The change in position of

the microtubule tips was measured for microtubules that were not moving laterally. The error in measurement was 0.1 μm based on repeated measurements of a microtubule. In a few cases, we measured the change in length between the tip of a microtubule and some static feature, such as a bend. An example of such a measurement is shown in Fig. 7, where a microtubule appears to shrink while it is simultaneously bending back toward the central region. The distance between the microtubule tip and a bend, which remains constant in shape, can be measured.

For clarity and detailed following of single microtubules (as seen in Fig. 8), some images of microtubules were traced by freehand from the video screen using modelling software (Chen et al., 1989).

The radius of gyration of the microtubules was determined by performing a line intensity scan across the growth cone in a direction perpendicular to the axon axis. A minimal cut-off intensity was determined for a single microtubules, and for each line intensity scan. This cut-off value was subtracted from all values, and any negative values were normalized to zero. The radius of gyration of the resulting distribution was determined with respect to the center of mass: $((\Sigma m_i r_i^2 - Ml^2)/M)^{1/2}$, where $m_i$ is the pixel intensity at a given position, $M$ is the total intensity across the line, $r_i$ is the distance of the pixel from the origin, and $l$ is the distance from the origin to the center of mass of the distribution. The width of the growth cone was determined from the same line intensity scans where a separate intensity cutoff was determined for the growth cone and the width of the resulting distribution was determined.

## Results

### Labeling Microtubules in Neurons

To label microtubules uniformly in neurons, we have developed a procedure in which labeled tubulin is injected into cells long before neuronal differentiation. The protocol for injection and neuronal culture is shown in Fig. 1. We injected rhodamine-labeled tubulin into *Xenopus* eggs during the first cleavage division and observed labeled microtubules 40 h later (at 18°C, 64 h at 13°C) in neurons explanted from the neural tube at the neurula stage. The embryo undergoes ~16 rounds of mitotic division to that stage, and generates 100,000 cells, but does not increase significantly in size. When the injected embryos were fixed and sectioned, or prepared as whole mounts, fluorescent tubulin could be easily seen in mitotic spindles and interphase asters throughout cleavage and gastrula stages (Reinsch, S. S., unpublished observations).

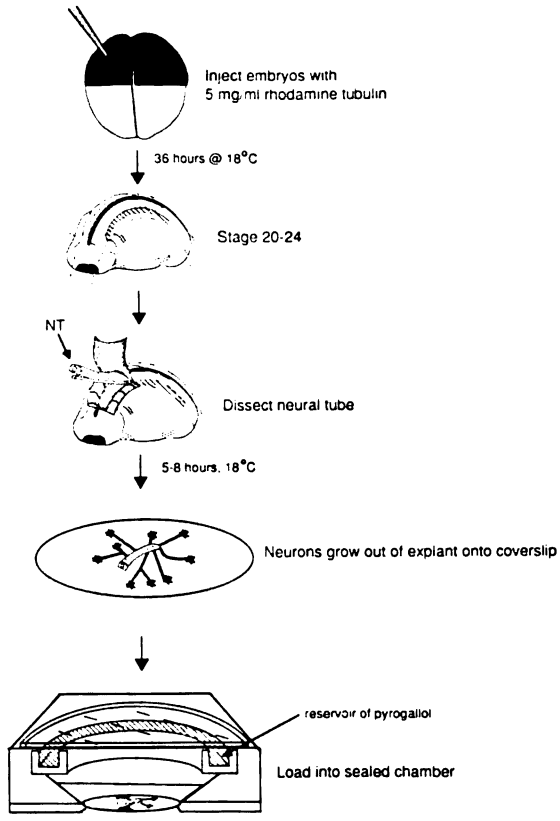


*Figure 1.* Outline of experimental procedure. Embryos are injected with 5 mg/ml rhodamine-tubulin at the two-cell stage. Neural tubes are dissected at stage 20–24, and plated as explants. Explants are viewed under anoxic conditions in a sealed chamber containing a reservoir of pyrogallol and n-propyl gallate.

To examine microtubules in neurons, we explanted small pieces of the neural tubes from normally developing embryos at ST 20–24 onto coverslips coated with a complex extracellular matrix. Fig. 2 shows a portion of an explant 5 h after plating, as neurons were beginning to emerge. The neurites had growth cones of various morphologies. In young cultures (4–10 h after plating), most growth cones had the classic features described for chick dorsal root ganglion and rat sympathetic neurons (Fig. 2, *inset*). They had significant regions of thin lamellipodia 5–10 μm in width with microspikes and filopodia emerging radially from the growth cone for distances up to 15 μm. Although most neurons generated straight axons, some branched or turned spontaneously. Axons grew out at rates of 70–250 μm/h at 19°C and reached lengths of several hundred microns. As the cultures aged (>12 h), the axons often developed varicosities and some of the growth cones started to become more bulbous, although they continued to grow. We concentrated our observations on the flat growth cones present in early cultures, because morphologically they resemble growth cones of well characterized neurons and because it was easier to visualize microtubules in thin flat regions of cells.

Under ambient conditions, overexposure to light (shuttered exposures more frequent than once every 15 s) caused growth cones to collapse, and the neurite to retract. During retraction, the microtubules and microtubule bundles became bent in response to the compression of the retracting growth cone and, as the microtubules bent, they appeared to twist around each other as they corkscrewed back toward the cell body. To reduce the cellular damage caused by singlet oxygen molecules generated during fluorophore excitation, the cultures were observed in a sealed chamber containing a reservoir of alkaline pyrogallol, to insure strict anoxic conditions throughout the experiment. Previous observations show that such explanted amphibian neurons can grow for several weeks in sealed chambers (Harrison, 1910). The removal of oxygen dramatically reduced photodamage and therefore increased the frequency of shuttered exposures (to every 5 s) that the cells could tolerate during fluorescence observation. The microtubules in the explanted neurons were imaged by epifluorescence optics and recorded digitally using a cooled charge-coupled device (CCD) camera.

### The Location of Microtubules in the Growth Cone

We will first describe the static images of microtubules in these neurons and then analyze properties of their distributions that could only be appreciated by time-lapse observa-

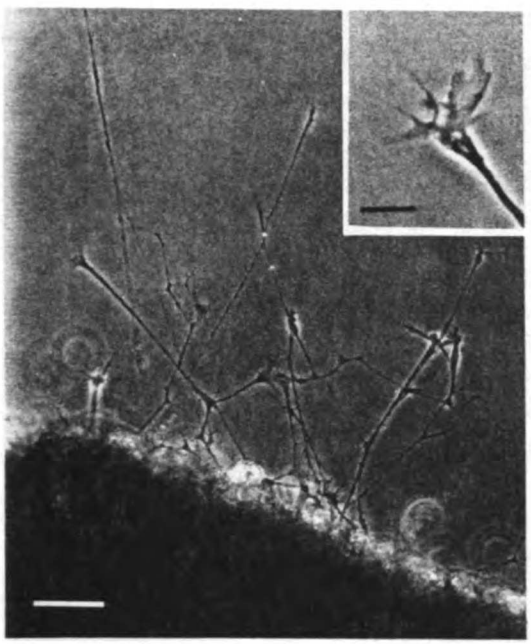

*Figure 2.* Low magnification phase image showing approximately one fifth of a typical neural tube explant, 5 h after plating. The cell bodies remain in the neural tube (lower portion of micrograph) as the neurites emerge. Later, additional neurons will grow out. (*inset*) High magnification view of one growth cone from the explant. Bars: (*lower portion of micrograph*) 50 μm; (*inset*) 8 μm.

tions at a level where single microtubules could be resolved. In growth cones, especially at their periphery, it was possible to distinguish single microtubules; in the most favorable cases we could describe in detail the distribution of microtubules in the entire growth cone. We recorded the microtubule distributions in 52 neurons in 24 experiments. In almost every instance we found that appreciable numbers of microtubules extended beyond the growth cone neck, deep into the peripheral lamella where they frequently touched or closely approached the membrane (Fig. 3, *A* and *B*, *arrows*). While individual microtubules in the lamella could be resolved, most of those in the central region were so closely packed that they could not be resolved. Organelle accumulations recorded by phase microscopy (Fig. 3, *A*, *C*, and *E*), corresponded roughly, but not precisely, to the regions of highest microtubule density; they are probably identical to the "organelle-rich regions" described in Aplysia neurons using Nomarski optics (Goldberg and Burmeister, 1986). Microtubules were not limited to these regions of high organelle density; for example, in Fig. 3, *A* and *B*, a small bundle of microtubules extended well beyond the dense organelle region (Fig. 3, *arrowheads*). Therefore, the use of organelle location to denote microtubule location may not always be justified.

The total number and distribution of microtubules in growth cones varied dramatically among different neurons. In some neurons, it was possible to resolve almost all of the microtubules, while in others, the thick tangle or close packing of microtubules in the central region made counting impossible. Our best estimate is that the number of microtubules per growth cone ranges from 10 to 40, and this number is roughly proportional to the size of the growth cone.

We could group the microtubule distributions into three general classes. A corresponding phase and fluorescence image of a typical growth cone from each class is shown in Fig. 3. In the first class, microtubules penetrated most of the projected growth cone area as seen in Fig. 3 (*A* and *B*). Many of the microtubules were bent or sinuous and were somewhat dispersed, even in the central region. We will refer to this distribution as the splayed distribution. In the second class, as seen in Fig. 3 (*C* and *D*), microtubules were also bent and spread, but they were not sinuous; rather, they formed loops that had a small radius of curvature. In such neurons, it was not uncommon to see microtubules that were bent by 90° or more. Such bending caused the distal ends of growth cone microtubules to be perpendicular to the direction of the axon bundle. We will refer to this configuration as looped. In the third category of growth cones (Fig. 3, *E* and *F*), almost all of the microtubules were straight, and even deep in the growth cone the width of the array did not deviate considerably from the width of the axon bundle. Sometimes, in this distribution, small bundles were resolvable whereas at other times, the array appeared to be of uniform brightness. This distribution, which we call bundled, left large regions of the growth cone unoccupied by microtubules (Fig. 3, *E* and *F*, *arrows*) with single microtubules occasionally straying from the main bundle (Fig. 3, *arrowhead*). In all three classes of neurons, microtubules extended to distal portions of the growth cone. Such diverse morphologies could represent distinct populations of neurons. However, when individual neurons were followed over time, as we discuss below, we observed an interconversion of the microtubule arrays among the splayed, looped, and bundled configurations.

### *The Origin of Microtubules in the Growth Cone*

***Microtubule Dynamics.*** Assembly of tubulin at steady state can be characterized by four parameters: the polymerization rate, the depolymerization rate, the rescue rate (shrinking to

*Figure 3.* Phase and fluorescence images of three living *Xenopus* neurons showing the three classes of microtubule distributions. (*A* and *B*) Phase and fluorescence images of a growth cone with a splayed microtubule distribution. Images were taken 44 s apart. Microtubules penetrate into the edges of the lamella in two places, shown by arrows. Arrowheads indicate areas where microtubules or small microtubule bundles extend beyond organelles. (*C* and *D*) Phase and fluorescence images taken 5 s apart, of a growth cone with a looped microtubule distribution. Microtubules penetrate to the edges of the growth cone. Many of the microtubules form acute bends which cause their distal ends to be perpendicular to the direction of the axon. (*E* and *F*) Images of growth cone with a bundled distribution taken 13 s apart. Microtubules in this growth cone are predominantly straight, and remain in a coherent axon-like bundle deep into the growth cone. Significant regions of the growth cone are left devoid of microtubules (*arrows*). A single microtubule is observed to form a loop near the neck (*arrowhead*). Bar, 5 μm.

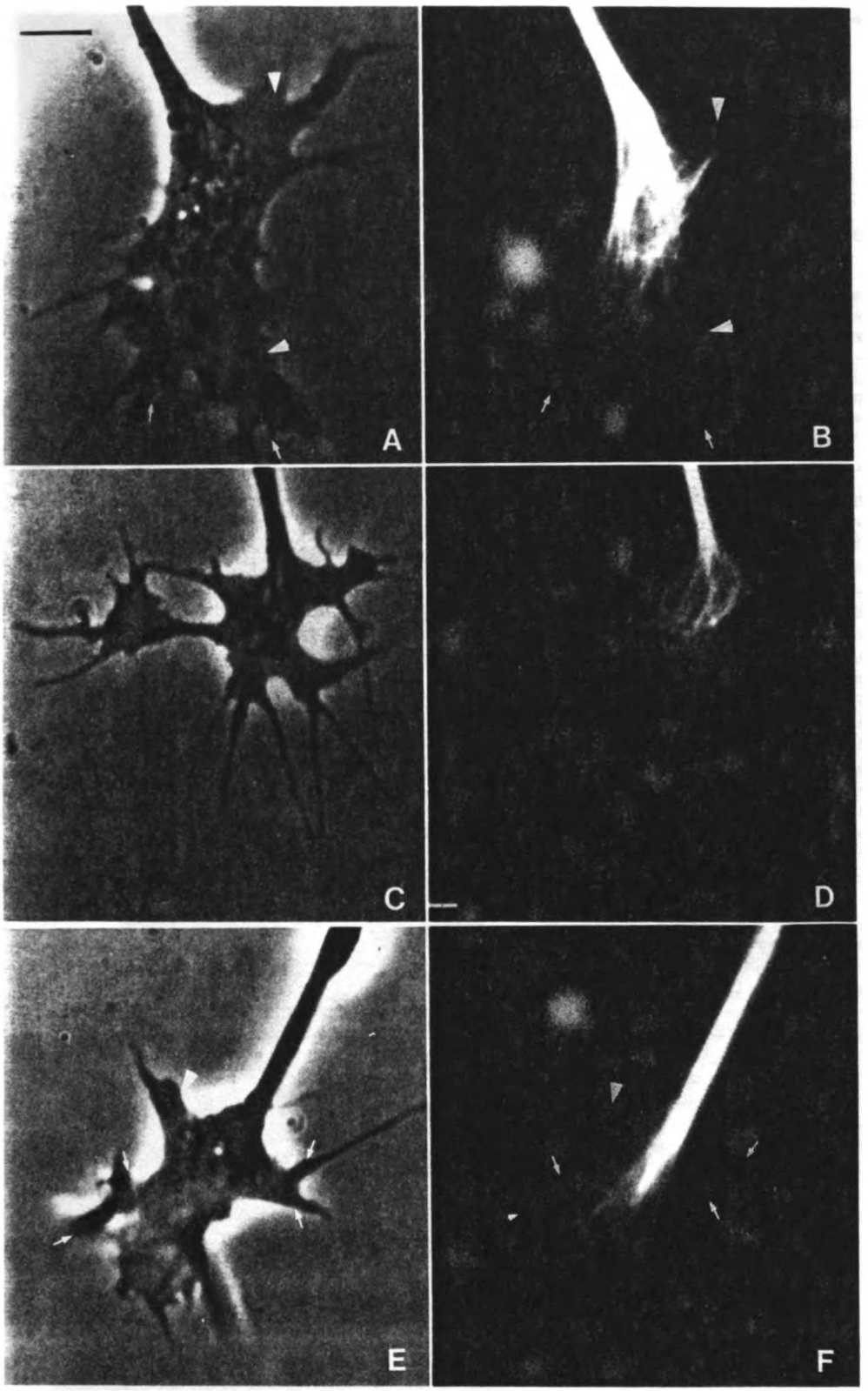
A
B
C
D
E
F

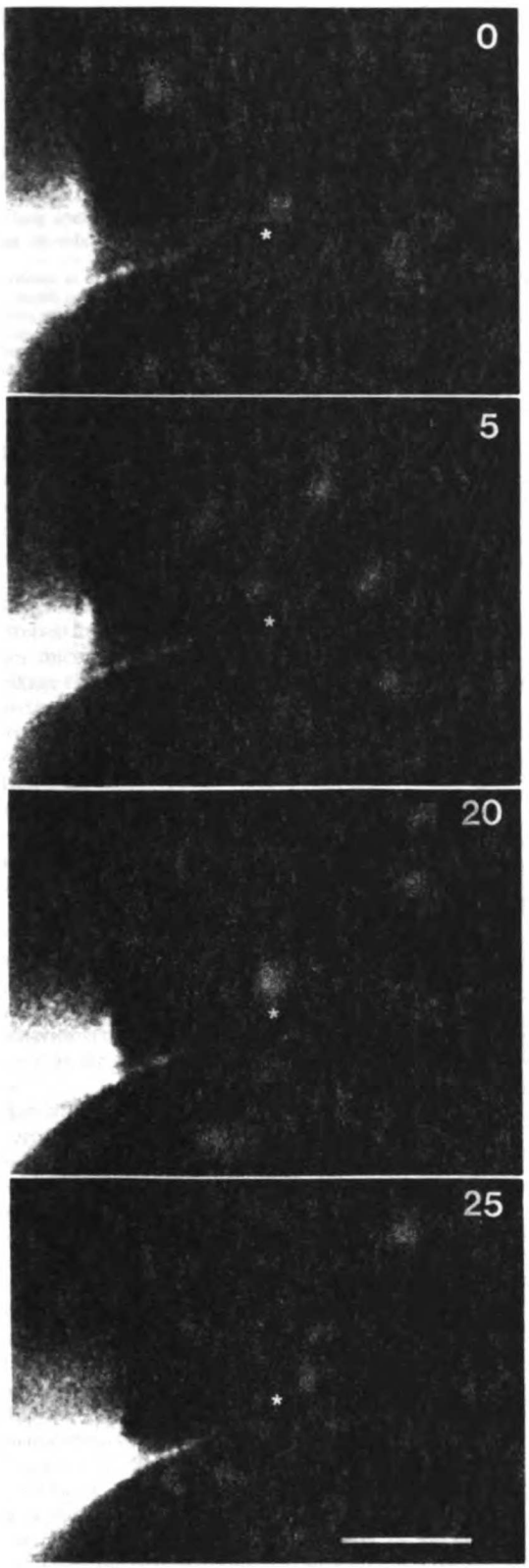


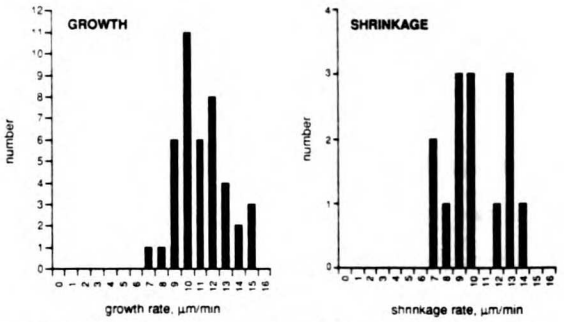


*Figure 5.* Histogram of growth and shrinkage rates. The movements of microtubule tips were measured (microtubules that simultaneously underwent lateral translocation were not included). Each measurement represents the measurement of a single tip between two frames. Measurements on the same microtubule at different times were considered independent measurements, as these rates varied considerably. Mean growth rate and SD, 10.6 ± 1.91 μm/min. Mean shrinkage rate, 9.7 ± 2.28 μm/min.

growing transition), and the catastrophe rate (growing to shrinking transition). To measure these assembly rates in growth cones, we acquired images of microtubules every 5–10 s in six cells. In general, we observed that isolated microtubules in peripheral areas had clear periods of sustained growth followed by sustained shrinkage (Fig. 4). For microtubules that showed little lateral movement, it was possible to measure with precision the change in the position of the microtubule end, as a means of measuring growth and shrinkage. In this way, we could measure the dynamics of 20–40% of the microtubules in these growth cones; the majority resided in densely populated regions of the growth cone where lateral motions and the high density of microtubules prevented accurate measurements. The mean growth rate for 42 measurements in the six neurons (Fig. 5) was 10.6 (SD 1.9) μm/min, while the mean shrinkage rate was 9.7 (SD 2.28) μm/min ($n$ = 14) (Fig. 5). Some microtubules did not appear to grow or shrink between two frames, as their tips remained stationary. We estimate that 15% of the microtubules whose tips we could follow were in this category.

The catastrophe rate was calculated as described previously (Walker et al., 1988; Belmont et al., 1990). We followed microtubules that could be discerned to be growing, and summed the total amount of time spent in growth for all of the microtubules. (This included microtubules that were growing and were subsequently lost from view.) This total time was then divided by the total number of transitions to shrinkage observed for these microtubules. Of 33 growing microtubules observed (1,560 s of growth), 18 were observed to shrink while 15 were lost. From these observations, we calculated a transition frequency of 0.72 $min^{-1}$. We could not measure rescue frequencies reliably, primarily because the region in which isolated microtubules are observable in

*Figure 4.* Growth and transition to shrinkage of a microtubule at a growth cone periphery. Microtubule extends 1.0 μm between 0 and 5 s, and recedes 1.9 μm between 5 and 20 s. The asterisk marks a constant position in the field. Bar, 5 μm.

*Table I. Comparison of Microtubule Dynamics in Growth Cones with Those in Non-neuronal Cells and in Cell Extracts*

| Cell type | Growth | Shrinkage | Catastrophe | Rescue |
|---|---|---|---|---|
| | μm/min (± SD) | μm/min (± SD) | $s^{-1}$ | $s^{-1}$ |
| Xenopus neurons | 10.5 ± 1.9 | 9.7 ± 2.2 | 0.012* | – |
| Xenopus extract (interphase)§ | 9.3 ± 4 | 12.8 ± 6.0 | 0.01-0.031* | 0.009-0.016* |
| BSC-1 fibroblasts‖ | 5.0 ± 2.4 | 7.4 ± 2.7 | – | – |
| Newt lung epithelia¶ | 7.2 ± 1.9 | 17.3 ± 4.1 | 0.014‡ | 0.044‡ |
| Human fibroblasts** | 3.5 ± 3.2 | 4.3 ± 5.7 | – | – |

* Determined as described in Walker et al. (1988).
‡ Determined as described in Cassimeris et al. (1988).
§ Belmont et al. (1990).
‖ Schulze and Kirschner (1988).
¶ Cassimeris et al. (1988).
** Sammak and Borisy (1988).

the lamella was very limited (≤12 μm), so shrinking microtubules were lost in the dense population of microtubules in the central region.

Such measurements do not distinguish growth or shrinkage at the distal end from the forward or backward translocation of stable polymer. We believe that at least some of the measurements represent actual polymerization and depolymerization for several reasons, none of which completely excludes microtubule translocation. First, both growth and shrinkage rates resemble rates found in other systems (Table I), and are especially close to rates found in *Xenopus* egg extracts. Second, 55% of the microtubules could be observed to transit from growing to shrinking. It seems less likely that translocating microtubules would change direction abruptly. Third, in some cases, we observed the change in length between the tip of a microtubule and some static feature, such as a bend. An example of such an event is shown in Fig. 7. The larger arrows follow the tips of two microtubules, while the smaller arrows mark the position of bends in these microtubules. In the upper microtubule, the distance between the microtubule tip and the bend increased between 5 and 35 s, while for the lower microtubule, the distance decreased between 10 and 25 s. Again, we believe that this type of behavior is more likely to be due to growth and shrinkage, rather than the translocation of a polymer through a sinuous track.

***Microtubule Translocation.*** New microtubule polymer in the growth cone also appeared to be generated by mechanisms other than polymerization. We have consistently observed what we interpret to be bulk sliding of microtubules from the axon into the growth cone. For single microtubules, this is an impression that would be difficult to prove without some marking on the microtubule that could distinguish translocation from polymerization off the free distal end. Bulk sliding was most clear when we observed the simultaneous movement of groups of microtubules. Loops consisting of several microtubules often maintained a stable configuration, and yet were translocated forward as a group within the growth cone. Loops in different regions of the growth cone moved at the same time, and approximately at the same rate. Fig. 6 shows such a translocation event. Within the 30-s sequence, though the morphology and position of the growth cone did not change relative to the substrate, there was a forward translocation of microtubule loops which maintained a coherent structure into the growth cone. The upper and lower arrows point to stable morphological features on the loops of microtubules, while the smaller arrows mark a constant position in the field; loops on both sides of the growth cone moved at the same time. The upper loop translocated 2 μm in 20 s while the lower loop translocated 1.6 μm during this time.

### *The Generation of Splayed, Looped, and Bundled Microtubule Configurations in the Growth Cone*

The most striking property of microtubules in growth cones were the forward and lateral translocations as well as bending movements that resulted in rapid changes in the overall distribution of microtubules in the growth cone. We have attempted to understand the cause of these movements and how they generate large-scale changes in the microtubule distribution, and finally, how these changing microtubule configurations are related to growth cone behavior and axon elongation. We analyzed in detail the microtubule distributions in 12 neurons over times ranging from 4 to 30 min. Phase images were not usually acquired during these sequences, but the signal generated from the fluorescence of tubulin monomer was used to define the edges of the cell, as can be seen in Fig. 2.

***Microtubule Splaying.*** When the microtubules in the growth cone were in the splayed configuration, the growth and shrinkage of microtubule ends was most easily visualized. We often observed that single microtubules that grew relatively straight into the lamella became bent or moved laterally. This resulted in the formation of wavy microtubules that would eventually shrink back to the central region. As in other cell types, the individual microtubules appeared to behave independently. Fig. 7 shows an example of such behavior. A single microtubule that extended rather straight into the periphery, as indicated by the lower arrow at 0 s, began to bend at 5 s (Fig. 7, *lower small arrow*). The bending continued through 20 s and the length from the microtubule tip to the bend shortened until the tip was barely visible at 35 s. The microtubule indicated by the upper arrow at 0 s also bent during the sequence (Fig. 7, *upper small arrow*), but its end lengthened with respect to the bend.

***Looping.*** During the generation of the looped configuration, we observed the formation of acute bends in many microtubules. Fig. 8 follows the formation of a looped structure. At 0 s, a single microtubule (Fig. 8, redrawn in the *right*

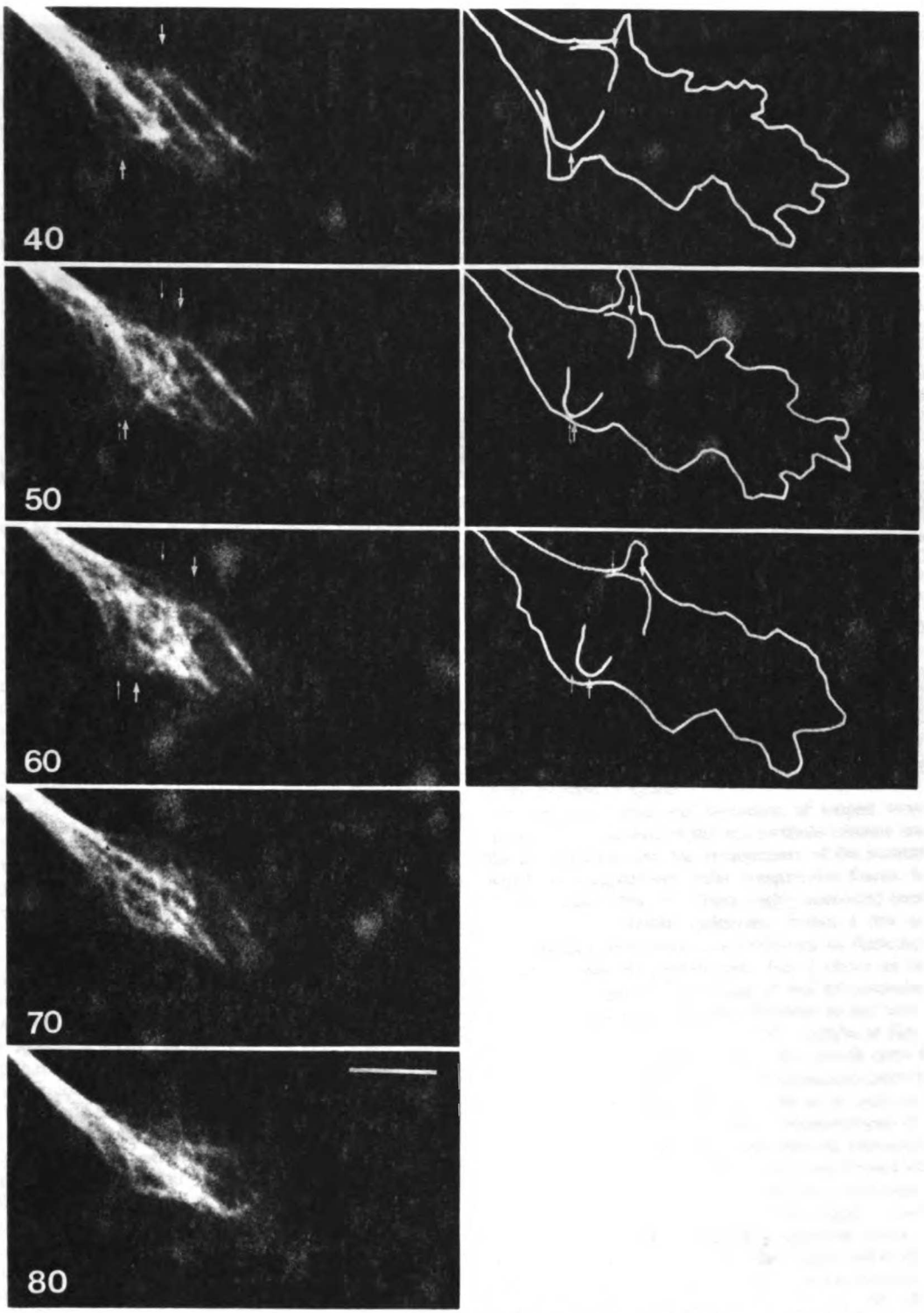


*Figure 6.* Forward translocation of microtubule loops in the growth cone. Larger arrows follow similar points on the microtubules (based on morphological criteria), while small arrows mark constant positions on the field (the positions of the arrows at 40 s). The upper loop moved forward 2.0 $\mu$m between 40 and 60 s, and the lower loop moved 1.6 $\mu$m within the growth cone, while the morphology and position of the growth cone is constant. The microtubules followed by the arrows and the outline of the growth cone have been redrawn on the right panel for clarity. Bar, 5 $\mu$m.

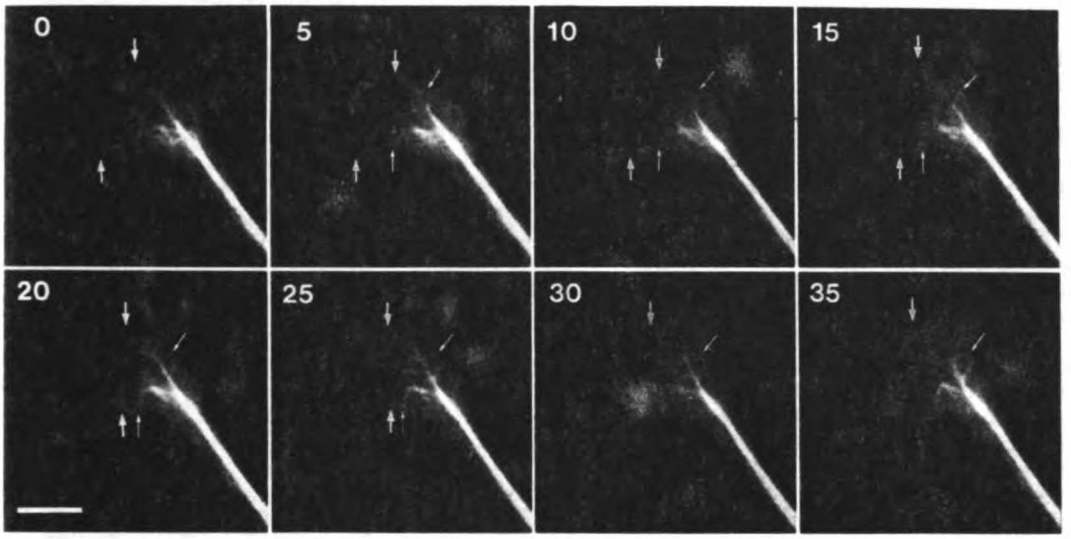


*Figure 7.* Bending of single microtubules in the peripheral regions of the growth cone. At time zero, two microtubules in the periphery (indicated by *larger arrows*) are relatively straight. Both microtubules form bends (marked by *smaller arrows*) at 5 through 15 s. For the upper microtubule, the length between the tip and the bend increases between 15 to 35 s. For the lower microtubule, the distance between the microtubule tip and the bend decreases during the same time. Bar, 5 μm.

*panel*) was quite contorted, making three bends, but most of the other microtubules were slightly spread, and pointed in the general direction of the axon. At 10 through 30 s, the bending of the redrawn microtubule became more acute, while the other microtubules began to bow out. By 40 and 50 s, multiple microtubules formed acute bends so that by 50 s, the distal ends of the microtubules looped back towards the axon rather than pointing out to the growth cone periphery.

Several forces could potentially have caused such microtubule bending and looping. First, the ends of the microtubules could have been pushed backward toward the axon; as a consequence, the sides of the microtubule would have bowed out. Second, the microtubules could have polymerized at their distal ends while in contact with a fixed barrier, resulting in increased microtubule length and in this constrained situation, buckling of the microtubule. Third, the microtubules could have been translocated forward into the growth cone against a fixed barrier. This forward translocation would have resulted in a compressive force on the microtubules that could have caused bending and buckling.

When single microtubules in the growth cone periphery became bent, as seen in Fig. 7, it was difficult to distinguish between these types of forces without a fiduciary mark on the microtubule. However, during the formation of looped configurations, the increase in the contour length of microtubules in the growth cone along with the forward movement of looped structures suggested that the formation of loops in the central region occurred primarily through the forward translocation and compression of microtubules. This can clearly be seen in the single microtubule that has been redrawn by in the right panel of Fig. 8. At 0 and 10 s, the contour length of the microtubule between two points that were fixed with respect to the substratum (Fig. 8, indicated by the *arrowhead* and the *arrow, right panel*) increased from 13.5 to 15.1 μm, while the tip of the microtubule moved forward ~0.7 μm. This could be due either to growth at the tips of the microtubule in the presence of a barrier and consequent buckling or to the translocation of polymer against a barrier and subsequent buckling. However, between 20 and 50 s the loop marked by the asterisk moved forward with respect to the substratum by 3.6 μm. It is unlikely that distal polymerization would cause the loop close to the neck to move forward in space.

***Bundling.*** During the formation of looped structures, there was an increase in the microtubule contour length in the growth cone, and the arrangement of the microtubules which were apparently under compressive forces, became more compact (Fig. 8). These highly contorted configurations were not stable endpoints; within a few minutes microtubules underwent a restructuring to form axon-like bundles within the growth cone. Fig. 9 shows an example where the looped arrangements of the microtubules rearranged into an axonal bundle. Previous to the time points shown, over a period from 0 to 175 s (relative to Fig. 9), we observed that the microtubules in the growth cone formed tight loops so that the distal ends of the microtubules pointed perpendicularly to the direction of the axon, with no microtubules pointing into the periphery. Measurements of microtubule contour length and of the forward translocation of loops, again, indicated that these loops had formed via buckling in response to forward translocation of polymer. By the first time point shown in Fig. 9 (280 s), these microtubules had begun to unfold so that they appeared partly splayed and partly looped. After 280 s, they continued to gradually straighten, so that at 315 and 350 s, microtubule ends entered the peripheral regions of the grow cone. By 385–455 s, the radius of curvature of the microtubules had decreased considerably, until at 490 and 525 s the microtubules, particularly in the proximal portion of the growth cone, coalesced to form the newest part of the axon.

During the formation of bundles in the growth cone, in ad-

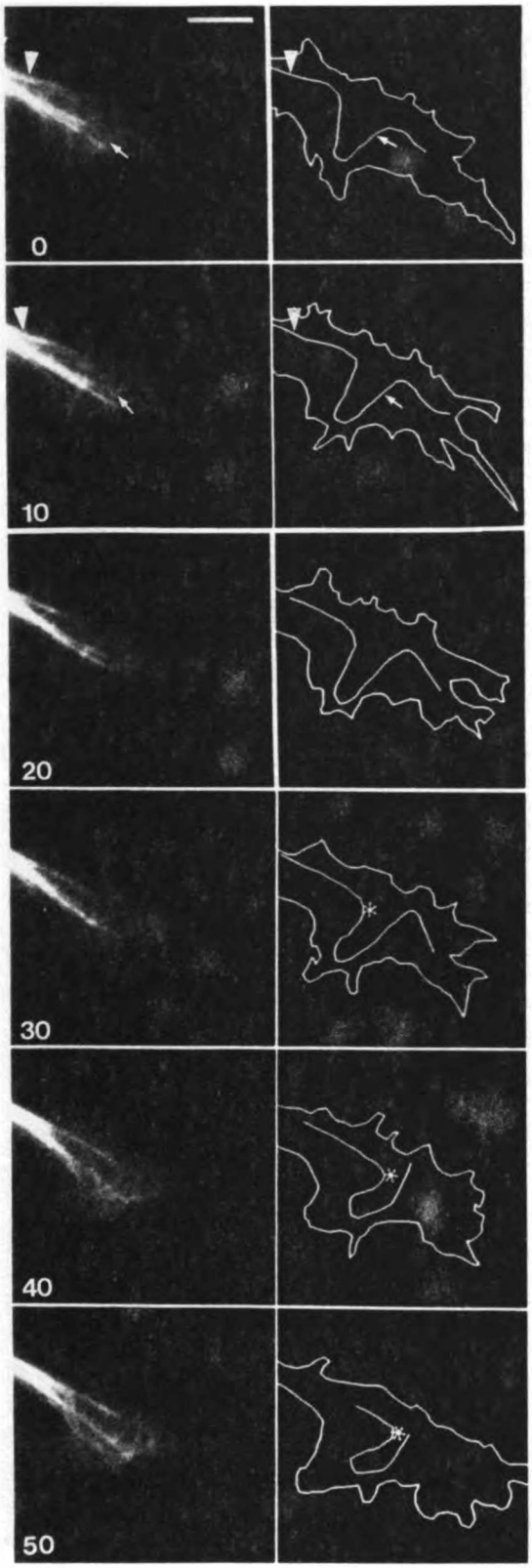


dition to the unfolding of compressed, looped microtubules, we also observed the extension of a microtubule bundle that had already formed in the growth cone. It is not known whether these microtubules grew by polymerization, or whether they emerged by sliding and translocation. In Fig. 10, three microtubules were seen to extend from the distal end of a bundle. At 0 s, three microtubule tips that emanated from the main microtubule bundle were barely discernable. From 15 to 45 s, these tips emerged from the bundle at rates of 8.9 μm/min (Fig. 10, *left microtubule*), 12.1 μm/min (Fig. 10, *center microtubule*), and 10.0 μm/min (Fig. 10, *right microtubule*). In contrast to the microtubules in Fig. 7, these microtubules pointed in the same direction as the microtubule bundle, and remained straight.

The conversion of bent (splayed or looped) microtubules and small microtubule bundles into larger, straight bundles was observed in five out of eight neurons. One of the five underwent three rounds of bending and straightening in 50 min with intervals of 330 and 297 s between bundling events. Of the remaining three growth cones, one (depicted in Fig. 7) had splayed microtubules that shrank back to the central bundle of microtubules. This was followed by the emergence of several microtubules from the bundle and subsequent elongation. One neuron maintained a looped microtubule array throughout the 50-min period of observation, while another displayed a splayed distribution throughout a rather short period of observation (4 min). The four neurons that branched or turned were not included in these classifications, though they too displayed episodes of bundling and splaying.

### *Microtubule Bundling and Growth Cone Advance*

Ultimately, the generation of new axon requires both the collapse and quiescence of the actin rich cortex and the bundling of microtubules. Thus, the finding that bundling occurred in the growth cone and often accompanied growth cone advance may simply reflect a passive response of the microtubules to a constriction of the plasma membrane generated by the actin cortex. If this were the case, we would expect that bundling would accompany collapse of the membrane. However, in several cases, we observed that microtubules that were looped or splayed, clearly formed bundles within the growth cone before the collapse of the growth cone membrane, and subsequent formation of new axon. Fig. 11 shows a growth cone that exhibited bundling before the collapse of the growth cone membrane. (Although images were acquired at 10-s intervals, here, we have only included images at 30-s intervals.) Bent microtubules accumulated in the first 60 s of the sequence mainly by translocation of loops into the growth cone. Between 60 and 90 s, the width of the

*Figure 8.* Forward translocation and looping of a single microtubule in the growth cone. The growth cone and a selected microtubule are redrawn in the right panel. The outline of the neurons looks larger than the diffuse fluorescence because it was not possible to reproduce all of the gray scales in the original image. Between 0 and 10 s, the contour length of the microtubule between the points marked by the arrowhead and the arrow (fixed with respect to the field) increases from 13.5 to 15.1 μm. The tip of the same microtubule moved forward 0.7 μm. Between 20 and 50 s, the microtubule loop marked by the asterisk moves forward 3.6 μm. Bar, 5 μm.

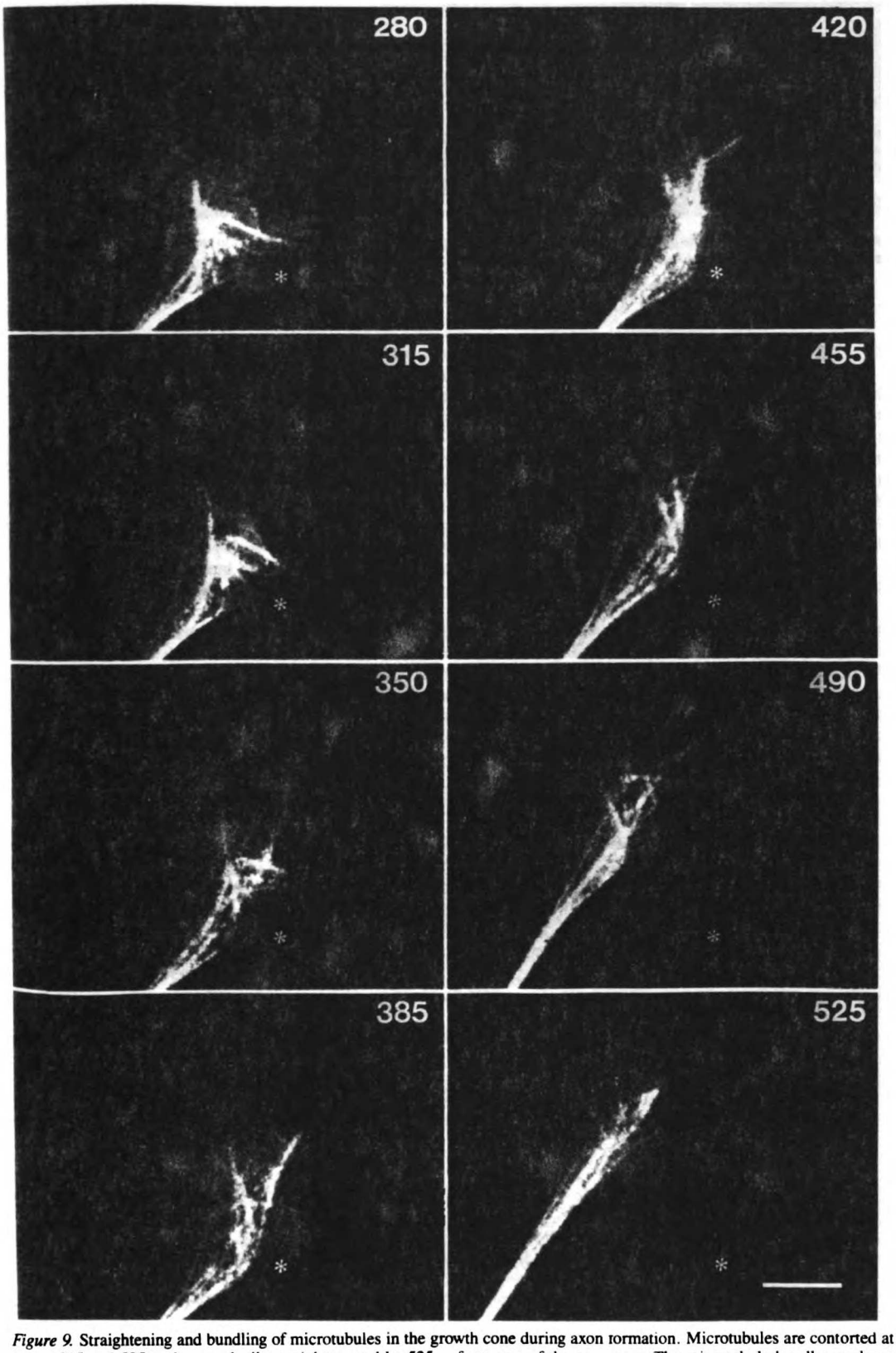


*Figure 9.* Straightening and bundling of microtubules in the growth cone during axon formation. Microtubules are contorted at 280 s. Between 315 and 525 s, they gradually straighten, and by 525 s, form part of the new axon. The microtubule bundles coalesce before the lamellar region on the right collapses between 455 and 525 s. Asterisk marks a constant position on the field. Bar, 5 $\mu$m.

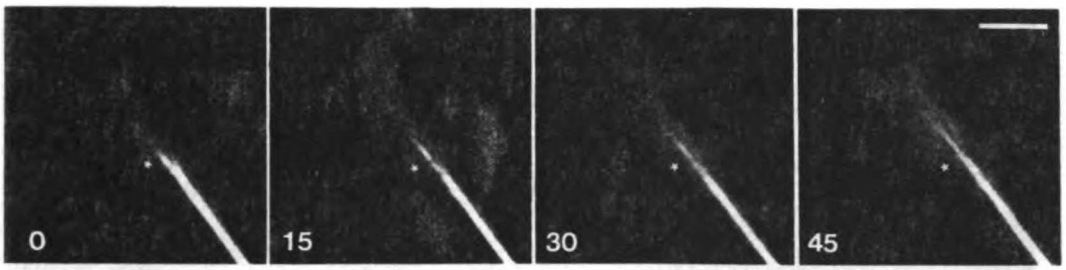


*Figure 10.* The extension of a microtubule bundle in the growth cone. Three microtubules simultaneously emerge from the end of the main axon bundle. These microtubules do not bend or deviate considerably from the main course of the bundle. Asterisk marks a constant position in the field. Bar, 5 μm.

growth cone did not change significantly but the microtubule array in the proximal region of the growth cone began to bundle. By 120 s, the width of the microtubule array in the proximal region of the growth cone closely resembled that in the axon, and by 180 s, the microtubules in the distal region of the growth cone also became restricted while a large lamellipodia extended forward. At 210 s, the proximal membrane collapsed around the microtubule bundle and a lamellipodia extended forward while the microtubules in the growth cone began to spread and loop. A second round of microtubule looping in the growth cone occurred between 210 and 300 s.

To assay bundling and membrane distribution quantitatively, we measured the diameter of the growth cone across a line that was fixed with respect to the field (the endpoints of the line are indicated by *arrows* in Fig. 11). This was correlated with the lateral distribution of microtubules along this line as measured by the radius of gyration of the microtubules on the line. The radius of gyration is a weighted measure of the radial distribution of the microtubules from the center of mass (see Materials and Methods for precise calculation). A plot of these parameters for the growth cone in Fig. 11 is shown in Fig. 12. Both the width of the growth cone and the radius of gyration of the microtubules were large in the early sections and both decreased as the growth cone advanced, and transformed into axon. The start of microtubule bundling (Fig. 12, *arrow A*) preceded by 20 s the beginning of the decrease in the width of the growth cone cortex (Fig. 12, *arrow B*). When we examined nine periods of rapid growth during which microtubules became bundled to form new axon, the initiation of microtubule bundling preceded growth cone collapse in four (for example, Fig. 11 at 180 s). In four, bundling and membrane collapse occurred so close together that they could not be distinguished. In one, the bundling had already occurred before the beginning of the sequence.

### *Microtubule Placement during Growth Cone Turning*

During our study of growing axons, we observed a few neurons that spontaneously made sharp turns, and one that branched. Though it is not our purpose to study turning in detail here, it was of particular interest to learn whether microtubules were oriented within the growth cone during turning, and, if so, whether similar mechanisms of microtubule translocation and bundling were used in the orientation of microtubules during turning. Of four growth cones that turned or branched, one had clearly begun to turn before observation began, but in the other three cases the morphology of the growth cones initially looked quite symmetrical and there was no indication to us that the growth cone would turn. When we examined the microtubules in these three growth cones, we found that several microtubules, but not all, were already oriented in the direction of future growth. For example, in Fig. 13, at 0 s, the growth cone had three large lamellipodial expansions, to the right, toward the center (Fig. 13, *arrowheads*), and to the left; the future direction of its course as judged by its cortical morphology was ambiguous. However, there was a slight asymmetry in the microtubule distribution, several microtubules curved gently to the right with a single microtubule protruding slightly into the right lamella, none entered the center, and only a few entered the left lamella. Because these microtubules were oriented before observation began, we do not know how they became oriented. Microtubules that subsequently entered the growth cone from the axon bundle were routed primarily to the right when they contacted the upper cortex. The small arrow at 10 through 45 s indicates microtubules as they initially extended straight into the growth cone. When they contacted the upper membrane they bent to the right. This bending resembled the bending observed during formation of the microtubule loops during forward growth. Whereas in looping, the microtubules bent back toward the center of the growth cone (as seen in Fig. 8) and crossed each other; during branching, the microtubules bent outward, and during turning, most microtubules bent in one direction. As in forward growth, we then observed the formation of microtubule bundles within the growth cone in the direction of growth. In Fig. 13, the pro-

*Figure 11.* Sequence of microtubule bending and bundling during outgrowth. In the first three frames, microtubules emerging from the neck bow out and fill most of the area of the growth cone. Many bent microtubules are observed in the central region. At 90 to 180 s, microtubules become extended and coalesce into a bundle within the growth cone. The formation of microtubule bundles precedes the collapse of membrane at the neck. Frames 210 to 300 show the recurrence of microtubule bending. The growth cone moves 15 μm in 300 s. The arrows indicate the endpoints of the line on which pixel intensity was measured for the radius of gyration measurement. Bar, 5 μm.

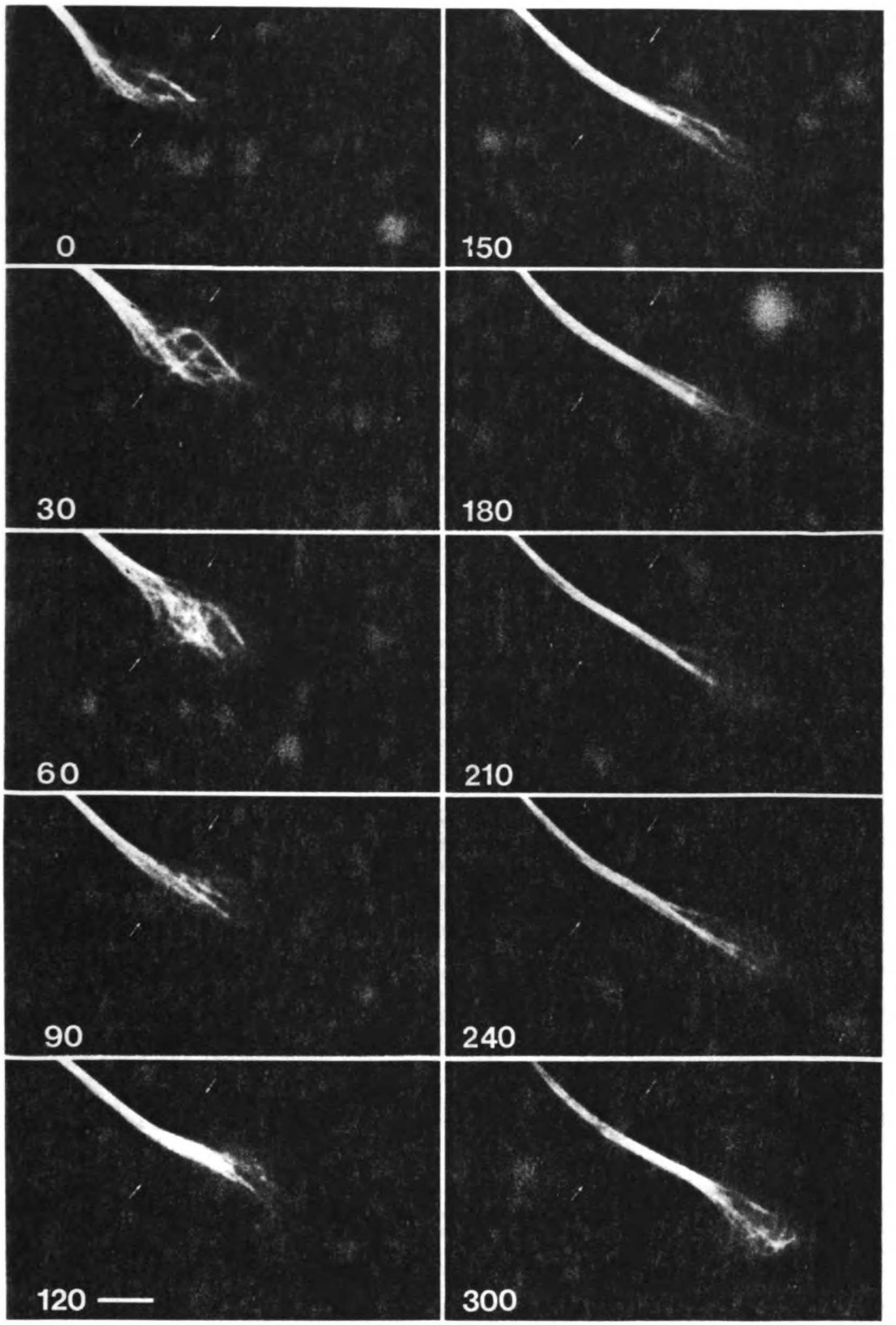
0
150
30
180
60
210
90
240
120
300

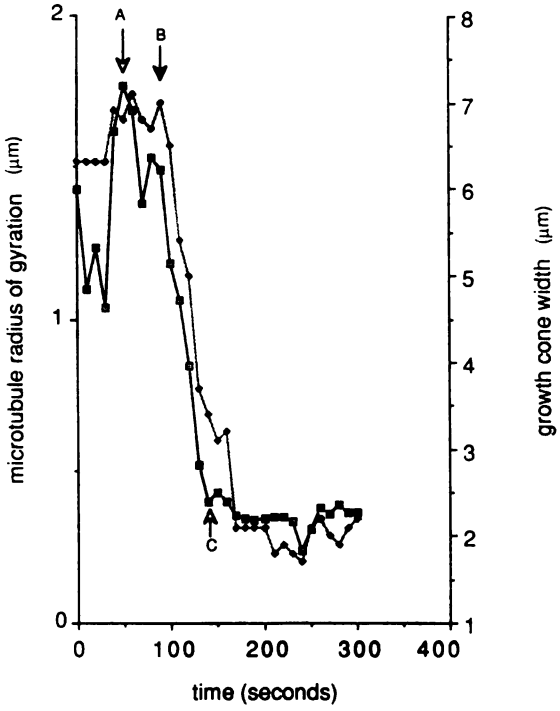


*Figure 12.* Comparison of the microtubule radius of gyration and the growth cone width along a constant line perpendicular to the axon for the growth cone in Fig. 11. (*open squares*) Microtubule radius of gyration. (*closed circles*) Growth cone width. The microtubules begin to bundle (as marked by *arrow A*) 20 s before the growth cone begins to collapse (*arrow B*). At 120 s (*arrow C*), the microtubules are bundled, while the growth cone has not completely collapsed.

gressive bundling of microtubules occurred between 55 and 185 s, well before the growth cone began to collapse to form the axon. The initiation of bundle formation before the collapse of the growth cone was observed in two neurons, while in the other two cases, the events occurred too close together to distinguish.

In two of the turning growth cones, microtubules that were not oriented in the future direction of growth were present and were seen to persist, even after the future direction of growth was quite clear. In Fig. 13, several microtubules occupied the left lamella from 0 s, and although the orientation of the axon bundle was clear by 55 s, a single microtubule persisted until 155 s. This microtubule, rather than shrinking back into the bundle, was zippered into the forming bundle. The arrows at 115 and 155 s follow the end of the microtubule, while the arrowheads (115, 155, and 185 s) follow the proximal region as it is dragged to the right and joins the bundle, forming an acute bend in the region where the microtubule joins the bundle (Fig. 13, *arrowheads*, 185 s). This leaves the left lamella unoccupied by any microtubules at 185 s.

## Discussion

The ability to observe microtubules in living cells offers several advantages over the use of fixed specimens. First, it avoids the potential artifacts due to fixation. Microtubules are difficult objects to preserve and recent knowledge of their dynamics provides an explanation for the early difficulties. (If a fixation process in a cell takes 10 s, a microtubule in this time can lose 50,000 subunits and shrink by 3 μm.) More importantly, by observing living cells we can describe microtubules as they grow and move, and in this way describe the process of generating new structures within the cell. These dynamic changes in microtubules can then be compared to other dynamic behaviors of the cell. In this report, we have examined the dynamic changes of microtubules within growth cones and correlated these changes with events involved in axon extension.

### *The Location of Microtubules in the Growth Cone*

Although microtubules were consistently found to extend deep into the periphery of the growth cone, the overall arrangement of microtubules was variable. We have grouped these distributions into three general categories: splayed, looped, and bundled. Although there were many times where the distribution exactly fit in a single category, intermediate distributions existed in which characteristics of two types were often seen. Thus, these categories are merely archetypes and do not reflect the existence of discrete states.

Similar variations in distribution have been described previously. The splayed configuration, in which microtubules extend and diverge into the periphery has been described by electron microscopy for chick retinal neurons (Cheng and Reese, 1985), and in rat superior cervical ganglion neurons using EM and immunofluorescence (Bridgman and Dailey, 1989). The looped distribution, in which microtubules loop backwards and form sharp bends, as well as the splayed distribution, have been seen by both Tsui et al. (1984) and Lankford and Klein (1990) in chick retinal cells. These two distributions have now been seen in living grasshopper pioneer neurons at the light level and in fixed specimens using EM (Sabry et al., 1991). Because previous analyses were limited to fixed cells, it was not clear whether these distributions were stable features of particular types of neurons or whether they were temporary features related to the activity of the nerve cell.

An important conclusion from our work is that the

*Figure 13.* Sequence of microtubule collapse and bundling as a neuron begins to turn. At zero seconds, the microtubules are already oriented to the left and to the right, even though a large lamella points along the central growth cone axis (*arrowheads*). Single microtubules, indicated by arrows, emerge from the central region of the growth cone (10, 20, 25). These microtubules extend into the periphery of the growth cone and bend to the right as the edge of the cell also collapses in this region. Subsequently (55–105), the dispersed microtubules become bundled toward the right. A single microtubule remaining in the left side of the growth cone retracts, leaving the left lamella without microtubules. At 115 through 155 s, the arrowheads follow the proximal portion of the single microtubule that remains in the left lamella, but is then zippered into the main bundle.

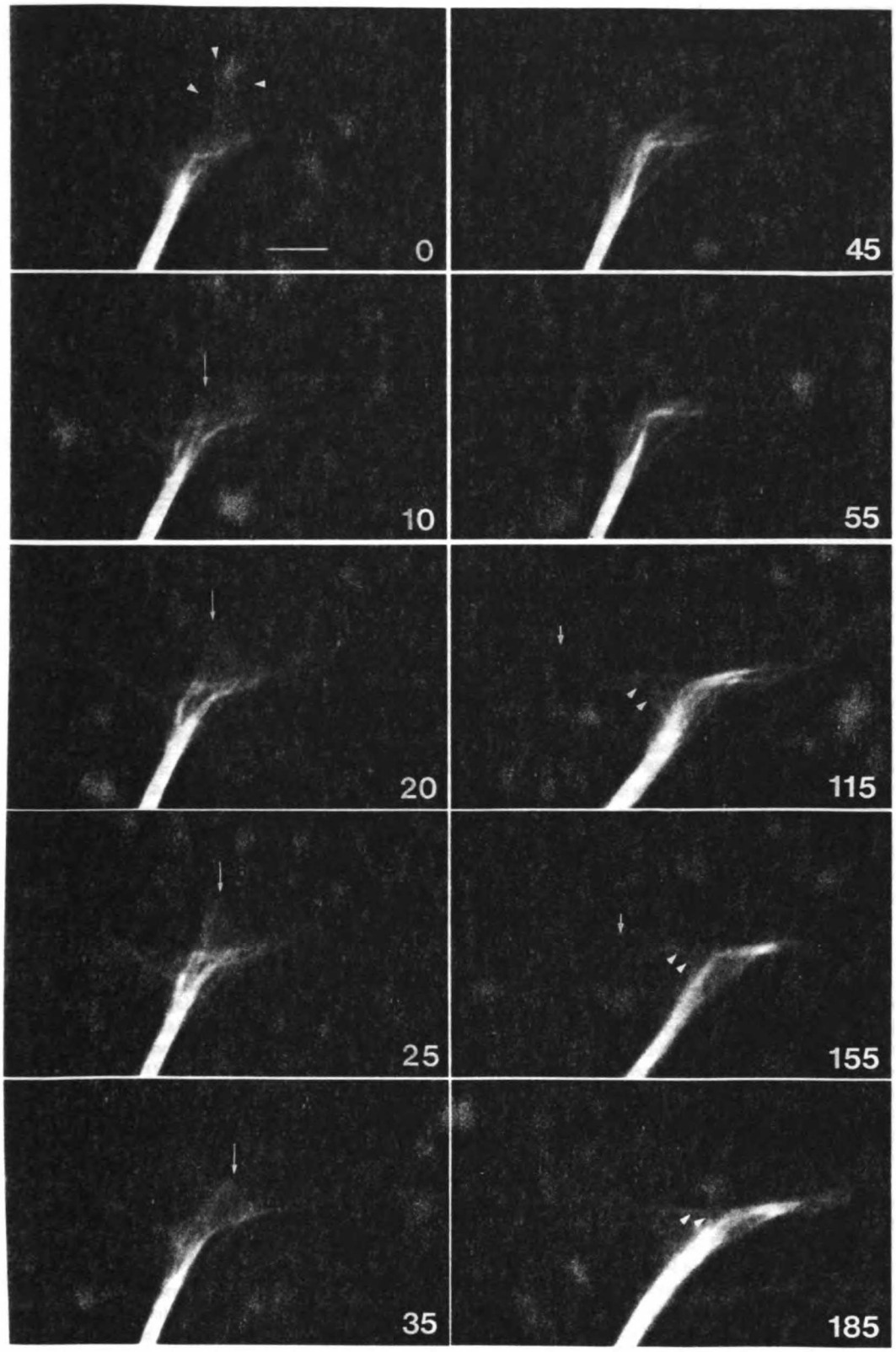
0
45
10
55
20
115
25
155
35
185

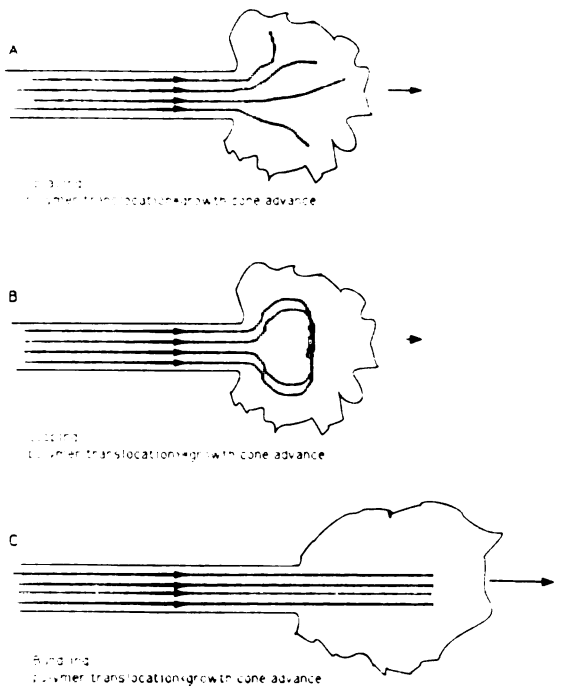


*Figure 14.* A schematized representation of the relationship between microtubule translocation and growth cone advance. The arrows superimposed on the microtubules represent the rate of translocation of the microtubules, while the arrows at the leading edges of the growth cones represent the rate of advance of the growth cone. For each growth cone, the relative rates of the microtubules and the growth cone are related to the configuration of the microtubules inside of the growth cone.

microtubules in a single neuron can alternate rapidly between these configurations during growth cone extension. We find that any of the three distributions—splayed, looped, or bundled—generally persists for several minutes. These configurations are generated by a variety of microtubule behaviors. A splayed distribution can be generated either by the growth and shrinkage of polymer in random directions (Fig. 7), by the dissociation of a bundle (Fig. 11, 210 s), or by the straightening of microtubule loops (Fig. 9, 350–455 s). In this paper we used the word splayed to refer to a distribution of spread microtubules that appears to be dominated by growth and shrinkage. Looped microtubules appear to be generated by the forward translocation of polymer into the growth cone (Fig. 6). Microtubule bundles in the growth cone can form either by the coalescence of splayed or looped microtubules (Figs. 9 and 11), or by the extension of microtubules from a preexisting bundle (Fig. 10). The origins of such distributions are difficult to infer from fixed specimens, but instead require knowledge of the history of the microtubules in the growth cone.

### *The Generation of Microtubule Polymer in the Growth Cone*

***The Role of Microtubule Dynamics.*** In theory, the properties of microtubules in extending neurites could be very different from their properties in other cells. In fibroblast cells, for example, there is rapid turnover of microtubule polymer by dynamic instability, but the overall quantity of microtubules is at or near steady state. By contrast, during axon outgrowth the cell volume increases as the growth cone moves away from the cell body, and total polymer must increase. For example, a *Xenopus* neuron can generate 150 μm of new axon per hour, requiring the assembly of perhaps 5 pg of tubulin—more tubulin than is present in a typical mammalian fibroblast cell. It is not known where this net assembly occurs or how the different requirements of the neuron affect the dynamics of microtubule polymerization and depolymerization or the transport of tubulin.

In principle, by measuring the four dynamic parameters (growth, shrinkage, catastrophe, and rescue rates) of a significant number of microtubules in the growth cone, we could assess whether net growth of microtubules occurred via growth of microtubules in the growth cone. Such an assessment has been limited by our ability to measure only a small proportion of microtubules and our inability to determine rescue frequency in these growth cones because of high microtubule density in the central region, and because of lateral movements.

The three dynamic parameters—growth rate, shrinkage rate, and catastrophe rate—that we could measure were similar to those found in other systems (Table I) where a mass balance of microtubules is maintained, and where there is no net growth over time. Though our measurements encompass a small proportion of microtubules, this suggests that if net growth of microtubules in the growth cone were occurring, it probably occurs through the modulation of rescue rates, a parameter which we were unable to measure directly.

An indirect measurement of rescue rates based on the number of growing microtubules, the number of shrinking microtubules, and the catastrophe frequency also indicates that microtubules in the growth cone may have high rescue frequencies. We can determine whether there is net growth (increase in polymer mass) of a microtubule array by examining the average behavior of the microtubules of the array although such an analysis will not tell us anything about the distribution or the fluctuations of the array. On average, microtubules in the growth cone grow for 1.39 min to a length of 14.6 μm (10.53 μm/min average growth rate, 0.72 $min^{-1}$ catastrophe frequency) before they transit to a shrinking phase and depolymerize at a rate of 9.8 μm/min. If mass balance were maintained, and these microtubules (or the average microtubule) showed no net growth, the rescue frequency would have to be 0.67 $min^{-1}$. If rescue were to occur on average in less than 14.6 μm, there would be net growth or if in more than 14.6 μm there would be net depolymerization.

In the growth cone, we have not been able to directly measure rescue frequencies. However, we can calculate the rescue frequency from the number of growing microtubules, the number of shrinking microtubules, and the catastrophe frequency. At steady state the number of microtubules growing at any time, $n_g$, and the number shrinking at any time, $n_s$, is related to the first order growing to shrinking transition, $k_c$ (for catastrophe) and $k_r$ (for rescue) by the equation: $n_g/n_s = k_r/k_c$ (Mitchison and Kirschner, 1987). We have found that the ratio of growing to shrinking microtubules in the growth cone is 2.4 (determined in 105 frames, for two neurons) resulting in a calculated $k_r$ of 1.74 $min^{-1}$.

From this rescue frequency we can say that, on average,

microtubules in the growth cone grow for 1.39 min to a length of 14.6 μm before they transit to a shrinking phase and depolymerize at a rate of 9.8 μm/min and shrink 5.6 μm before being rescued. This would produce net growth or 9 μm for a 2-min excursion of growth and shrinkage. In terms of the dimensions of an average growth cone, such a microtubule would grow from a region close to the neck of the growth cone out to the periphery, and shrink back into the densely populated central region.

The accuracy of the calculated rescue frequency and subsequent calculations depend on our ability either to measure all growing and shrinking microtubules or to estimate accurately the fraction of microtubules that are growing or shrinking and to determine that such events are actually occurring through polymerization and depolymerization, rather than through polymer translocation. These estimates are therefore very crude. Furthermore, because the calculation assumes steady-state conditions, it does not account for new nucleation of microtubules. In the growth cone, these factors are largely unknown, and for these reasons, we cannot quantitatively determine how much growth actually occurs through polymerization in the growth cone.

These calculations are not accurate enough for us to determine the contribution of polymerization to the net extension of the microtubule array, but they do provide a tool for thinking about possible mechanisms of polymer growth. Given the high rescue rates expected from the calculations and the rarity of rescue observed in the periphery, we might expect that rescue is frequent in microtubule bundles, where we could not resolve single microtubules. The progressive advance of microtubule bundling during axon formation, and the formation of microtubule bundles in the growth cone as it advances could generate a forward wave of the stabilizing (rescuing) activity. In this way, the bundling of microtubules would play a role not only in restricting the microtubules to an axonal configuration, but also in driving net polymer growth.

***Translocation of Polymer.*** Our observations suggest that new polymer in the growth cone is also generated by assembly within the cell body or the axon and subsequent translocation into the growth cone. Although we could not find or make fiduciary marks directly on the growth cone microtubules, we have seen clear, indirect indications that such a process occurs. In many circumstances we observed the forward movement of coherent arrays of microtubules within the growth cone. Microtubule polymerization could not have caused simultaneous movements of microtubule loops that were in different regions of the growth cone. The forces acting on microtubules that cause them to loop and bend are also best explained by the forward translocation of microtubules against a barrier. Although increasing contour length and bending could be explained by growth against a barrier, the combination of backward movement of microtubule ends, and the forward movement of the forming loops make this possibility unlikely, in our view.

The coordinate nature of the polymer translocation that we observe resembles the translocation of polymer observed by Reinsch et al. (1991) using photoactivation in the axons of *Xenopus* neurons. We measured rates of translocation as high as 10 μm/min over short intervals of <1 min. This polymer translocation rate in the growth cone is faster than the overall rate of 1 μm/min found in the axon (Reinsch et al., 1991). However, it should be noted that the neurons used by Reinsch et al. (1991), most of which were dissociated from the neural tube, had about half the growth rates than the explanted neurons used here. In addition, they found that instantaneous rates were quite variable and often high especially near the growth cone, while those averaged over 30 min were slower. We only measured translocation when it was rapid and significantly exceeded the rate of growth cone advance and made no effort to calculate time-averaged translocation rates. For this reason, we cannot quantitatively estimate the contribution of translocation to the generation of new polymer.

### *The Coupling of Growth Cone Advance and Microtubule Extension*

During axon elongation, the growth cone moves forward and the membrane behind it collapses, becomes quiescent, and forms new axonal structure. Over time, the microtubules must elongate equal to the rate of growth cone movement. If microtubule growth and growth cone movement were tightly coupled, the density of microtubules in the growth cone would be constant. We observed, however, that the configuration of microtubules as well as the amount of microtubule polymer in the growth cone is not constant. Furthermore, the shape of the growth cone does not always reflect the microtubule array. Such observations indicate that the advance of the growth cone and the extension of the microtubule array are not strictly coordinated.

The generation of the various microtubule configurations appears, in some respects, to reflect the relationship between the rate of microtubule extension, and the rate of growth cone advance. Fig. 14 illustrates the three types of microtubule distributions that we observed and the predicted relationship between microtubule translocation, microtubule bundling, and growth cone advance. When microtubules in the growth cone are splayed (growth cone A), the amount of polymer in the growth cone appears to remain constant, and we do not see obvious signs of polymer translocation into the growth cone (see Fig. 7). Single microtubules appear to grow and shrink independently and fill the space of the growth cone. These observations suggest that during splaying, the rate of microtubule polymer translocation (*arrows* on microtubules) matches the rate of growth cone advance (*arrow* leading the growth cone), and that bundling is primarily restricted to the axon or the neck of the growth cone. It is also possible that translocation is slower than growth cone advance, and that additional polymer is generated by net growth of microtubules in the growth cone; unfortunately the detailed mass balance is impossible to extract from our data.

During looping (growth cone B), the amount of polymer in the growth cone increases and the microtubules appear to be under compression. We believe that the increase in polymer, and the formation of loops is best explained by the translocation of polymer into the growth cone without compensating depolymerization. Furthermore, after the loops have formed, they are translocated forward within the growth cone. Altogether, these observations suggest that during looping, the rate of polymer translocation exceeds the rate of growth cone advance, but that microtubule bundles are still restricted to the axon.

Microtubule bundling (growth cone C) can occur through the coalescence of splayed microtubules, by the extension of looped microtubules, or the extension of a preexisting bundle. Because the microtubules do not loop or form bends, they do not appear to be under high compressive forces. This is most clearly seen as looped microtubules unfold and extend during conversion to microtubule bundles. This suggests that the rate of microtubule polymer translocation is slower or the same as growth cone advance, and that this allows bundling to occur within the growth cone.

These models predict that the relative rates of polymer translocation and growth cone advance determine the microtubule configuration in the growth cone. Polymer translocation rates appear to be highly variable near the growth cone (Reinsch et al., 1991), and there appears to be only a loose coupling of polymer translocation and growth cone advance. The exact nature of the relationship between growth cone advance and polymer translocation remains to be determined.

### *Microtubule Bundling May Be the Critical Step in Converting the Growth Cone into New Axonal Structure*

We have seen on several occasions that the bundling of microtubules in the growth cone precedes the constriction of the membrane and consequent formation of new axon. Therefore, the formation of bundles cannot depend on physical squeezing by the cortex around the microtubules, although it is possible that microtubule bundling is caused by the constriction of an internal structure that is invisible to us. We cannot say whether microtubules actually cause the collapse of the cortex or whether both are caused by another event. The organization of microtubules may in fact feed back on the actin cortex, since microtubule depolymerizing drugs can stimulate growth cone-like activity along the axon (Bray, 1978). Bundling, therefore, may be the first morphological event related to axon formation.

### *Microtubule Placement May Be an Early Event in Growth Cone Turning*

Although in this study we have not focused on pathfinding in response to natural cues, we have examined some cases where neurons spontaneously turned. The microtubule polymer events in turning neurons were similar to those found in neurons that were growing straight. The difference was that with turning neurons, microtubule polymer was laid down in a new direction. In several examples we found that there were changes in the orientation of the microtubule array that signified the direction of turning before the growth cone showed obvious signs of asymmetry. While it is not surprising that the microtubules adopt an orientation consistent with the ultimate direction of the neuron, it is important that in several cases the microtubule reorganization preceded obvious changes in overall growth cone morphology. This does not prove that microtubules respond directly to extracellular cues for turning, since there may be a whole sequence of invisible events that precede the asymmetric microtubule organization. However, these other processes must have an early effect on microtubule polymer organization.

The sequence of events that we observed in these spontaneously turning neurons resembles those found in growth cones that were making turns in response to physiological turning cues. In an accompanying paper, Sabry et al. (1991) used similar methods of microinjection of fluorescently labeled tubulin to study the pathfinding process of pioneer neurons in the grasshopper leg. Although visualization in this system was more difficult due primarily to the unevenness of the natural epithelial substrate, the turning signals in this system were more physiological. In these neurons, an asymmetric distribution of microtubules was also generated very early in the response of these neurons to specific external turning cues, before any obvious asymmetry could be seen in the overall shape of the growth cone. It will be particularly interesting to study the processes of microtubule dynamics in the grasshopper neurons at the resolution we have employed here. Similarly, we would like to study the response of *Xenopus* neurons to external signals generated by the substrate or by chemotactic agents. Such studies could examine whether asymmetric microtubule bundling is a causal agent only during the spontaneous turning seen here, or whether these early microtubule redistributions are an obligate part of the normal turning response of neurons to external signals.

In the past it had been convenient to separate the process of axonal growth from the process of pathfinding. Axonal growth was defined as the laying down of new structures in the axon of which microtubules are the most prominent. Pathfinding was defined as an event in the growth cone that biased axonal growth in response to extracellular signals. The assumption that the microtubule cytoskeleton was restricted to the axon implied that its major role was to provide dimensional support. The assumption that the actin cytoskeleton, though not restricted to the growth cone, played its most active role there implied that actin was involved in shaping of the growth cone. For primary *Xenopus* neurons in culture this distinction is untenable. Microtubules are found both in the axon and deep in the growth cone. During axon elongation they assume a series of configurations in the growth cone indicating that the microtubule array does not merely elongate in response to growth cone movements generated by the actin cortex. Most importantly, it appears that microtubule bundling in the growth cone is the critical event in converting the typical organization of tubulin in the growth cone to the very different organization in the axon. Similarly, in turning, the early orientation and bundling of microtubules in the new direction of growth suggests that these events are important to directing axon growth. These observations, and the ability to observe microtubules with high time resolution in these living neurons has set the stage for a more precise understanding of the interaction between microtubules and other important elements that control axon elongation and pathfinding. We can now begin to determine how directly growth and turning cues act on microtubules. In addition, it will be interesting to define the interaction of microtubules with other components of the cytoskeleton, such as actin.

We would like to thank Tim Mitchison and David Drechsel for valuable advice and encouragement throughout this work. We are deeply grateful to Dr. Louis F. Reichardt for allowing us to use his microscope and Dr. John Sedat, Dr. David Agard, Jason Swedlow, Hans Chen, and Dr. Jon Minden for their generosity and patience in teaching us how to use their CCD acquisition and analysis systems. We wish to thank Douglas McVay for constructing modifications for the sealed chamber; the growth cone collective, James Sabry and Sigrid Reinsch, for helpful comments and discussion throughout; and Andrew Murray, Jeremy Minshull, Douglas Kellogg, and Michael Glotzer for critical readings of the manuscript.

These studies were supported by a grant from the National Institutes of General Medical Sciences to M. W. Kirschner.

Received for publication 17 May 1991 and in revised form 24 June 1991.

### *References*

Belmont, L. D., A. A. Hyman, K. E. Sawin, and T. J. Mitchison. 1990. Real-time visualization of cell cycle-dependent changes in microtubule dynamics in cytoplasmic extracts. *Cell.* 62:579–589.

Bentley, D., and A. Toroian-Raymond. 1986. Disoriented pathfinding by pioneer neurone growth cones deprived of filopodia by cytochalasin treatment. *Nature (Lond.).* 323:712–715.

Bray, D. 1978. Growth cone formation in cultures of sensory neurons. *Proc. Natl. Acad. Sci. USA.* 75:5226–5229.

Bridgman, P. C., and M. E. Dailey. 1989. The organization of myosin and actin in rapid frozen nerve growth cones. *J. Cell Biol.* 108:95–109.

Bunge, M. B. 1973. Fine structure of nerve fibers and growth cones of isolated sympathetic neurons in culture. *J. Cell Biol.* 56:713–735.

Cassimeris, L., N. K. Pryer, and E. D. Salmon. 1988. Real-time observations of microtubule dynamic instability in living cells. *J. Cell Biol.* 107:2223–2231.

Chen, H., J. Sedat, and D. A. Agard. 1989. Manipulation, Display, and Analysis of Three-dimensional Biological Images. *In* The Handbook of Biological Confocal Microscopy. J. Pawley, editor. IMP Press, Madison, WI. 127–135.

Cheng, T. P. O., and T. S. Reese. 1985. Polarized compartmentalization of organelles in growth cones from developing optic tectum. *J. Cell Biol.* 101:1473–1480.

Daniels, M. P. 1972. Colchicine inhibition of nerve fiber formation in vitro. *J. Cell Biol.* 53:164–176.

Forscher, P., and S. J. Smith. 1988. Actions of cytochalasins on the organization of actin filaments and microtubules in a neuronal growth cone. *J. Cell Biol.* 107:1505–1516.

Gard, D. L., and M. W. Kirschner. 1987. A microtubule-associated protein from *Xenopus* eggs that specifically promotes assembly at the plus-end. *J. Cell Biol.* 105:2203–2215.

Goldberg, D. J., and D. W. Burmeister. 1986. Stages in axon formation: observations of growth of *Aplysia* axons in culture using video-enhanced contrast-differential interference contrast microscopy. *J. Cell Biol.* 103:1921–1931.

Harris, W. A., C. E. Holt, T. A. Smith, and N. Gallenson. 1985. Growth cones of developing retinal cells in vivo, on culture surfaces, and in collagen matrices. *J. Neurosci. Res.* 13:101–122.

Harrison, R. G. 1910. The outgrowth of the nerve fiber as a mode of protoplasmic movement. *J. Exp. Zool.* 17:521–544.

Heidemann, S. R., J. M. Landers, and M. A. Hamborg. 1981. Polarity orientation of axonal microtubules. *J. Cell Biol.* 91:661–665.

Hinkle, L., C. D. McCaig, and K. R. Robinson. 1981. The direction of growth of differentiating neurones and myoblasts from frog embryos in an applied electric field. *J. Physiol.* 314:121–135.

Hyman, A. A., D. N. Drechsel, D. Kellogg, S. Salser, K. Sawin, P. Steffan, L. Wordeman, and T. J. Mitchison. 1991. Preparation of modified tubulins. *Methods Enzymol.* 196:478–485.

Lankford, K. L., and W. L. Klein. 1990. Ultrastructure of individual neurons isolated from avian retina: occurrence of microtubule loops in dendrites. *Brain Res. Dev. Brain Res.* 51(2):217–224.

Marsh, L., and P. C. Letourneau. 1984. Growth of neurites without filopodial or lamellipodial activity in the presence of cytochalasin B. *J. Cell Biol.* 99:2041–2047.

Mitchison, T., and M. Kirschner. 1988. Cytoskeletal dynamics and nerve growth. *Neuron.* 1:761–772.

Mitchison, T. J., and M. W. Kirschner. 1987. Some thoughts on the partitioning of tubulin between monomer and polymer under conditions of dynamic instability. *Cell Biophys.* 11:35–55.

Newport, J., and M. W. Kirschner. 1982. A major developmental transition in early *Xenopus* embryos. I. Characterization and timing of cellular changes at the midblastula stage. *Cell.* 30:675–686.

Nieuwkoop, P. D., and J. Faber. 1956. Normal table of Xenopus laevis. Amsterdam: North-Holland., *Daudin.* 168–170.

Peters, A., S. L. Palay, and H. Webster. 1991. The fine structure of the nervous system: neurons and their supporting cells. Oxford University Press, New York. 101–137.

Porter, K. R. 1966. Cytoplasmic microtubules and their functions. *In* Principles of Biomolecular Organization. G. E. W. Wolstenholme and M. O'Connor, editors. Little, Brown, and Co., Boston. 308–356.

Ramon y Cajal, S. 1890. Sur l'origine et les ramifications des fibres nerveuses de la moelle embryonaire. *Anat. Anz.* 5:609–613.

Reinsch, S. S., T. J. Mitchison, and M. W. Kirschner. 1991. Microtubule polymer assembly and transport during axonal elongation. *J. Cell Biol.* 115:365–379.

Sabry, J. H., T. P. O'Connor, L. Evans, A. Toroian-Raymond, M. W. Kirschner, and D. Bentley. 1991. Microtubule behavior during guidance of pioneer neuron growth cones in situ. *J. Cell Biol.* 115:381–395.

Sammak, P. J., and G. G. Borisy. 1988. Direct observation of microtubule dynamics in living cells. *Nature (Lond.).* 332:724–726.

Schnapp, B. J., and T. S. Reese. 1982. Cytoplasmic structure in rapid-frozen axons. *J. Cell Biol.* 94:667–679.

Schulze, E., and M. Kirschner. 1988. New features of microtubule behaviour observed in vivo. *Nature (Lond.).* 334:356–359.

Tsui, H. T., K. L. Lankford, H. Ris, and W. L. Klein. 1984. Novel organization of microtubules in cultured central nervous system neurons: formation of hairpin loops at ends of maturing neurites. *J. Neurosci.* 4:3002–3013.

Walker, R. A., E. T. O'Brien, N. K. Pryer, M. F. Soboeiro, W. A. Voter, H. P. Erickson, and E. D. Salmon. 1988. Dynamic instability of individual microtubules analyzed by video light microscopy: rate constants and transition frequencies. *J. Cell Biol.* 107:1437–1448.

Yamada, K. M., B. S. Spooner, and N. K. Wessells. 1971. Ultrastructure and function of growth cones and axons of cultured nerve cells. *J. Cell Biol.* 49:614–635.

# Chapter 3
# Movement and localization of microtubules in growth cones during turning at substrate borders

## INTRODUCTION

As neurons extend processes through the embryo, they must often take complex paths to reach their targets [1,2]. During this process, the terminal portion of the neurite, called the growth cone integrates diverse extracellular cues, including ECM, cell-surface proteins, and gradients of chemoattractants, and transduces these signals into morphological changes that direct the growth cone in the proper orientation[3-6].

While many extracellular molecules capable of guiding growth cones have been identified, the cellular mechanisms used by the growth cone to respond to orientation signals remain unclear. Crucial to elucidating these mechanisms will be understanding how the cytoskeleton reorganizes to change the direction of growth cone motility. Since the cytoskeleton ultimately determines the shape and the dynamic properties of the growth cone it must be one of the major targets of signaling from extracellular cues.

The examination of cell shape changes during turning decisions has shown that the dynamic actin-containing structures at the cell edge such as lamellipodia, the thin veils of a meshwork of filamentous actin, and also filopodia, small spikes of bundled actin filaments, respond to guidance cues [5,7,8]. Direct visualization of F-actin in Aplysia and grasshopper neurons further revealed that actin dramatically re-distributes to the site of future growth [9,10]. While actin-rich structures clearly respond to guidance cues, other cytoskeletal structures must coordinately respond to produce re-orientation of outgrowth [7].

The microtubule array also re-arranges during turning to generate the bend in the axon that re-directing the trajectory of growth. While it is clear that this re-direction of the microtubule array occurs, it is still unclear how it occurs, and to what extent this re-arrangement directs the

turning of the whole growth cone. In grasshoppers, heterogeneous behavior during different turning decisions indicated that microtubules may sometimes pay a decisive role in guidance decisions [11]. At segment boundaries, microtubules entered multiple filopodia, only one of which became the new axon. In this case, microtubules did not predict the direction of turning. At the guide post cell, however, microtubules only entered the branch that contacted the guide post cell, and this branch became new axon. The microtubules in Aplysia bag neurons during contact mediated guidance appear to resemble the former situation in grasshopper, as microtubules appeared to invade only the lamella at the contact site [10]. Such observations suggest that the commitment of microtubules to the new orientation of growth can be quite early, but no one has observed the behavior of microtubules in living neurons with sufficient time or spatial resolution to reveal the mechanism of their rearrangements and the relative time of microtubule rearrangements with the changes in actin containing structures. Such information is pivotal in any attempts to determine how actin and microtubules interact and furthermore to identify the molecular activities that control the cytoskeletal rearrangements during guidance decisions.

For this reason, we have chosen to follow microtubules in the growth cones of living cultured Xenopus neurons as they encounter a substrate border. As shown previously, the Xenopus system allows us to follow microtubules with high spatial and temporal resolution [12]. In this paper, we describe the sequence of rearrangements for single microtubules and also for microtubule bundles that occur during turning decisions. We find two contrasting turning behaviors termed "motility" and "growth" mediated re-orientation. These two classes represent cases where two distinct steps in

turning- the adhesion of lamella and the re-orientation of the microtubule array- appear limiting .

## MATERIALS AND METHODS

*Preparation of patterned substrate* A) Collagen-coating: 25 mm diameter round coverslips were washed with 1 N HCl for 14 hours at 65 C then washed extensively with glass distilled $H_2O$ and air dried. Prior to the experiment, coverslips were coated with 150 µl of 200 µg/ml collagen type IV (Collaborative, Bedford, MA). After incubation for 1-3 hours, coverslips were rinsed with distilled $H_2O$ and air dried. B) Producing Matrigel stripes. Concentrated Matrigel (Collaborative, Bedford, MA) was stored in small (10 µl) aliquots at -20 C. To make stripes, stock Matrigel was diluted 50-fold, then labeled with 2 X $10^{-6}$ M N-hydroxy-succinimydyl-ester-coumarin ( kind gift of Tim Mitchison). The mix was then incubated at 37 C for 1 hour in the dark to gel the Matrigel. Stripes of Matrigel were then aspirated onto 0.1 µm nucleopore polycarbonate filters (Costar, Pleasanton, CA) as described for membrane particles [6] --(see figure 1). Matrigel-patterned filters were stored on top of a thin layer of 1% agarose/$Ca^{++}$,$Mg^{++}$-free PBS at 4 C. C) To make alternating stripes of Matrigel and collagen, The filter plus the a garose underneath it were excised from the rest of the surrounding agarose by cutting a square around the filter with a razor blade. This block was carefully picked up with forceps and inverted onto the dried, collagen-coated coverslip so that the Matrigel was facing the collagen-coated surface. This assembly was incubated for 30-60 min. at room temperature. The coverslip was then flooded with $Ca^{++}$,$Mg^{++}$-free PBS and the agarose block and filter were removed. All coverslips were checked for proper patterning (sharp stripes)

with epi-fluorescence micrscopy before use. Just before plating explants, the PBS was replaced with Steinberg's plating media.

*Neural cultures and mt labelling* Labelling of neuronal mts and culturing of neural tube explants was performed exactly as described previously [12] (Chapter 2). Imaging of cultured neurons was also performed as previously described.

## RESULTS

### Xenopus neurons turn at a substrate border

We chose a turning paradigm that resembles guidance decisions in Xenopus embryos where motor neurons growing out of the neural tube appear to follow patterns of extracellular matrix (ECM) molecules such as laminin [13]. It seemed likely that the neurons emerging from cultured Xenopus neural tube explants would respond to borders of different ECM molecules. Explants of the Xenopus neural tubes responded strongly to culture on different ECMs. Laminin or laminin-rich crude substrates such as Matrigel induced rapid outgrowth. In contrast, explants cultured on fibronectin or collagen type IV supported very poor outgrowth (data not shown). We tested whether Xenopus motor neurons growing on the favorable laminin-rich substrate would turn to stay on the laminin if they encountered a border with collagen type IV.

In order to observe individual neurons at high magnification during turning, we developed a turning assay in which we had a relatively high chance of seeing a turning event. To make patterns of ECM we adapted a method used for guidance assays on membranes prepared from different regions of chick optic tectum [6] (see Materials and Methods). This resulted in coverslips patterned with alternating 100 μm-wide stripes of

Matrigel and collagen type IV. The substrate pattern was visible using epi-fluorescence since the Matrigel was fluorescently labeled prior to application (figure 1a). Eight to fifteen hours after plating neural tube explants on the patterned coverslips extended neurites over Matrigel-containing regions but avoided collagen resulting in patterns of neurite outgrowth that matched the patterns of fluorescent stripes (figure 1b).

**Observation of growth cones during turning at substrate borders**

To follow microtubules during turning decisions we fluorescently labeled neuronal microtubules in Xenopus embryonic neurons by injecting eggs at the two-cell stage with rhodamine-labeled tubulin as previously described [12]. We plated the neural tubes from injected embryos onto the patterned coverslips and began to observe the neurons 8-12 hours after plating. We chose growth cones growing towards substrate borders and collected images at 30-second intervals. Both the growth cone and the microtubules could be followed simultaneously using rhodamine epi-fluorescent illumination since the general shape of the growth cone was visible due to the cytoplasmic signal from the tubulin monomer. The turns took between 10 to 87 minutes averaging 28 minutes. In total we observed 33 neurons growing on Matrigel that encountered a collagen border. In 7 of the sequences the growth cone interacted with other cells during the turn obscuring and complicating its behavior while in 3 cases the growth cone had already initiated turning before observation. These observations were not included in this study. Of the 23 remaining sequences, two growth cones remained paused at the border throughout the observation period and two growth cones grew through the border onto the collagen. Four suddenly retracted after reaching the border and only two of these grew back in a new

direction, successfully avoiding the border; the other two failed to grow back during the observation period. 16 neurons clearly changed their direction of movement at the border. These neurons showed differences in behavior dependent on how strongly the growth cone and axon adhered to substrate at the border. Four neurons underwent what we term "sidestepping" behavior, in which the growth cone moved laterally along the border. Since both the central part of the growth cone and the axon were not attached to the substrate, the axon remained straight. The microtubule behavior in these cases resembled that found in neurons extending on uniformly coated coverslips described previously [12]. Thirteen neurons clearly changed direction when they approached the border by developing an axonal bend. It is these 13 neurons that we will describe in this paper. Three of the neurons underwent two of the behaviors (such as sidestepping and then turning) during observation, so they were counted twice.

*Angle of Approach* The average angle at which the 22 neurons approached the border was 52±23 degrees. There was no significant difference in the average approach angle for the neurons that displayed collapsing, sidestepping or turning behaviors at the border (51 ± 45, 52 ± 25, 46±18, respectively). In the two instances in which the growth cone grew through the border the approach was nearly perpendicular at 84 and 90 degrees.

**Two types of growth cone turning at substrate borders: motility mediated and growth mediated re-orientation**

The behavior of the 14 growth cones that changed their direction of growth when they encountered the substrate boundary could be categorized into two groups, which we shall term "motility mediated" and "growth mediated" re-orientation.

*Motility Mediated Reorientation* Five growth cones exhibited motility mediated re-orientation. When growth cones approached borders they extended lamellae or branches in multiple directions. In four out of five cases growth cones extended lamellae onto collagen. A single lamella spread on Matrigel acquired dominance by forming a strong attachment to the substrate. The other lamellae appeared weakly adherent compared to the dominant lamella that pulled the entire growth cone away from the border into a new orientation. The dominant lamella pulled on the entire microtubule array in the growth cone so that a bend in the axonal microtubule bundle developed before the border and within the axon, not the growth cone. The configuration of the microtubules did not change during motility mediated reorientation i.e. splayed microtubules did not bundle during turning.

Figure 2 shows a neuron turning by motility mediated reorientation. At 0 minutes the growth cone growing on Matrigel approached the border, and extended a lamella (the c lamella) across the collagen border marked by the white stripe. By 2.0 minutes, the upper lamella (the m lamella) on the Matrigel expanded, while the c lamella shrank slightly. Note, however, that some microtubules have invaded the base of the c lamella (arrow). At 6.0 minutes, the growth cone assumed a fairly symmetric shape with microtubules contained in the central region. At 9.0 minutes the growth cone began expanding the m lamella (arrowheads) perpendicular to the axon. At 14.0 and 15.0 minutes, the m lamella lengthened, and became stably attached to the substrate while the c lamella continued to retract from the border. By 22.0 minutes, microtubules entered the growing m lamella. However, at 26.5 minutes, the c lamella detached completely and the m lamella pulled the growth cone and the distal portion of the axon away from the border. This

tugging bent the axon parallel to the border. Reorientation occurred with little net growth of either the microtubule array or the axon.

Our general observations suggested that the lamella on Matrigel was more stable, and eventually pulled the growth cone onto the Matrigel, keeping it from straying onto the collagen. We compared the life span of lamella on Matrigel to those extending onto collagen at the substrate boundary for 25 lamellae on each substrate from six cells. The life spans of most lamella on collagen and Matrigel were quite similar (figure 3). However, a small proportion of the lamella showed extremely long life spans, (greater than or equal to 1200 seconds) on Matrigel making the average life span on Matrigel 396 ± 360 seconds versus 198±149 for lamella on collagen. The distribution of life spans suggests that most lamella are short lived whether extended onto collagen or Matrigel but occasionally lamellae on Matrigel became stable (figure 3). In addition, the sizes of the lamellae extended onto the collagen (455± 296) or the Matrigel (532± 305) did not differ.

*Microtubules enter lamella that eventually retract* We determined whether lamella crossing the border onto collagen ever contained microtubules. If the entry of microtubules into a lamella were sufficient to stabilize it then we would never expect them to enter lamella on collagen. However, in all cases, we saw microtubules enter at least one lamella that eventually retracted although microtubules rarely extended far enough into the lamella to cross the border.

In three out of five cases, microtubules left the lamella prior to its retraction. In those cases the microtubules evacuated the lamella by bending and translocation rather than by depolymerization. In figure 4 microtubules enter the c lamella at 2.0 minutes (arrow) At 0 and 1.5 minutes, the growth cone has formed two main lamella, with a few single microtubules emerging

from the main microtubule mass. At 3.5 minutes, single microtubules exclusively reside in the lower lamella that will eventually detach (arrow). At 4.5 minutes, these microtubules are bent and pulled out of the lamella so that by 5.0 minutes no microtubules extend into the lamella (arrow). The empty lamella remains spread (arrowheads). This lamella began to shrink at 5.5 minutes to become a small branch at 10.0 minutes. Meanwhile, single microtubules began to invade the stable lamella at 6.0 minutes (arrow). The main microtubule mass extended forward into this lamella at 8.5 minutes and further consolidated growth in that direction.

***Growth Mediated Reorientation*** The other major class of turning exhibited distinct microtubule behavior. In this type of turning, the microtubules did not extensively explore multiple areas of the growth cone. In 6 out of 9 cases, we did not see microtubules enter other lamellae before the turn. Instead, the bulk of the growth cone microtubules bent towards a single lamella and bundled. After elongation of the bundle, this lamella collapsed around the bundle and the distal end developed growth cone activity and morphology. This behavior contrasts with motility mediated re-orientation where the entire growth cone moved away from the border because adherence was lost in portions of the growth cone. In growth mediated reorientation, the growth cone maintained tight substrate contact throughout the growth cone so that turning was accomplished via directed growth.

Two examples of growth mediated reorientation are shown in figures 5 and 6. In figure 5 at 0 minutes, a single microtubule (arrow) extended into the peripheral lamella on Matrigel. This microtubule was immediately shored-up by the invasion of other microtubules into that region at 1.5 minutes (arrow) so that by 5.5 minutes, a substantial bundle of microtubules accumulated and a new lamella (arrowhead) formed at the end of the bundle.

By this time, a sharp axonal bend formed where the growth cone originally encountered the border. From 7 to 19.5 minutes the microtubule bundle continued to elongate by the same sequence of events.

Figure 6 illustrates microtubule bending towards the new direction of growth followed by subsequent invasion of a branch that is eventually transformed into new axon. In this case turning was initiated by bending of multiple microtubules rather than exploration of a lateral lamella by a single microtubule. At 0 minutes the microtubules in the growth cone were pointing in the same direction as the axon growing towards the collagen. The arrow indicates the microtubule ends. By 0.5 minutes, the microtubules bent laterally so that their terminal portions paralleled the substrate boundary. The top arrow marks a constant position in the field. At 1.5 minutes, the bending continued, and the microtubules coalesced into a more cohesive bundle. At 2.0 minutes, a single microtubule (arrow) entered the branch parallel to the border (arrowheads). This branch expanded and formed wider veils at its end at 2.0 and 2.5 minutes so that it now resembled a growth cone. By 3.5 minutes, multiple microtubules entered the region following the single pioneer (arrow). This invasion continued beyond the original area explored by the single microtubule. The original bending of the growth cone microtubules at 0.5 minutes was preserved in the axonal bend at 3.5 minutes.

*Invasion of lamella by individual microtubules precedes consolidation*
As illustrated in both figures 5 and 6 one or a few individual microtubules emerged out of the bundle into a lateral lamella or branch before the rest of the bundle invaded that area. In all 6 cases where we could clearly resolve single microtubules, single microtubules preceded the invasion by the microtubule bundle. In the other three cases, we lacked single microtubule resolution.

## DISCUSSION

### Characteristics of growth cones turning at a substrate border

In this paper we have used borders between laminin-rich Matrigel, and collagen type IV to induce turning of Xenopus neurons. Patterned substrates have previously been used to induced guided neurite outgrowth [5,7,14]; Kleinfeld, 1988 #782. As yet, it is still controversial what the nature of the difference between the substrates must be to guide neurons, and how the growth cone detects these differences. Here we do not attempt to directly address this issue but we note that in our experiments, neurons were growing on a substrate which promoted very robust outgrowth and turned to avoid a substrate (collagen IV) that poorly supports outgrowth. In this paper, we focused on the relationship between lamellipodial behavior and microtubule behavior during turning.

*Stability of lamella.*

During turning at the substrate boundary growth cones paused and in many cases extended lamellae over the boundary onto collagen. We found no difference in the size of lamellae spreading over the two substrates, but we found that lamella extending on Matrigel were two-fold more stable than those on collagen. A histogram of the lamellipodial life spans revealed that most of the lamella on Matrigel had similar life spans to those on collagen but a few were much more stable than the rest. This profile of lamellipodial life span reflects the observation that most of the lamella eventually retract after spreading over the preferred substrate and suggests that turning occurs by the selective stabilization of lamella rather than selective spreading. The greater stability of lamella on the preferred substrate during turning has previously been documented in chick DRGs and Aplysia bag cell neurons [5,7]

. Gundersen found a four-fold increase in stability of lamella on laminin compared to collagen. It was not determined if this average increase in stability was due to increased life span of all lamella extended on laminin, or if, similar to our observations, a subset of lamella showed much greater stability.

The selective stabilization of lamella on Matrigel suggests that Matrigel does not induce lamella that are inherently different than lamella on collagen. Rather, there is a higher frequency on Matrigel at which the lamella will be stabilized and subsequently mature into an axon. It is not known why Matrigel can stabilize lamella while collagen does not. Different spectrums of integrin subtypes are known to bind collagen and laminin. It is possible that the subtypes present on Xenopus motor neurons have a higher affinity for Matrigel than collagen. Alternatively, Matrigel may induce stronger contacts of integrins with the internal cytoskeletal elements or signaling complexes required for lamellipodial stability compared to collagen.

*Microtubules are important but not sufficient to stabilize lamellae*

During growth mediated reorientation the invasion of the branch or lamella by single microtubules preceded the invasion by the microtubule bundle. A similar sequence of events was observed in the grasshopper Ti1 neuron at guidepost cells [11]. These observations, as well as the inhibition of axonal growth by vinblastine treatment of Xenopus neurons, indicate that the polymerization of single microtubules into the peripheral lamella may be an essential first step in axonogenesis (Tanaka et al., manuscript in preparation). Actin accumulates at the tips of the growing branch or lamella that is invaded by microtubules in both grasshopper and Aplysia neurons during guidance decisions [9,10]. Such high local concentrations of actin could also localize factors that capture the peripheral microtubules which then act as templates

for further bundling. Observations in fixed neurons have found the association of microtubules with the bases of filopodia and other actin structures [15-18].

During turning we also observed microtubules entering lamella extended over the substrate border that eventually retracted. This indicates that the entry of microtubules into a lamella is not sufficient to confer stability. Similar behavior has also been observed in the grasshopper Ti1 neuron during re-orientation at the segment boundary where microtubules sometimes invaded multiple branches even though only one survived [11]. Unlike the grasshopper system, we could follow the growth cones at higher time and spatial resolution to determine whether when a lamella retracted, the microtubules receded from the lamella first, or if the lamella and the microtubules collapsed simultaneously. We observed both situations. When microtubules evacuate a lamella prior to the lamella's collapse, this occured at least in part by the movement of microtubules out of the lamella as they are bent backwards out of the lamella (figure 4). Translocation of microtubules rather than their disassembly appeared the major mechanism by which a labile lamella lost microtubules. It appears that forces in the lamella push microtubules out of it. The retrograde flow of actin away from the leading edge might provide the motive force for this movement and this flow might result from either the polymerization of actin at the leading edge or the activity of actin-based motor proteins . A third possibility for generating this microtubule movement are as yet unidentified microtubule motor proteins anchored to actin filaments in the lamella. The retrograde flow of microtubules in the lamella has previously been observed in non-neuronal cells (Hollifield ASCB abstract, Tanaka, unpublished). Furthermore, in mature Aplysia bag neurons, the zone of retrogradely

flowing actin in the lamella excludes entry of most microtubules into the lamella and treatment with cytochalasin relieves this exclusion allowing microtubules to invade [19]. It is interesting to note that Burmeister and Goldberg observed that branches of Aplysia neurons crossing the substrate border appeared to shrink by losing components rather than by loss of adherence [7]. Our observations indicate that microtubules comprise one of the internal elements lost during branch regression.

**Two types of turning: motility and growth mediated re-orientation**

When growth cones on Matrigel encountered a collagen border, we observed two types of behaviors: motility mediated and growth mediated re-orientation.

*Motility Mediated Reorientation*

During motility mediated re-orientation, the growth cone was not tightly attached to the substrate and changed its direction when a dominant lamella pulled it away from the border. Little axonal growth accompanies this type of turning. The configuration of microtubules in the Xenopus neurons during motility driven reorientation resembled some of the grasshopper Ti1 neuron growth cones turning at the segment boundaries. Both types of neurons extended lamella or branches in multiple directions and microtubules invaded multiple lamella. In both cases, one branch or lamella was eventually chosen and the others retracted.

*Growth Mediated Reorientation*

During growth mediated turning, the entire growth cone maintained tight attachment to the substrate and the entry of microtubules into a lamella appeared to be the limiting step. At the collagen border, microtubules within the growth cone bent and elongated in the new direction of growth. The

invasion of a lateral lamella by these microtubules predicted the location of new growth cone formation.

This type of turning resembled grasshopper Ti1 turning at guidepost cells where microtubules only invaded the branch that would eventually become the axon. This invasion was followed by the further infiltration of microtubule bundles that eventually formed the axon.

Our data supports a model for growth cone guidance with two sequential steps that are represented by the two types of turns we observed. The first essential step that appears rate-limiting in motility mediated turning is the strong attachment of a lamella to the substrate. In the next step the movement of the growth cone away from the border changes the orientation of the microtubule bundle and leads to the transformation of a lamella into a growth cone. In growth mediated reorientation the entire growth cone strongly attaches to the substrate so turning depends on the reorientation of microtubules and subsequent growth.

1.Bentley, D. and Keshishian, H. 1982. Pathfinding by peripheral pioneer neurons in grasshoppers. Sci 218: 1082-1088.

2.Holt, C. E. 1989. A single-cell analysis of early retinal ganglion cell differentiation in Xenopus: from soma to axon tip. . J Neurosci 9: 3123-45.

3.Tessier-Lavigne, M., Placzek, M., Lumsden, A. G., Dodd, J. and Jessell, T. M. 1988. Chemotropic guidance of developing axons in the mammalian central nervous system. Nature 336: 775-8.

4.Gundersen, R. W. and Barrett, J. N. 1979. Neuronal chemotaxis: chick dorsal-root axons turn toward high concentrations of nerve growth factor. Sci 206: 1079-1080.

5.Gundersen, R. W. 1987. Response of sensory neurites and growth cones to patterned substrata of laminin and fibronectin in vitro. . Dev Biol 121: 423-31.

6.Walter, J., Henke, F. S. and Bonhoeffer, F. 1987. Avoidance of posterior tectal membranes by temporal retinal axons. . Development 101: 909-13.

7.Burmeister, D. W. and Goldberg, D. J. 1988. Micropruning: the mechanism of turning of Aplysia growth cones at substrate borders in vitro. J Neurosci 8: 3151-9.

8.O'Connor, T., Duerr, J. and Bentley, D. 1990. Pioneer growth cone steering decisions mediated by single filopodial contacts. J Neurosci 10: 3935-3946.

9.O'Connor, T. P. and Bentley, D. 1993. Accumulation of Actin in Subsets of Pioneer Growth cone Filopodia in Response to Neural and Epithelial Guidance Cues In Situ. J. of Cell Biol. 123: 935-948.

10.Lin, C. H. and Forscher, P. 1993. Cytoskeletal remodeling during growth cone-target interactions. . J Cell Biol 121: 1369-83.

11.Sabry, J. H., O'Connor, T. P., Evans, L., Toroian-Raymond, A., Kirschner, M. W. and Bentley, D. 1991. Microtubule behavior during guidance of pioneer neurons growth cones *in situ*. manuscript submitted

12.Tanaka, E. and Kirschner, M. 1991. Microtubule behavior in the growth cones of living neurons during axon elongation. J Cell Biol 115: 345-363.

13.Perris, R., Krotoski, D., Lallier, T., Domingo, C., Sorrell, J. M. and Bronner, F. M. 1991. Spatial and temporal changes in the distribution of proteoglycans during avian neural crest development. . Development 111: 583-99.

14.Hammarback, J. A., McCarthy, J. B., Palm, S. L., Furcht, L. T. and Letourneau, P. C. 1988. Growth cone guidance by substrate-bound laminin is correlated with neuron-to-pathway adhesivity. Dev. Biol. 126: 29-39.

15.Gordon-Weeks, P. R. 1991. Evidence for microtubule capture by filopodial actin filaments in growth cones. NeuroReport 2: 573-576.

16.Bridgman, P. C. and Dailey, M. E. 1989. The organization of myosin and actin in rapid frozen nerve growth cones. . J Cell Biol 108: 95-109.

17.Letourneau, P. C. 1981. Immunocytochemical evidence for colocalization in neurite growth cones of actin and myosin and their relationship to cell--substratum adhesions. . Dev Biol 85: 113-22.

18.Letourneau, P. C. 1983. Differences in the organization of actin in the growth cones compared with the neurites of cultured neurons from chick embryos. J Cell Biol 97: 963-973.

19.Forscher, P. and Smith, S. J. 1988. Actions of cytochalasins on the organization of actin filaments and microtubules in a neuronal growth cone. J Cell Biol 107: 1505-16.

**Figure Legends**

Figure 1 *Xenopus neurons follow patterns of Matrigel and avoid collagen.* 1A Alternating 100 μm stripes of Matrigel (white stripes) and collagen (dark stripes) were made as described in Materials and Methods. The Matrigel was fluorescently labelled with coumarin. 1B Matched picture of neurons and grown on the patterned substrate. Neurons follow the stripes of Matrigel. In this picture, neurons were fixed and visualized by immunofluroescence against tubulin. Each fine strand represents an axon or multiple fasciculated axons.

Figure 2 *Turning at substrate border by motility-driven reorientation.* In this sequence the white line denotes the border between Matrigel (above) and collagen (below). 0 minutes The growth cone reached the border and extended a lamella across onto the collagen (c lamella). Microtubules remained well behind the border. 2 minutes The c lamella shrank and the upper lamella on Matrigel (m lamella) expanded. A single microtubule bent into the base of the c lamella (arrow). 6.0 minutes The m and c lamellae are similar in size while microtubules remain at their bases. The m lamella expanded laterally and the c lamella no longer extended across on collagen. 14 minutes Lateral m lamella remained stable (arrowheads) and microtubules began to fill the growth cone. The c lamella shrank. 19 minutes The m lamella continued to extend laterally, and a few microtubules have bent to enter the base of the m lamella (arrow). The c lamella collapsed close to the microtubule bundle. 22.0 minutes Lateral m lamella has expanded, and two microtubules entered deep into it (near asterisk). The remnants of the c lamella continued to lose adherence. The movement of the growth cone away from the border created a gentle bend in the axon behind the

growth cone neck. 26.5 minutes The m lamella has pulled the central region of the growth cone and the c lamella lost its attachment close to the border. Consequently, the whole growth cone moved away from the border. This can be seen both by the increased distance between the growth cone and the border, and the relationship of the growth cone to the asterisk that marks a constant position in the field at 22.0 and 26.5 minutes. Scale bar, 5 μm.

Figure 3 *Life spans of lamellae spread on Matrigel and collagen.* Average life span on Matrigel is 396±360 and on collagen is 198±149. Although average life spans differ two-fold, histograms show that most lamellae on the substrates have similar life spans but a small proportion of stable microtubules skew the distribution. The means are significantly different at a level of $p < 0.001$???? by the two-tailed t-test.

Figure 4 *Microtubules that enter a lamella that is not stabilized translocate out of the lamella prior to its collapse.* 0 minutes The growth cone had two large lamellae. Microtubules enter both lamellae. The border is irregularly shaped. Lamella on the right extends partly onto Matrigel and partly onto collagen while left lamella is entirely on Matrigel. 1.5 minutes Several single microtubules enter peripheral lamellae and growth cone looks fairly symmetrical. 3.5 minutes Several microtubules have entered the right hand lamella (arrows). These microtubules originally were from the left side of the axonal bundle (arrow heads) and gently curve into the lamella. The left lamella remains empty of microtubules. 4.5 minutes The microtubules in the right lamella receded somewhat so that they only penetrate the base of it. This has occurred in part because the microtubules form a more acute bend (arrowheads) and because the entire axon had begun the move to the left.

The left lamella expanded. 5.0 minutes The right lamella remained extended (arrowheads) although devoid of microtubules. (arrow). 5.5 minutes The right lamella (arrowheads) narrowed and the left lamella remained expanded while microtubules remain looped in the central region. 6.0 minutes A single microtubule (arrow)penetrated the left lamella as the right lamella remained attached. The axon continued to angle to the left. 7.5 minutes The right lamella collapsed into a thin branch. Microtubules further invaded the left lamella. 8.5 minutes and 10 minutes The microtubule bundle continued to move into the left lamella, further consolidating the choice to the left. Only a strand of the right branch remained. 10.0 minutes The growth cone moved to the left, and continued to grow in that direction as a single microtubule emerged from the bundle. Scale bar, 5 μm.

Figure 5 *Turning by growth mediated reorientation.* 0 minutes As the growth cone approached the border, a single microtubule entered the peripheral lamella (arrow), while other lamella remained devoid of microtubules. 1.5 minutes The region explored by the microtubule at 0 minutes was invaded by more microtubules. (arrow at 0, 1.5, and 5.5 minutes marks the same point in the field) 5.5 minutes Microtubules invading the region consolidated into a thick bundle (arrow) and new lamellipodia sprouted at the end of the bundle (arrowhead). The microtubule array at the border formed a discrete bend. 7.0 minutes A single curled microtubule (arrow) extended into the lamella from the distal end of the microtubule bundle. 11.5 minutes A few microtubules have followed the single microtubule, so that a thin bundle forms in the region marked by the arrow at 7.0 and 11.5 minutes. From the end of the bundle emanates a small curled microtubule (upper arrow). 14.5 minutes More microtubules invaded

the region between the two arrows so a thick microtubule bundle formed. 18.0 minutes The small growth cone has moved away form the end of the microtubule bundle (arrowhead). 19.5 minutes Several microtubules infiltrate the base of the growth cone, beginning the cycle of bundle elongation again. Scale bar, 5 μm.

Figure 6. *Growth cone microtubules bend toward new direction of growth.* 0 minutes The growth cone grew to the border and extended a branch laterally (arrowheads). Most microtubules remained straight, pointing in the direction of the axon. 0.5 minutes The lateral branch remained stable, and all growth cone microtubules bend towards it. The upper arrow marks the same point in field as at 0 minutes. The lower arrow marks the new position of microtubule ends. 1.5 minutes The base of the branch dilated with microtubules invading it. The distal portion of the branch (arrowheads) has widened and assumed some protrusive activity. 2.0 minutes The stable lateral branch expanded further (arrowheads) and a single microtubule infiltrated the base of the branch (arrow). No microtubules invaded the branch on the right. 2.5 minutes The base of the branch widened with more microtubule ends invading it, while tthe right branch remained free of microtubules. (arrows in 2.0, 2.5, 3.0, 4.5, 5.0 minutes mark the same point in the field). At the point where the growth cone originally approached the border, a discrete bend in the axon formed due to the bending and extrusion of microtubules at previous times. 3.5 and 4.5 minutes The distal area (arrow) was buttressed by the arrival of more microtubules. 5.0 minutes Several single microtubules emerged beyond the area marked by the arrow, infiltrating the new growth cone that formed. Microtubules at the bend (arrowheads) clearly form an axonal bundle.

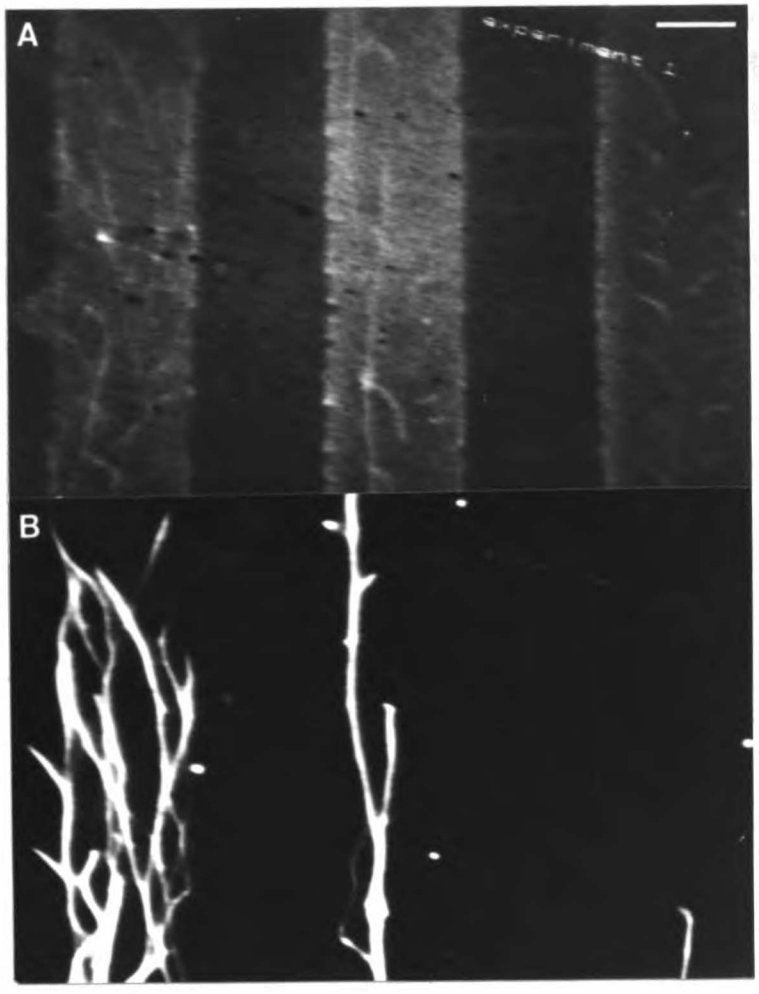
A
B

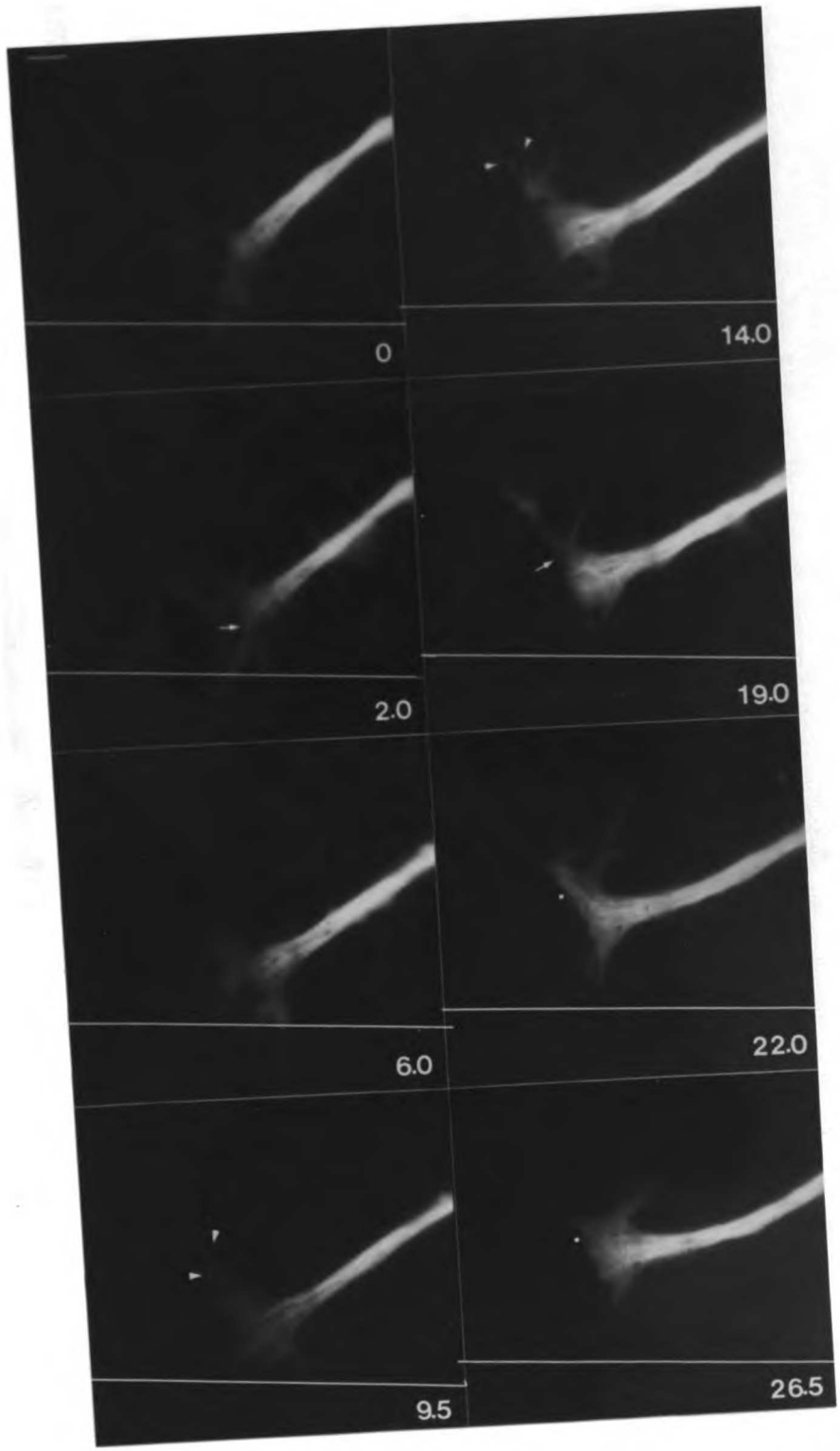
0
14.0
2.0
19.0
6.0
22.0
9.5
26.5

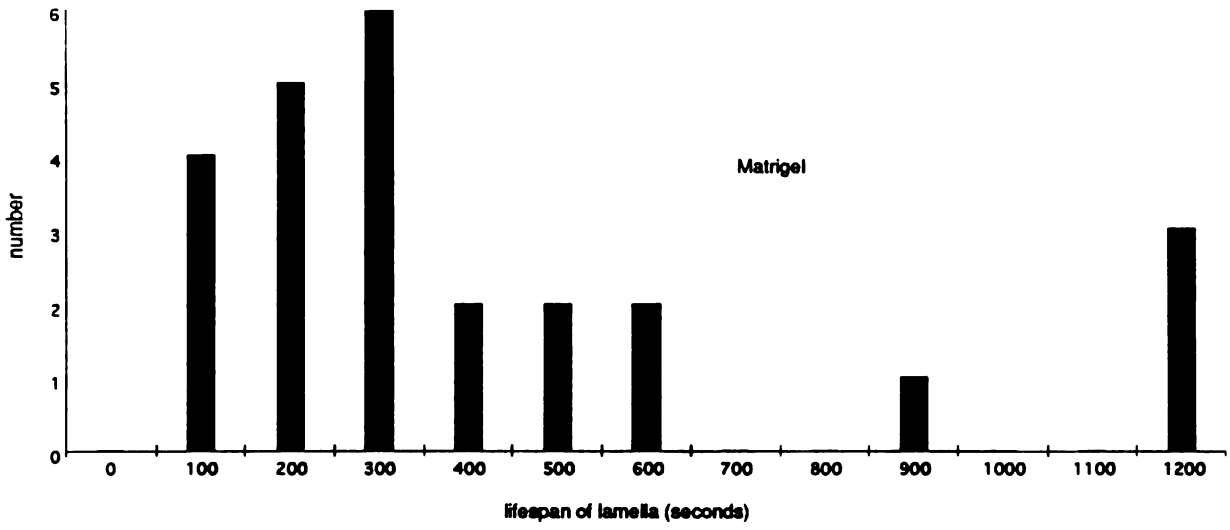
number
Matrigel
lifespan of lamella (seconds)
0
1
2
3
4
5
6
0
100
200
300
400
500
600
700
800
900
1000
1100
1200

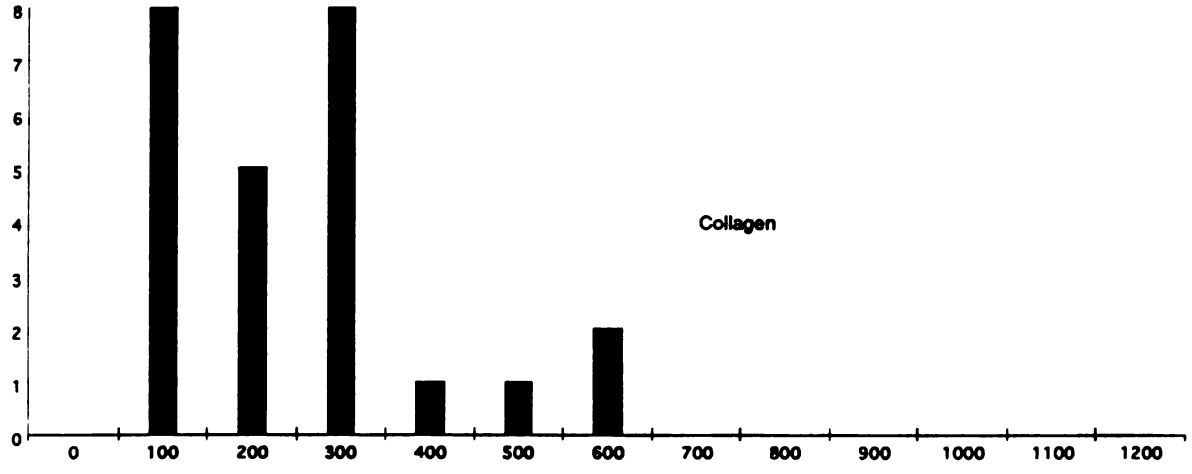
Collagen
0
1
2
3
4
5
6
7
8
0
100
200
300
400
500
600
700
800
900
1000
1100
1200

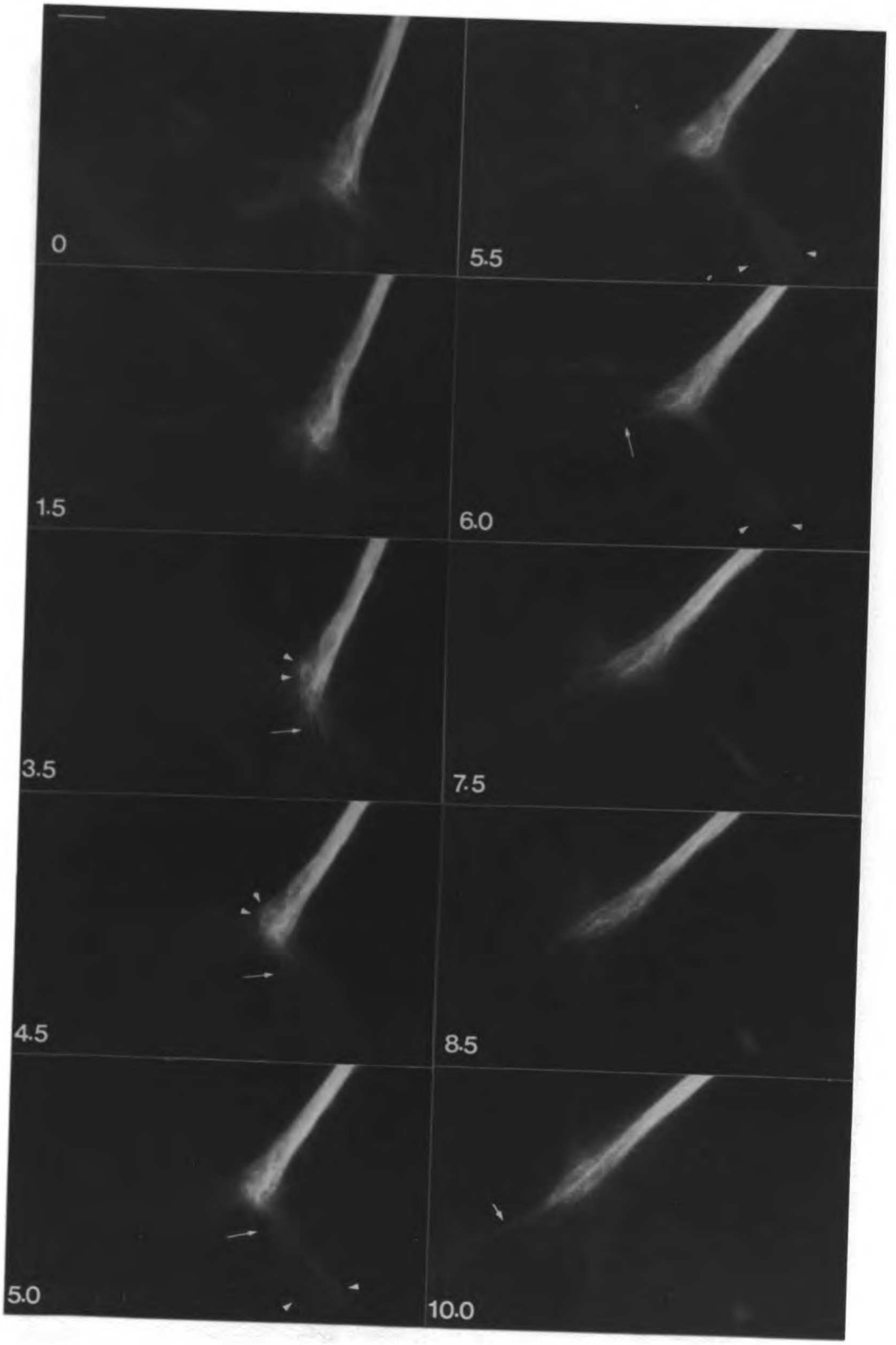
0
5.5
1.5
6.0
3.5
7.5
4.5
8.5
5.0
10.0

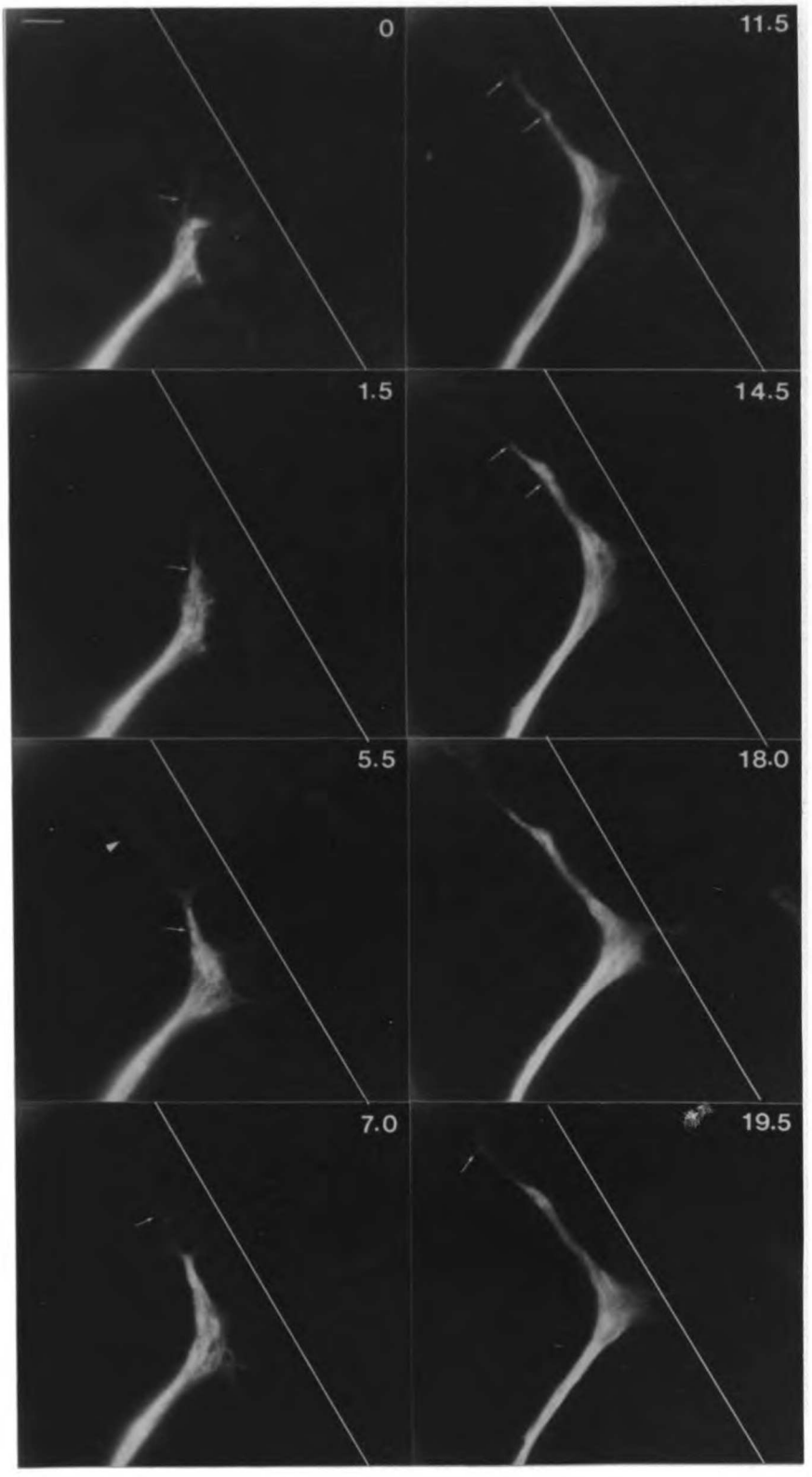
0
11.5
1.5
14.5
5.5
18.0
7.0
19.5

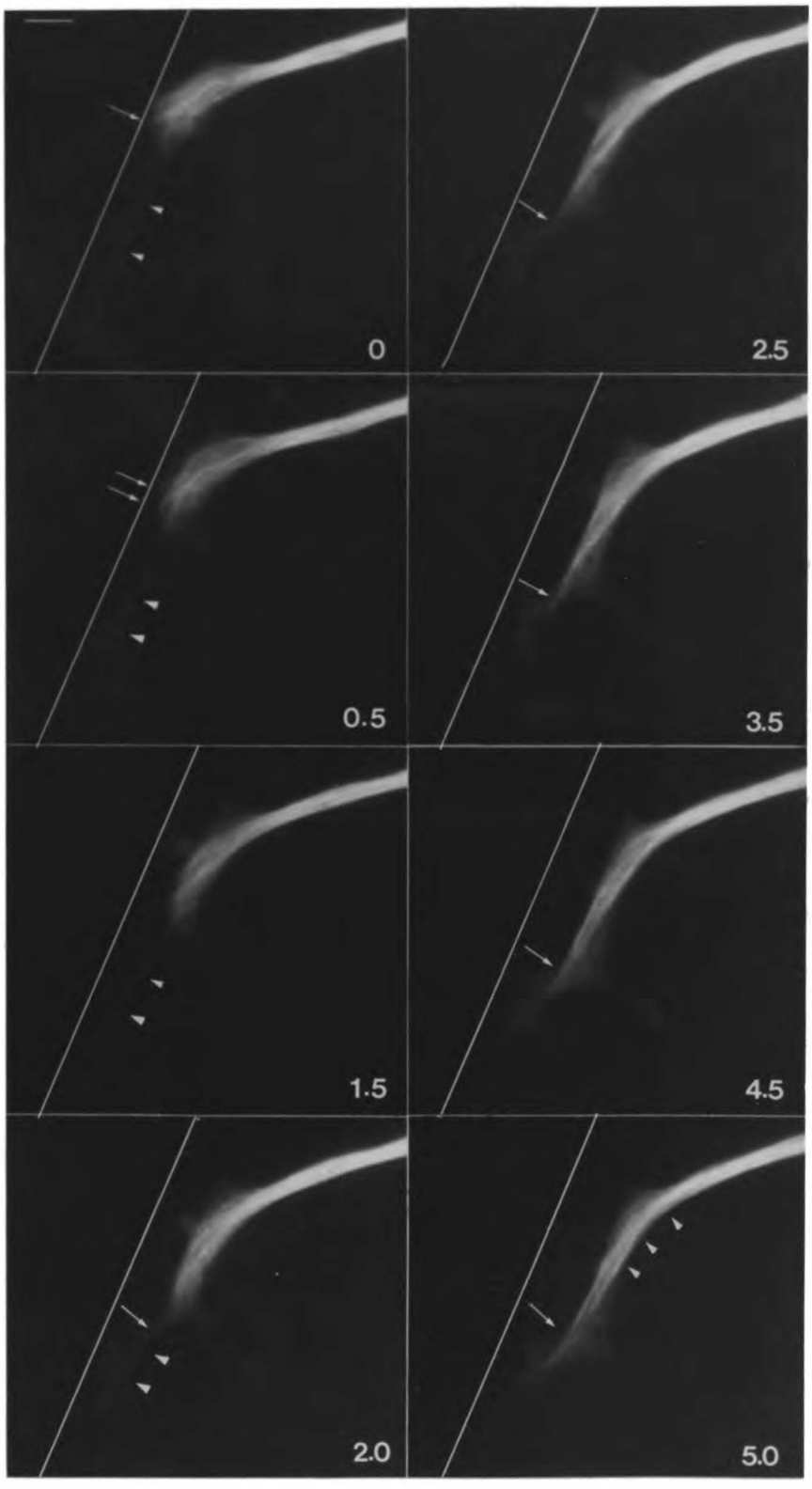
0
2.5
0.5
3.5
1.5
4.5
2.0
5.0

# Chapter 4
# The role of dynamic microtubules in coordinating growth cone motility and axon elongation

## INTRODUCTION

During neurite outgrowth, the movement of the growth cone away from the cell body results in the generation of new axonal structure. Therefore, the direction of movement chosen by the growth cone in response to extracellular cues determines the ultimate path of the axon [1-3]. In this process then, the motility of the growth cone must somehow be coordinated with the assembly of new cellular components that is required for axonogenesis. While the mechanism of this coordination is still unclear, the cytoskeleton is likely to be a key element through which this coordination is achieved. The actin and microtubule cytoskeleton comprise the motile apparatus of the growth cone as well as the structural framework the axon [4-7]. Microtubules, the cytoskeletal system we will focus on in this paper, extend in parallel bundles down the length of the axon into the growth cone [8-11]. Within the growth cone, microtubules form a dense, frequently bundled network in the central region, with a smaller number of single microtubules penetrating the peripheral lamella [9,12]. FRAP studies showed that the microtubules in the axon are relatively stable, while the growth cone microtubules turnover similarly to microtubules in fibroblasts [13,14]. Direct observation of microtubules in growth cones showed that at least the peripherally extending microtubules undergo dynamic instability [15]. Microtubules appear to be important for maintaining axonal structure as application of microtubule depolymerizing drugs to cultured neurons induces axonal collapse [4,5,7]. The local application of such drugs showed that the growth cone was particularly sensitive, and resulted in growth cone collapse, suggesting that microtubules may play an important role in growth cone motility as well [16].

The sensitivity of the growth cone to microtubule drugs and the lack of movement seen of a photobleached mark made on fluorescently labeled axonal microtubules suggested that the growth cone is the site of the microtubule polymerization required for axonogenesis [13,14,16]. This is an appealing model as the growth cone, the site of motility, would also be the site of assembly. Studies examining rhodamine microtubules in growth cones of living neurons could not determine if this occurred, and a specific mechanism is yet unknown [15]. Other studies in cultured Xenopus neurons, and PC12 neuronal cell lines, found that a mark made on axonal microtubules translocated as a coherent phase down the axon [17]. These studies suggested that assembly of polymer occurred in the cell body or all along the axon, and polymer was extruded down the axon. In this model then, the site of assembly is dissociated from the site of growth cone motility. Indeed, observations of microtubules in Xenopus growth cones found that the coupling between growth cone movement and microtubule elongation was not exact. At times, microtubule polymer would accumulate in the growth cone, while at other times the movement seemed to outrun the polymer [15]. With the observation of microtubule translocation in Xenopus neurons, it was unclear if the dynamic microtubules in the growth cone were necessary for axonal elongation, or whether axonal outgrowth could be achieved purely by the extrusion of polymer down the axon. It is possible that the dynamic microtubules in the growth cone are necessary purely to maintain the motile properties of the growth cone. In the Xenopus system atleast, it is unclear whether the cytoskeleton assumes two separate functions in growing neurons--one for fueling growth cone motility, and one for assembling axonal structure--or whether the motility of the growth cone is more directly linked to axonogenesis.

To examine such issues, we have sought to understand the role of microtubule dynamics in growth cone motility and axonal outgrowth. We have utilized low concentrations of vinblastine in neurons to inhibit microtubule dynamics without causing massive depolymerization. The action of low concentration of vinblastine on microtubules has been investigated in interphase cells and in vitro [18-20] . In vitro studies of purified tubulin showed that vinblastine inhibits turnover while tracking of individual microtubule dynamics in vitro showed that dynamics of ends are indeed suppressed. It has been postulated that vinblastine binds to microtubule ends and inhibitions both addition and loss of monomer. Hela cells and rat superior cervical ganglia treated with low vinblastine arrest in mitosis with intact spindles while neurons incubated with low doses of vinblastine polymer maintain constant levels of polymer [21] . Our examinations of axonal outgrowth in the presence of vinblastine combined with our observations of microtubules in vinblastine-treated growth cones suggest that the dynamic growth cone microtubules play a critical role in coordinating growth cone motility and axonogenesis.

## MATERIALS AND METHODS

*Xenopus neural tube cultures* Neurons from neural tubes explants were cultured as described previously [15] . Briefly, dorsal regions were dissected from ST 22-24 Xenopus embryos and placed in 1 mg/ml collagenase in Steinberg's solution. After 40 min., neural tubes were further dissected and stored in Steinberg's media until further use (15-30 min.) Neural tubes were plated as explants on large coverslips (35X50 mm, Carolina Biological Supply) coated with Matrigel as previously described.

Fibroblast cells were cultured from dorsal tissue of ST 24 embryos. Instead of using embryo extract, media was supplemented with the defined media supplement, 5%% Ultroser HY. This promoted spreading of non-neuronal cells. All other manipulations of the cells are as described for neurons.

*Perfusion chamber* Perfusion chambers were constructed on large rectangular coverslips (35X50 mm) that had been acid-cleaned with 1N HCl for 12 hours at 65 C. 22x22 mm, 1.5 thickness coverslips were cut into 3x22 mm strips, coated on both sides with high vacuum grease, and attached to the large coverslip parallel to each other 15 mm apart so that they made 15x22 rectangular flow cell between them. The area between the strips was coated with Matrigel and washed as previously described. The area was then flooded with Steinberg's plating media containing 0.3% methylcellulose (Dow Corning) and the coverslips were placed in a humidified chamber. Neural tube explants were then plated between the strips and allowed to attach and send out neurites for 8 to 16 hours depending on the type of experiment. Just before observation, the perfusion chamber was sealed by placing a 22x22 mm coverslip on top, making sure that plating media filled the volume between the coverglasses.

*Time-lapse observation of vinblastine treatment* For phase observations, cells in the perfusion chamber were observed on a Zeiss IM35 microscope at magnifications ranging from 25 to 60X and recorded using a Hamamatsu video rate CCD camera to a Panasonic 2025 optical memory disk recorder (Secaucus, NJ) via Image-1 image processing system (Universal Imaging, Brandywine, PA.). All growth rate measurements were mead using Image-1.

For perfusing control, vinblastine, or wash media through the chamber, 150 µl Steinberg's/0.3% methylcellulose with or without vinblastine was added to one side of the chamber and wicked through by placing wedges

of Whatman no. 1 paper on the other side. This was repeated three times. Vinblastine was stored as 10 μg/ml stock in $H_2O$ at 20 C, and diluted before each experiment.

For observation of microtubules during vinblastine treatment, Xenopus eggs were injected with rhodamine-labeled tubulin as previously described [15]. For observation, explants were plated in perfusion chambers as for phase observations. To maintain anoxic conditions, the coverslip was attached to a custom built chamber which covered the perfusion chamber, but had inlets for nitrogen input, two hypodermic needle inputs for adding media for washes, and a thin slit for inserting the wicking paper. The constant flow of nitrogen through the chamber maintained an anoxic atmosphere. The vinblastine and wash media for perfusion were made anoxic by incubation in a nitrogen-filled glove box for 15-20 min. with occasional shaking. After incubation, the media was sucked into 1 ml syringes and sealed by inserting it into a hypodermic needle plunged into a rubber stopper. The syringes were then transferred to the cell chamber that had been perfusing with nitrogen. Prior to observation, the cells were perfused with wash media from the syringe both as a control and to ensure that they were growing in anoxic conditions.

*Fluorescence imaging* Mts were imaged on an Olympus IMT-2 microscope with a 60x objective. Mercury light was attenuated to 7-12% of full illumination with neutral density filters and light was shuttered to 0,1 sec exposures. Images were acquired onto a cooled CCD camera with a Tektronix 1024D chip. The field was magnified approximately 270-fold to the chip so that 0.107 μm was imaged onto a pixel width. Images were acquired and processed using a Sun Sparcstation +1, running Inovision software (Research Triangle, NC.) For viewing of sequences and crude analysis, digital images

were transferred to optical disk. All fluorescence intensity measurements were made directly from digital images using the ISee software from Inovision.

## RESULTS

### Low doses of vinblastine induce growth cone wandering.

To determine the effect of vinblastine on growth cone behavior and neurite outgrowth, we treated cultured Xenopus neurons with concentrations of vinblastine varying from 5 nM to 20 nM. While the growing neurons were being observed with time-lapse video microscopy using phase optics, they were first perfused with normal media (control) to establish the baseline reaction of the cells to perfusion. After 10 to 30 minutes, cells were perfused with vinblastine-containing media and then observed for 25 to 60 minutes. The vinblastine was subsequently washed out and the cells observed for another 30 to 60 minutes.

In general, we observed decreased axonal elongation, and an increase in growth cone wandering in response to 5-20 nM vinblastine. Prior to vinblastine treatment, the net motion of the growth cone was straight although lamella transiently extended in all directions, resulting in efficient formation of new axon. Perfusion of control media did not affect this movement. The growth cone movement which is in the same orientation as the axon and which results in axonal outgrowth we shall refer to forward movement of the growth cone. Figure 1, 0 to 10 minutes shows a typical growth cone prior to vinblastine treatment. At 0 minutes, the growth cone has extended a lamella at approximately 30 degrees away from the orientation of the axon (arrowhead). By 5 minutes, the growth cone, however, has continued the move in the general direction of the axon, and although it

transiently extends lamella and branches in three directions (arrowheads), continues to move forward so that by 10 minutes, it has moved forward about 40 μm from its position at 0 minutes. In contrast, after vinblastine addition, growth cones lost their persistent forward motion. Rather, the entire growth cone would explore the area around it, often extending a lamella or branch laterally then moving in the direction of that lamella, then and exploring another branch or lamella--a behavior which we will term wandering. Figure 1 between 14 minutes and 37 minutes shows the reaction a growth cone to vinblastine. Initially, after vinblastine perfusion, the growth cone looks relatively normal (figure 1, 14 min.). By 20 minutes, the growth cone has ceased forward movement, and by 25 minutes, has begun moving toward a laterally toward the upper right corner of the field. 6 minutes later, however, a lateral sprout at the base of the growth cone (asterisk), forms a thin veil, which thickens, and pulls on the growth cone at 37 minutes. In many cases this behavior resulted in the formation of branched configurations, as in figure 1, 37 min., of the growth cone. Under these conditions the net elongation rate of the axon decreased markedly, while area of exploration increased.

The effect of vinblastine was reversible, and the growth cones resumed more persistent forward movement resulting in the resumption of axonal elongation. In figure 1, by 74 minutes when the vinblastine has been washed out, the lower branch (asterisk) has become the dominant one, and a new growth cone sprouts from the end of it at 80 minutes. This growth cone then resumes forward movement so that by 91 minutes, the growth cone has grown 38 mm. Of 13 growth cones treated with 5-20 nM vinblastine, 10 began wandering. Of the remaining growth cones, 1 rounded up and essentially stopped, and two 2 continued to grow fairly normally.

*Vinblastine affects persistent growth cone movement but not overall motility.* From our visual observations of the time-lapse sequences, it appeared that when treated with vinblastine, growth cones lost their persistent forward movement, but that their motility--their ability to move by extending and retracting filopodia and lamella--was not affected. To quantitatively distinguish between vinblastine's affect on persistent forward movement (or axonal elongation) and growth cone motility we quantitated the growth cone behavior by the three different methods represented for three growth cones in figure 2. In 2A the trajectory of the growth cone is plotted by simply tracing the xy coordinates of the growth cone centroid at 1 minute intervals. At 5 nM, vinblastine addition (v) only slightly affects growth cone movement. Intermittently after vinblastine treatment at 60, 70, and 90 minutes (asterisk, figure 2a) the growth cone briefly wanders to the side and steps back before resuming some growth. In contrast, at 10 nM, the effect of vinblastine is apparent after 8 minutes. At 75 minutes, the growth cone wanders back along the direction in which it was growing, and then starting at 90 minutes, stalls in one spot until the vinblastine is washed out (w). At 20 nM (figure 1a), the effect is drastic. In this case, the growth cone had spontaneously begun to move backwards. With the addition of vinblastine, it remains stalled in a small area throughout vinblastine treatment. The neuron does not recover persistent movement for approximately 15 minutes after washing out vinblastine. At 50 and 200 nM vinblastine, growth cones collapsed, and the neurites began to retract (data not shown).

To measure how much vinblastine treatment inhibited forward motion or axon elongation, we calculated the velocity with respect to its starting point, in other words, the rate at which the growth cone was moving away from its

starting point. This was done by treating each xy coordinate as a vector, and subtracting the initial vector ($x\hat{}_0$, $y\hat{}_0$) from each of the subsequent vectors ($x_i\hat{}$,$y_i\hat{}$) This results in a series of vectors between the first point and each point of the trajectory. The magnitude of each vector was then calculated giving the distance ($d_i$) of each point to the original point. Each distance was subtracted by the distance previous to it ($d_i$-$d_{i-1}$). Since the points were one minute apart, this calculation yielded the instantaneous velocity of the growth cone with respect to the first point of the graph. This analysis is a reasonably good indicator of the persistent movement of the growth cone. We will refer to this velocity measurement as persistent velocity. If the growth cone starts retracting or moving backwards, the velocity is negative, if the growth cone stalls, the velocity approaches zero and if the growth cone wanders laterally, the velocity also approaches zero. In Figure 2B at 5 nM, the dip in the graph around 70 minutes reflects the lateral motion seen in 2A, and the negative values at 90 minutes reflects some brief backwards movement. In contrast, at 10 nM, the growth cone begins stepping backwards 15 minutes after vinblastine addition, with a much larger magnitude of backward movement (2 μm/min., than at 5 nM, 0.5 μm/min.). At 20 nM the growth cone hovers around zero during vinblastine treatment. Therefore, at 10 and 20 nM, there is a marked effect on persistent growth cone advance. The average persistent velocities for multiple growth cones is given in table 1. At 5 nM the persistent velocity decreases to about 50% from control treatment, while at 10 and 20 nM, the velocity decreases to 24% and 36% respectively.

As a measure of the basic motility properties of the growth cone, we measured the absolute velocity of the growth cone by simply calculating the distance, irrespective of direction, between each successive xy position of the

growth cone. Therefore, if the growth cone froze in its tracks, the velocity would approach zero, whereas if the growth cone wandered, the motility would remain high. We will refer to this velocity as motility velocity. As seen in figure 2C, while it is clear that the motility velocity decreases somewhat upon vinblastine addition, it is reduced far less than the relative velocity. The average decrease of motility for all growth cones in 10 nM is only 25% in contrast to the average decrease of 75% for persistent velocity (table 1). This indicates that the growth cone maintains much of its motility during vinblastine treatment. The decrease in persistent velocity without a matching decrease in motility velocity reflects that the growth cone is exploring a larger lateral area.

**Vinblastine inhibits microtubule dynamics in non-neuronal cells.**

Since microtubules are the cellular target of vinblastine, we wished to determine how microtubules in the growth cone changed in response to vinblastine, and how this change results in growth cone wandering. While vinblastine was shown to inhibit microtubule dynamics on purified tubulin in vitro, it has not been determined if vinblastine acts by the same mechanism inside cells. To analyze the effect of vinblastine on cellular microtubules, we first wanted to directly measure the effect of vinblastine on microtubule polymerization in the cell. It is, however, extremely difficult to make such measurements in growth cones themselves because the rapid incorporation of the microtubules into bundles makes it very difficult to follow any one microtubule for an extended period of time and frequent microtubule translocations makes it difficult to distinguish polymerization from movement. We therefore measured microtubule polymerization in the non-neuronal cells that are present in the Xenopus culture. These cells are

fibroblastoid cells which extend large, flat lamellae that are optimal for dynamics measurements.

Using the same procedure for fluorescently labeling Xenopus neurons with rhodamine-tubulin (Tanaka and Kirschner), we cultured neural tubes and somites, but in this case included serum factors which would stimulate the spreading of non-neuronal cells. Cells were observed under anoxic conditions every 8.5 to 15 seconds using epi-fluorescence microscopy. We measured over 40 microtubules in both the control and vinblastine, and 28 microtubules during recovery in three cells.

Prior to vinblastine treatment, microtubules exhibited normal dynamic instability behavior. They underwent growth alternating with rapid shrinkage at rates and transition frequencies comparable to those measured previously (figure 5, table 2). This behavior is illustrated in figure 3 which shows normal microtubule dynamics between time 0 and 36 seconds. The larger arrow shows a microtubule which begins shrinking at 19 seconds, and by 36 seconds, has shrunk 2.5 microns. The smaller arrowheads highlight another shrinking microtubule. These microtubules co-exist with growing microtubules that are highlighted by the arrows. The individual histories of microtubules (figure 4A) show that they undergo the characteristic phases of growth and shrinkage with two of the microtubules disappearing from the field in less than five minutes (figure 4A). As in some other cells, these microtubules undergo some extended lengths of pausing where no growth or shrinkage can be discerned. In the normal condition, after 8 minutes it is very difficult to identify the same microtubules at the edge of the cell, because when they shrink back to toward the cell center, they are lost.

In contrast, microtubules in vinblastine treated cells undergo much longer periods of pausing, and have reduced growth and shrinkage rates making

them relatively undynamic (figure 4,5, table 2). In vinblastine, the average growth and shrinkage rate decreased from 6.4 +/- 3.25 to 3.1 +/-3.4 μm/min. and 14.3+/- 8.5 to 5.1+/-4.0 μm/min. respectively (table 2). Under these conditions, it becomes easy to follow a microtubule for more than 8 minutes, as they are relatively undynamic. As seen in the microtubule life histories (figure 4B), a proportion of the microtubules undergo very little growth or shrinkage during the time of observation, while some others do shrink. This is illustrated in figure 3. At 52 seconds the cell has just been treated with vinblastine. Three microtubules in the periphery (arrowheads, 56s-8 min. 53 s), are still visible after 8 minutes. The upper one , although it appears to shrinks 1.21 microns between 2:33 and 3:51, has actually translocated back, as the proximal portion of the microtubule, towards the cell center, becomes kinked. Such microtubules were not included in the measurements. The middle microtubule becomes kinked between 2:33 and 3:51, and then eventually shrinks back to the asterisk in 8:53. Another microtubule in the upper left (large arrow) which is stable throughout the 8 minutes also becomes kinked between 2:33 and 3:51, and is then actually severed between 3:51 and 8:53. Similarly, of two microtubules highlighted by the smaller arrows, the lower one is stable, and visible for the entire 8 minutes, while the upper one shrinks back between 52 seconds and 2:33.

After washing vinblastine out, microtubules began to regain their dynamic properties. The proportion of time the microtubules spend pausing decreased while the time spent growing increased (table 2). During the time of observation, the growth and shrinkage rates, however, remained depressed, at 3.8 +/-2.8 and 5.6 +/-3.4 respectively (table 2, figure 3). As seen in individual life histories, this results in some microtubules that grow slowly but steadily (figure 4). In figure 3, the arrowhead at 53:41 highlights a

microtubule that has barely grown by 57:36, but microtubule just below it grows 2.3 mm. During recovery from vinblastine, microtubule fragments presumably generated through severing as seen at 8:53 (fig 3) would propel forward into the lamella (arrows at 56:02 and 57:36). Any events resembling this were not included in measurements.

**The effect of vinblastine on growth cone microtubules**

Our studies in the fibroblasts suggested that vinblastine may affect the forward movement of the growth cone and axonal elongation by inhibiting microtubule dynamics. To determine how vinblastine affected neuronal microtubules, we observed fluorescently labeled microtubules in directly in growth cones during vinblastine treatment. We chose to look in the growth cones themselves rather than the axon for several reasons. First, the response of the growth cone to vinblastine is very rapid--usually less than 10 minutes, so it seems that the growth cone may be particularly sensitive at early time points. Indeed, local application of colcemid to cultured chick neurons(?) showed that the growth cone is 100-fold more sensitive to colcemid than the axon. Furthermore, previous photo bleaching of fluorescent microtubule studies have shown that the most dynamic microtubules are in the growth cone. Third, because at least some the microtubules in the growth cone are not bundled, we can resolve the changes in individual microtubules.

We labeled neurons with rhodamine-tubulin and cultured them as described previously. Then while observing the growth cones using epifluorescence at time-lapse intervals ranging from 8.4 to 30 seconds, vinblastine was perfused through the cell chamber. After 10-30 minutes, vinblastine was washed out and observed for 20-45 minutes. Of 23 neurons observed, 13 were analyzed. 7 cells did not grow significantly after wash out

and were not counted while 3 cells were too difficult to analyze because they interacted with other cells during observation.

*Vinblastine selectively eliminates the peripheral, dynamic microtubules in the growth cone.* Prior to vinblastine treatment, growth cones displayed the typical splayed, looped or bundled configurations described previously. In these growth cones, particularly in the splayed and looped configurations, dynamic microtubules extended into the peripheral regions of the growth cone (figure 6, 0 minutes). After addition of vinblastine, the dynamic microtubules no longer extended into the growth cone periphery and only straight, stable microtubule bundles of microtubules or a mass of looped bundles remained in the central region of the growth cone (figure 8, 9). Because perfusion temporarily disturbed the focus, we were unable to determine to what extent the dynamic microtubules incorporated into the bundle, and to what extent the microtubules shrank back and never re-emerged. After vinblastine was removed, single microtubules re-emerged from the bundle and invaded the peripheral regions of the lamella. In figure 7, at time 0, a single microtubule bundle is present a growth cone that has just been washed out of vinblastine. After 4 min. 35 s, three microtubules have grown out into the distal regions of the growth cone (small arrow), while other microtubules have invaded an flat adhesion point further down the axon (large arrow). After 17:03, the growth cone in figure 6 has recovered a normal appearance, with single microtubules spread out through the central region of the growth cone, and filling the bases of the two lamellae (two small arrows).

*Forward translocation of microtubules continues during vinblastine treatment* Our previous studies showed that in addition to undergoing dynamics, microtubules translocate forward during axon outgrowth. In

vinblastine treated neurons, although the dynamic microtubules disappeared, microtubule translocation was still evident. The rate of this translocation could be approximated by measuring the position of the end of the microtubule bundle with time. Since our studies in fibroblasts showed that microtubule dynamics become quite quiescent in vinblastine, we assumed that the coherent movement of an microtubule bundle reflects the forward translocation of polymer. One instance of translocations shown in figure 8. At 0 seconds, the neuron has been treated with vinblastine for approximately 10 minutes. The arrow marks the end of the brightest region of the microtubule bundle. In subsequent frames, this bundle moves forward until, at 132 seconds, the edge of the bundle is more than 2 μm beyond the arrow giving an approximate rate of 1 μm/min. movement. Such bundle movement could measured in 5 growth cones, and yielded an average rate of 0.8 μm/min. We do not know if the lower rate of translocation compared to normal neurons is due to vinblastine treatment itself, or whether the vinblastine treatment results in slower growth which inhibits rapid translocation.

A much more dramatic manifestation of forward translocation was seen in some growth cones with looped microtubules, where it was difficult to measure actual rates of translocation. In 4 cases, when the growth cone stalled after vinblastine treatment, instead of forming a straight bundle, the microtubules continued to translocate forward, so the microtubules accumulated as a twisted mass in the growth cone, with a concomitant depletion of fluorescence in the axon. This phenomenon is shown in figure 9. At 0 min., the growth cone has just been treated with vinblastine. The microtubules are already somewhat looped, and there is a small bulge containing microtubules in the axon behind the growth cone (arrow). At 1

min. 40 sec, the microtubules in the neck area (arrowheads) have become contorted by compression due to microtubule forward translocation into the stalled growth cone. The movement of the microtubule bulge toward the growth cone neck most likely marks the forward translocation of microtubule polymer (arrow, 1:40). At 3:00, the microtubules are even more contorted, and by 6:00, the intensity of fluorescence in the growth cone due to accumulation of microtubule polymer has become noticeably brighter, while the width and intensity of the axon has diminished. This re-distribution of fluorescence is most extreme at 10:00, where the total intensity due to microtubules in the growth cone has increased 1.6-fold from 1.8 million (arbitrary fluorescence units) at 0 min. to 2.9 million at 10 min., while the intensity per unit length in the axon has decreased 2.5-fold from 5803 a.u./pixel, to 2333 a.u./pixel. We interpret this re-distribution to be the wholesale movement of axonal microtubules into the growth cone.

*Microtubules do not invade peripheral lamella during vinblastine treatment*

Although microtubules translocate forward even during vinblastine treatment, in general, these stable polymers do not penetrate or extend into the peripheral lamella. During vinblastine treatment lamella are often unoccupied by microtubules. In normal growth cones, while this may occur transiently, in most cases, some microtubules will eventually populate the lamella. For instance, in figure 6, a large lamella is free of microtubules at 5:00 (arrowheads). 17.5 minutes later, at 22:30, most of the lamella is still unoccupied by microtubules. After vinblastine wash out at 27:30 and 30:30, microtubules fill the lamella (arrows). When the growth cone consolidates into an axonal morphology (34:30 to 35:30), a new lamella extends which is transiently free of microtubules, but at 41:00, a small microtubule bundle has

begun invading the base of the lamella, and at 44:00, a number of microtubules fill the new growth cone in a splayed configuration.

*Correlation of microtubule behavior with growth cone movement* We have described the changes in microtubule morphology and behavior that occur during treatment with 10 nM vinblastine. To relate these observations with our initial phase observations of decreased persistent movement, and increased growth cone wandering in vinblastine, we tracked the growth cone in our fluorescence sequences and correlated the growth cone motility with the changes in microtubule distribution We analyzed 11 cases where we could clearly discern the outline of the growth cone from the tubulin monomer fluorescence, or from matching phase pictures that were taken alternating with the fluorescence pictures. We did not find a particularly strong temporal correlation of the disappearance of peripheral microtubules with the initial inhibition of persistent growth cone movement. In 4 cases, we could not discern any difference between the time at which the dynamic microtubules were lost, and the initial decrease in the growth cone's persistent velocity. In 3 cases, the loss of significant dynamic microtubules lagged the growth cone slowing down by 2-5 minutes. In 3 cases, the growth cone stopped 2-5 minutes after the microtubules were lost. When the growth cone stalled, the microtubules would either remain in a bundle (figure 8) or they would accumulate looped microtubules as in figure 9.

During growth cone wandering, we observed that after a lamella formed, instead of the growth cone microtubules being consolidated into a bundle, with the growth cone then consolidating into new axon as would often occur during normal growth (see figure 6 between 34:30 and 44:00), the vinblastine-treated lamella would either collapse back to the bundle, or it would pull the whole growth towards it, and the microtubule bundle with in the growth

cone would get dragged in that direction. This can be seen in figure 6 between 10 minutes and 22 min. 30 sec. At 10 minutes, substantial portions of the lamella points out to both to the lower left, and the lower right-hand corner of the field (arrowheads). Subsequently, at 14:30 to 22:30, while the gross shape of the growth cone remains similar, the microtubule-free lamella that extends out toward the bottom right corner, pulls the whole growth cone toward that corner (the growth cone moves closer to the asterisk which marks a constant point in the field) even though the microtubules are pointed 90 degrees from that direction.

When we correlated the re-emergence of single microtubules in the lamella with the resumption of persistent growth cone movement, in 10 of 11 cases, we found that the microtubules re-emerged prior to the resumption of growth. In one case, it was difficult to discern any effect of vinblastine on either the growth cone motility or the microtubule distribution. The lag between microtubule emergence and growth cone movement ranged from 2 to 8 minutes. Such a relationship can be seen in figure 7. The growth cone has not moved significantly between 0 and 4 min. 35 sec, yet by the latter time point 3 microtubules have already emerged from the distal end of the microtubule bundle. By 17:03, when there are many microtubules, the growth cone has moved about 40 mm so that the position of the growth cone at time 0 is no longer in the field of view. Figure 6 shows in more detail sequence of events that occur after the vinblastine is washed out. Single microtubules fill the peripheral lamella (27:30, arrow). In 30:30, the arrow at the left points to microtubules that have looped to the left. By 34:30, these microtubules have mostly straightened, and a new lamella has formed in the most distal part of the growth cone. The growth cone clearly begins consolidating into axonal structure at 35:30. The microtubules have

straightened and become bundled, and the growth cone membrane has begun to collapse around the microtubules. At 41:00. new microtubules (arrow) invade the mew lamella, and by 44:00, the growth cone has spread into a fan-like shape, with splayed microtubules (arrows) extending into it.

## DISCUSSION

### Low doses of vinblastine induce growth cone wandering

We have examined the role of microtubule dynamics in growth cone motility and axonal elongation by watching the changes in growth cone behavior and in microtubule distribution induced by low doses of vinblastine. 5-20 nM vinblastine had two immediate effects--the rate of axonal elongation was decreased and growth cones lost their persistent movement. Under these conditions the growth cones would "wander"--they would explore more lateral areas than during normal growth. These observations indicate that at this level of disrupting normal microtubule function, the actin-rich motile apparatus of the growth cone is still intact but the ability of the growth cone to continue directed movement has been compromised. Both the effect on axonal elongation and growth cone wandering are likely derive from the cessation of microtubule dynamics were readily reversible upon removal of vinblastine. It is not necessarily clear whether these two striking effects that are rapidly induced by vinblastine are linked. Do microtubule dynamics play a separate role in the growth cone that may be importance guidance decisions from in the axon, where its primary role may be to supply polymer mass? Or does inhibition of axonal elongation inherently induce growth cone wandering? As discussed below, our observation of microtubules in growth cones during vinblastine treatment lead us to believe that the dynamic growth cone microtubules play an

important role in coordinating growth cone movement with elongation of the microtubule polymer mass.

**Vinblastine inhibits microtubule dynamics in non-neuronal cells**

We confirmed that vinblastine was indeed suppressing microtubule dynamics in cells by measuring microtubule dynamic instability parameters in non-neuronal cells. Similar to in vitro studies of purified tubulin, we found that microtubules in vinblastine spent much of the time in a non-dynamic "paused" state, and that both growth and shrinkage rates are depressed [20]. While high concentrations of vinblastine induce massive microtubule depolymerization, Jordan et al. has postulated that at low concentrations, vinblastine binds to a "high affinity" binding site that exists only at the ends of microtubules, and that this binding inhibits both monomer addition and loss. Our results indicate that this model could be correct, and that vinblastine has similar effect on microtubules inside cells as in vitro.

Although we have followed the dynamics of individual microtubules in cells, we have not determined by other methods whether the whole microtubule array is more stable because of vinblastine addition. In cells, since it is possible only to measure the subset of microtubules that extend sufficiently far out toward the cell periphery where microtubule density is low, it is possible that addition of vinblastine results in the depolymerization of the most dynamic microtubules, uncovering more central microtubules that are more stable and thus have different dynamic properties. We believe that this is unlikely for two reasons. First, our findings are similar to previous results examining purified microtubules in vitro where this problem is less likely to occur. Second, although it is difficult to follow

microtubules during perfusion of vinblastine, it was occasionally possible for us to follow previously dynamic microtubules which became stable in vinblastine.

**The effect of vinblastine on growth cone microtubules**

When we examined microtubules in growth cones during vinblastine treatment, several characteristics were evident. We saw loss of the peripheral microtubules that populate lamella. Most of the growth cone polymer, however, remained in the growth cone as bundles and loops. We did not see retraction of microtubules to the neck or into the axon. When growth cones were followed over time, we observed the translocation of these stable bundles. The forward movement of loops suggests that the machinery for translocation has not been disabled by inhibiting microtubule polymerization. Although we saw quite dramatic instances of translocation, the lamella was not invaded by single microtubules again. This indicates that peripheral microtubules enter lamella by polymerization.

The growth cone wandering that we observed in the phase sequences occurred when a lamella would form and remain unoccupied by microtubules, so they did not consolidate into a bundle and give growth, instead, the lamella would drag the growth cone, (and microtubule bundle) in that direction--it would pull the growth cone toward it, and the microtubules acted as an inflexible, passive mass. In several cases, the growth cone would pull forward but then lose adhesion. When the vinblastine was washed out, straight microtubules re-emerged from the distal end of the bundle and entered the lamella. This appearance of these microtubules preceded resumption of growth. In contrast to the aimless wandering characteristic of vinblastine treated neurons, during recovery, microtubules in the growth

cone would enter the lamella and then the microtubule array would become organized into an elongated bundle, and the membrane would collapse around the microtubules to form new axon.

**The relationship between growth cone motility and axonal elongation.**

Why does the inhibition of the dynamic microtubules by vinblastine result in growth cone wandering? Is growth cone wandering coupled to the inhibition of axonal elongation? It is possible that the persistent movement of the growth cone is directly tied to the microtubule polymerization necessary for axonal elongation. As microtubules assemble and become stable, the growth cone is driven by some mechanism to move away from the stabilized bundle of microtubules. Inhibiting polymerization with vinblastine thus would stop the supply of growing polymer necessary for axonal elongation, and consequently stop growth cone. movement. Therefore, the effect of vinblastine on growth cone wandering is a result of inhibiting the elongation of the axonal microtubules. We do not prefer this model for several reasons. First, when growth cones are treated with vinblastine, we still observe many microtubules in the central part of the growth cone--the microtubules do not recede out of the growth cone. Furthermore, in many cases we still observe the translocation of microtubules into the growth cone. In the most extreme examples, the amount of polymer in the growth cone increases by 50% (figure 9) while the growth cone has stalled. These observations suggest that there is still ample polymer available for axonal elongation. In addition other studies indicate that driving microtubule polymerization, which might be expected to stimulate persistent growth cone movement and axon elongation is not sufficient to drive axonal elongation. The application of taxol to neurons,

which causes microtubule polymerization actually inhibits neurite outgrowth [22]. When microtubules in growth cones treated with taxol were observed, many microtubules formed in the growth cone but the growth cone rapidly stopped its forward progression (preliminary observations). Furthermore, it has been found that rat superior cervical ganglia cells, when treated long term with similar doses of vinblastine continue to slowly extend neurites even though the microtubule polymer mass does not increase, suggesting that translocation mechanisms may be sufficient to support less efficient outgrowth [21]. While the rat cells were not followed by time lapse microscopy so we can not compare the behavior of those growth cones with the present study, it is interesting to note that the authors observe that the rat cells extend more arborized axons in vinblastine. This suggests that the rat growth cones probably underwent similar meandering during vinblastine treatment.

We therefore interpret our results as implicating a role of dynamic growth cone microtubules in guiding the persistent movement of the growth cone, and in controlling the formation of the new axonal microtubule bundle. As mentioned above, our observations indicate that ample polymer remains in vinblastine treated neurons, but these microtubules can not organize themselves and the growth cone into an axonal form. In the absence of this organization the growth cone is remains capable of forming large areas of lamella which can either exert force on the growth cone or retract. We believe that the microtubules could act in two ways. First, we found that the extension of single microtubules into the base of lamella precedes the resumption of outgrowth. In addition to the observation that the stable bundles in vinblastine do not invade lamella, it suggests that the role of the dynamic microtubules is to enter the peripheral lamella. While

we know from our previous studies that microtubules transiently enter lamella that are not eventually stabilized, indicating that entry of microtubules is not sufficient to stabilize a lamella, we believe our present results suggest that the peripheral microtubules are necessary or important in the stabilization of a lamella that will eventually become consolidated into new axon by the bundling of microtubules.

In terms of mechanism, we speculate that there may be two activities of the peripheral microtubules that are important for the consolidation of the lamella. First, we predict that there may be discrete sites in the lamella that bind the microtubules at least transiently. These microtubules may be then important in then allowing the other, more stable microtubules to bundle around them. Thus, the dynamic microtubules would help guide the direction and rate of bundling within the growth cone. This bundling may be mediated by microtubule-microtubule sliding. The dynamic microtubules in the lamella would have two properties that would be important for organizing the bundling of microtubules. First, unlike the stable microtubules, which become more kinked the longer they have survived in the cytoplasm, the newly formed dynamic would be relatively straight, providing a good template for bundling microtubules in the proper orientation [23]. Second, having just formed, the microtubules would not be coated with proteins, or would not be modified by mechanisms that depend on longer residence in the cytoplasm, allowing accessibility to other binding proteins, such as, perhaps lamella. The organized bundling of microtubules into a lamella may then itself induce the growth cone cortex to collapse around it. In vinblastine, the dynamic microtubules no longer invade the lamella, so the efficiency of bundles forming at the bases of lamella becomes very inefficient.

The association of microtubules with sites in the lamella, particularly the bases of filopodia have previously been noted using immunofluorescence and EM [24-26] and observations of translocating microtubules in fibroblast lamella (Chapter 3) also support the existence of such binding sites. It is likely that such an association has not been clearly distinguishable in our initial and our present observations of microtubules in living growth cones for two reasons. First, during microtubule bundling and the consolidation of the growth cone into axon when microtubule binding to such sites would be occurring, the bundled microtubules quickly overtake the dynamic microtubules that extend into the lamella. Therefore, it is impossible to follow the peripheral microtubules for extended periods of time to determine if these microtubules persist in the lamella longer than expected by their dynamic instability properties. Second, the association of microtubules with such sites may be transient. Because other dynamic microtubules are likely to invade the same area, it may not be necessary for any single microtubule to persist for an extremely long time, if another microtubule may replace it by binding the lamella in the same region.

It is worth considering briefly that the dynamic growth cone microtubules main role may not be as a structural scaffold, but as a detector of cellular conditions. During mitosis, the proper assembly of the mitotic spindle appears to be an important point of feedback control for the progression in mitosis [27]. Treatment of dividing Hela cells with similar doses of vinblastine or other microtubule-disrupting agents results in mitotic arrest [19]. It has been suggested that cells monitor the association of microtubules with other spindle components such as kinetechores, and activates a feedback control mechanism that delays mitosis if the proper associations have not been made. It is possible that microtubules play an

analogous role in sensing the state of the cell during neurite outgrowth. A feedback system may monitor the binding of microtubules to specific sites in the growth cone. If the proper sites are not bound, then the cell may stimulate a signal that inhibits the further consolidation of the axon. In the realm of cell signaling, many of the same molecules, such as ras, the receptor tyosine kinases and MAP kinase, that govern regulation of mitogenesis are important for neuronal differentiation [28]. There may certainly be other parallels between the control of mitogenesis and control of neuronal differentiation.

1.Harris, W. A., Holt, C. E. and Bonhoeffer, F. 1987. Retinal axons with and without their somata, growing to and arborizing in the tectum of Xenopus embryos: a time-lapse video study of single fibres in vivo.. Development 101: 123-33.

2.Harris, A. K., Pryer, N. K. and Paydarfar, D. 1990. Effects of electric fields on fibroblast contractility and cytoskeleton.. J Exp Zool 253: 163-76.

3.Gundersen, R. W. and Barrett, J. N. 1980. Characterization of the turning response of dorsal root neurites toward nerve growth factor. J. Cell Biol. 87: 546-554.

4.Daniels, M. P. 1973. Fine structural changes in neurons associated with colchicine inhibition of nerve fiber formation in vitro. J. Cell Biol. 58: 463-470.

5.Yamada, K. M., Spooner, B. S. and Wessells, N. K. 1970. Axon growth: role of microfilaments and microtubules. PNAS 66: 1206-1212.

6.Yamada, K. M., Spooner, B. S. and Wessells, N. K. 1971. Ultrastructure and function of growth cones and axons of cultured nerve cells. J Cell Biol 49: 614-635.

7.Daniels, M. P. 1972. Colchicine inhibition of nerve fiber formation *in vitro.* J.Cell Biol. 53: 164-176.

8.Porter, K. R. 1966. Cytoplasmic microtubules and their functions. Principles of Biomolecular Organization 308-356.

9.Bunge, M. B. 1973. Fine structure of nerve fibers and growth cones of isolated sympathetic neurons in culture. J Cell Biol 56: 713-735.

10.Heidemann, S. R., Landers, J. M. and Hamborg, M. A. 1981. Polarity orientation of axonal microtubules. J. Cell Biol. 91: 661-665.

11.Heidemann, S. R., Hamborg, M. A., Thomas, S. J., Song, B., Lindley, S. and Chu, D. 1984. Spatial organization of axonal microtubules. J. Cell Biol. 99: 1289-1295.

12.Cheng, T. P. and Reese, T. S. 1988. Compartmentalization of anterogradely and retrogradely transported organelles in axons and growth cones from chick optic tectum. . J Neurosci 8: 3190-9.

13.Lim, S., Sammack, P. J. and Borisy, G. G. 1989. Progressive and spatially differentiated stability of microtubules in developing neuronal cells. J. Cell Biol. 109: 253-264.

14.Okabe, S. and Hirokawa, N. 1990. Turnover of fluorescently labeled tubulin and actin in the axon. Nature 343: 479-482.

15.Tanaka, E. and Kirschner, M. 1991. Microtubule behavior in the growth cones of living neurons during axon elongation. J Cell Biol 115: 345-363.

16.Bamburg, J. R., Bray, D. and Chapman, K. 1986. Assembly of microtubules at the tip of growing axons. Nature 321: 778-790.

17.Reinsch, S. S., Mitchison, T. J. and Kirschner, M. W. 1991. Microtubule polymer assembly and transport during axonal elongation. manuscript submitted

18.Jordan, M. A. and Wilson, L. 1990. Kinetic analysis of tubulin exchange at microtubule ends at low vinblastine concentrations. . Biochemistry 29: 2730-9.

19.Jordan, M. A., Thrower, D. and Wilson, L. 1992. Effects of vinblastine, podophyllotoxin and nocodazole on mitotic spindles. Implications for the role of microtubule dynamics in mitosis. . J Cell Sci

20.Toso, R. J., Jordan, M. A., Farrell, K. W., Matsumoto, B. and Wilson, L. 1993. Kinetic stabilization of microtubule dynamic instability in vitro by vinblastine. . Biochemistry 32: 1285-93.

21.Baas, P. W. and Ahmad, F. J. 1993. The transport properties of axonal microtubules establish their polarity orientation. J Cell Biol. 120: 1427-1437.

22.Letourneau, P. C., Shattuck, T. A. and Ressler, A. H. 1987. Pull and push in neurite elongation: observations on the effects of different concentrations of cytochalasin B and taxol. Cell Motility and Cytoskel 8: 193-209.

23.Schulze, E. S. and Kirschner, M. W. 1987. Dynamic and Stable Populations of Microtubules in Cells. J. Cell Biol. 104: 277-288.

24.Letourneau, P. C. 1983. Differences in the organization of actin in the growth cones compared with the neurites of cultured neurons from chick embryos. J Cell Biol 97: 963-973.

25.Letourneau, P. C. 1981. Immunocytochemical evidence for colocalization in neurite growth cones of actin and myosin and their relationship to cell--substratum adhesions. . Dev Biol 85: 113-22.

26.Bridgman, P. C. and Dailey, M. E. 1989. The organization of myosin and actin in rapid frozen nerve growth cones. J Cell Biol 108: 95-109.

27.Murray, A. W. 1992. Creative blocks: cell-cycle checkpoints and feedback controls. Nature 359: 599-604.

28.Borasio, G. D., John, J., Wittinghofer, A., Barde, Y. A., Sendtner, M. and Heumann, R. 1989. ras p21 protein promotes survival and fiber outgrowth of cultured embryonic neurons. Neuron 2: 108-1096

**Figure legends**

Figure 1 Timelapse sequence of a growth cone responding to 10 nM vinblastine. Prior to vinblastine treatment *(c)*, the growth moves along a straight line, resulting in rapid axonal elongation. In 14 minutes the growth cone has traveled 34 μm. Arrowheads at 0 and 5 minutes show lamella that are transiently extended in multiple directions while the growth cone generally proceeds toward the bottom right corner of the field. Vinblastine was added at 11 minutes *(v)*. At 20 minutes (9 min. after vinblastine addition), the growth cone has stopped its forward progression, and by 25 min. has begun exploring laterally. At 37 minutes, the growth cone is shrinking back from its upper branch, and the lower branch (asterisk) is gaining dominance. Vinblastine was washed out at 66 minutes *(w)*. By 74 minutes, the lower branch (asterisk), is remaining, and a growth cone sprouts from its end at 80 min. At 86 minutes, that growth cone has consolidated into new axon, and the growth cone has continued to move forward at 91 minutes. The frame of reference is the same for 0 through 14 minutes. It is changed but constant for 20 through 37 minutes, and then again, for 74 through 91 minutes. The white asterisks in frame 37 and 74 mark approximately the same spot on the substrate. Scale bar, 10 μm

Figure 2. (A). Growth cone trajectories of three neurons treated with 5, 10, 20 nM vinblastine. Each point represents the XY position of the growth cone centroid at a given time with constant time between each point (1 min.). The large arrow at the beginning of each trajectory denotes the direction of growth cone movement and axonal growth. At point *(c)*, control media is washed through, *(v)* vinblastine is washed in, and *(w)*, vinblastine is washed out.

Asterisks denote times during vinblastine incubation where the growth cone wanders astray from a uniform path. (B). Growth cone velocity along the direction of growth. The distance of each point from the initial point of each trajectory shown in (A) was calculated and the instantaneous velocity was calculated from these distances. Plot represents the running average of five instantaneous velocities with respect to time. (C). Absolute growth cone velocity. Instantaneous velocities were calculated from the distance between each point. Plots repellent the running average of 5 growth cone instantaneous velocities with respect to time.

Figure 3. Microtubule dynamics in a non-neuronal cell before, during and after 10 nM vinblastine treatment. 0 to 36 seconds (*control (c) column*) shows microtubule dynamics prior to vinblastine treatment. Microtubules display typical dynamic instability behavior. Large and small arrowheads highlight two microtubules that undergo rapid shrinkage events while arrows show microtubules undergoing growth. At 52s to 8 min. 53 s *(vinblastine (v) column)* the cell has been treated with 10 nM vinblastine. Many microtubules are stable during this interval. Of three microtubules (arrowheads), two are stable for the 8 minute interval, while one depolymerizes. Similarly, one of the two microtubules (small arrows) remains stable while the other depolymerizes. The stable microtubule in the upper left region (larger arrow) becomes kinked (3:51) and is eventually severed (8:53). At 53:41 through 57:36 (*wash (w) column)* the cell has been recovering from vinblastine treatment for (29 minutes). In the upper region (arrowhead), two microtubules grow out between 53:41 and 57:36. The arrows at 56:02 and 57:36 indicate a microtubule fragment that appears. Scale bar, 5 μm.

Figure 4. Histories of individual microtubules in non-neuronal cells before vinblastine treatment (A.), in 10 nM vinblastine (B.), and after washing out vinblastine (C.)

Figure 5. Histograms of growth and shrinkage rates. *(a,d)* Growth and shrinkage rates for control cells prior to vinblastine treatment. Mean growth and shrinkage rates were 6.4+/-3.25 and 14.3 +/- 8.5 μm/min. respectively. *(b,e)* 10 nM vinblastine treated cells. Mean growth and shrinkage rates were 3.1 +/- 3.4 and 5.1 +/- 4.0 μm/min. *(c,f)* Cell after washing out vinblastine. Mean growth and shrinkage rates were 3.8+/-2.8 and 5.6 +/-3.4 μm/min.

Figure 6. Complete timelapse sequence of microtubules in a growth cone treated with 10 nM vinblastine. Before vinblastine addition (time 0), single microtubules spread throughout the growth cone. Just after vinblastine addition (5:00), single microtubules can still be seen. During the remainder of vinblastine treatment, sparse bundles of microtubules populate the growth cone. The bundles move forward within the growth cone (arrows, time 10:00-22:30). During vinblastine the lamella becomes quite large, but remains unoccupied by microtubules (arrowheads, 5:00 through 22:30). After vinblastine wash out( 27:30-44:00), microtubules populate the distal regions of the lamella (arrows, 27:30 and 30:30). These microtubules become consolidated into a bundle (34:30-41:00) and axon growth resumes. During this rapid outgrowth, a long lamella forms at the end of the growth cone in 35:30, but is quickly invaded by microtubules at 41:00 and 44:00 (arrows). The field is moved several times during the sequence, the asterisk marks a constant position on the substrate. Scale bar, 10 μm

Figure 7. Recovery of the growth cone from vinblastine. At time 0, 10 nM vinblastine has just been washed out. While a bundle remains in the growth cone, no single microtubules are evident in the distal end or the protrusion in the lower right corner. 4 min. 35s later, the growth cone has spread but not moved forward and several single microtubules (small arrow) have merged at the distal end of the bundle, as well as several in the lower protrusion (large arrow). At 17 min. 3s, many single microtubules have re-populated the distal regions of the growth cone (small arrows). The growth cone at 0:00 and 4:35 are in the same frame of reference. In 17:03, the stage was moved to keep the growth cone in the field of view. The growth cone has grown approximately 40 μm between 4:35 and 17:03. Scale bar, 5 μm.

Figure 8. The forward translocation of microtubule bundles during vinblastine treatment. The growth cone has been treated with 10 nM vinblastine for approximately 10 minutes. During 132 seconds, the microtubule bundle translocates approximately 3.5 μm with respect to the substrate. The arrow marks a constant position on the substrate. Scale bar, 5 μm.

Figure 9. Accumulation of microtubule loops in the growth cone with depletion of microtubules from the axon during vinblastine treatment. The neuron has been treated with vinblastine for 4 minutes. In the course of 10 minutes, microtubule loops accumulate in the growth cone by the translocation of microtubules from the axon into a stationary growth cone. The arrow at time 0 and 1 min. 40s follows the forward translocation of a nodule of microtubules towards the neck of the growth cone. Comparison of

10:00 with 0:00 shows that the microtubules in the growth cone have become compacted, with the total intensity of fluorescence signal increasing 1.6-fold, while the caliber markedly and fluorescence intensity of the axon per unit length has decreased 2.5-fold. Scale bar, 5 μm

| concentration | | MOTILITY VELOCITY (microns/min) pre-control | control | vinblastine | wash | PERSISTANT VELOCITY (microns/min) pre-control | control | vinblastine | wash |
|---|---|---|---|---|---|---|---|---|---|
| 5 nM | *(rate)* | 4.00 | 3.11 | 2.53 | 2.99 | 3.34 | 2.02 | 0.99 | 1.2 |
| | *(percent)* | 129% | 100% | 81% | 96% | 165% | 100% | 49% | 59% |
| 10 nM | | 2.88 | 3.07 | 2.3 | 2.7 | 1.79 | 2.17 | 0.51 | 1.71 |
| | | 94% | 100% | 75% | 88% | 82% | 100% | 24% | 79% |
| 20 nM | | 2.68 | 2.84 | 2.05 | 2.14 | 1.91 | 2.04 | 0.73 | 1.7 |
| | | 94% | 100% | 72% | 75% | 94% | 100% | 36% | 83% |

| | control | vinblastine (10nM) | wash |
|---|---|---|---|
| catastrophe frequency (s -1) | 0.015 | 0.007 | 0.009 |
| rescue frequency (s -1) | 0.015 | 0.004 | 0.009 |
| percent growth time | 36.5 | 7.9 | 25.9 |
| percent shrinkage time | 20.5 | 11.2 | 16.1 |
| percent pause time | 42.9 | 80.8 | 58 |
| mean growth rate (microns/min) | 6.5+/-3.255 | 3.2+/-3.4 | 3.8+/-2.8 |
| mean shrinkage rate (microns/min) | 14.3 +/-8.5 | 5.1+/-4.0 | 5.6+/-3.4 |

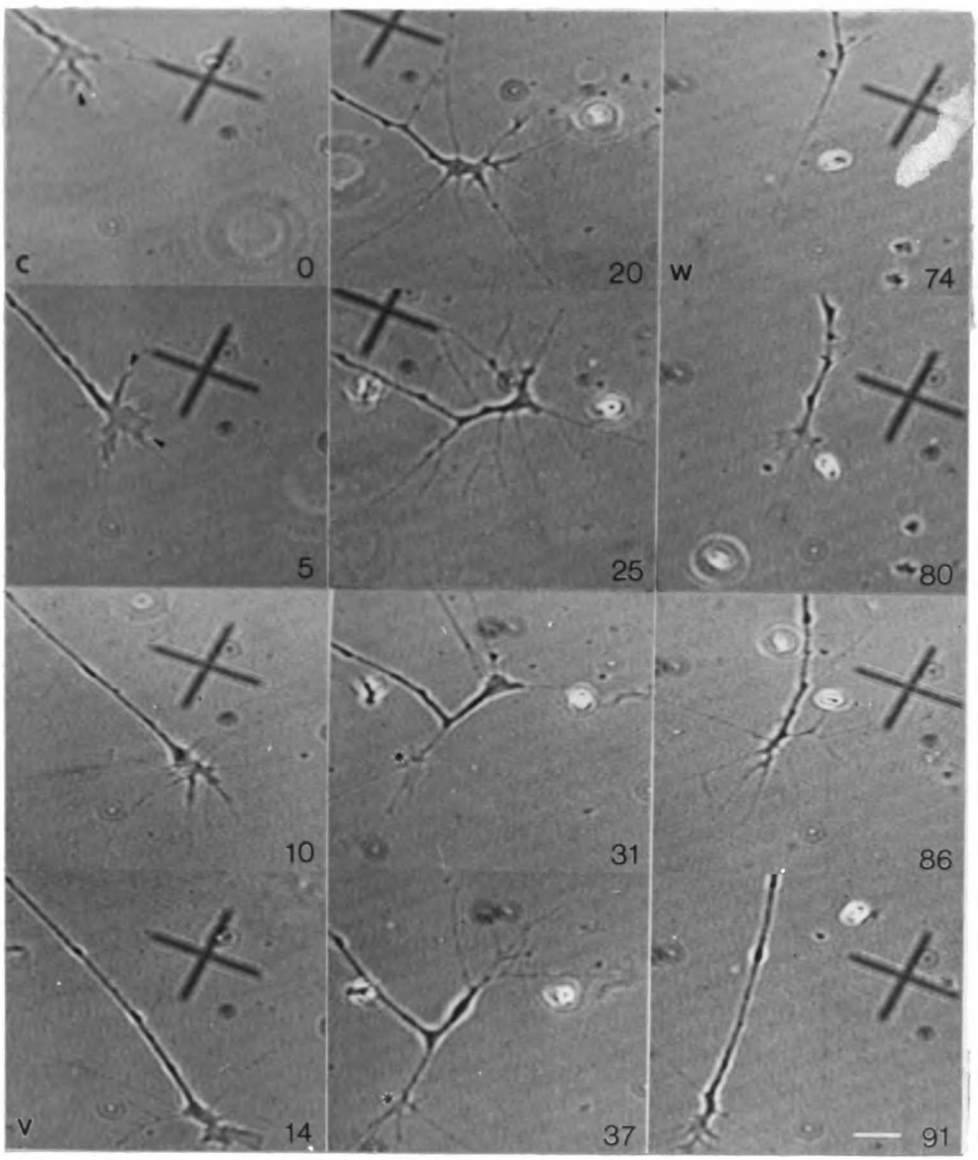
C
0
20
W
74
5
25
80
10
31
86
V
14
37
91

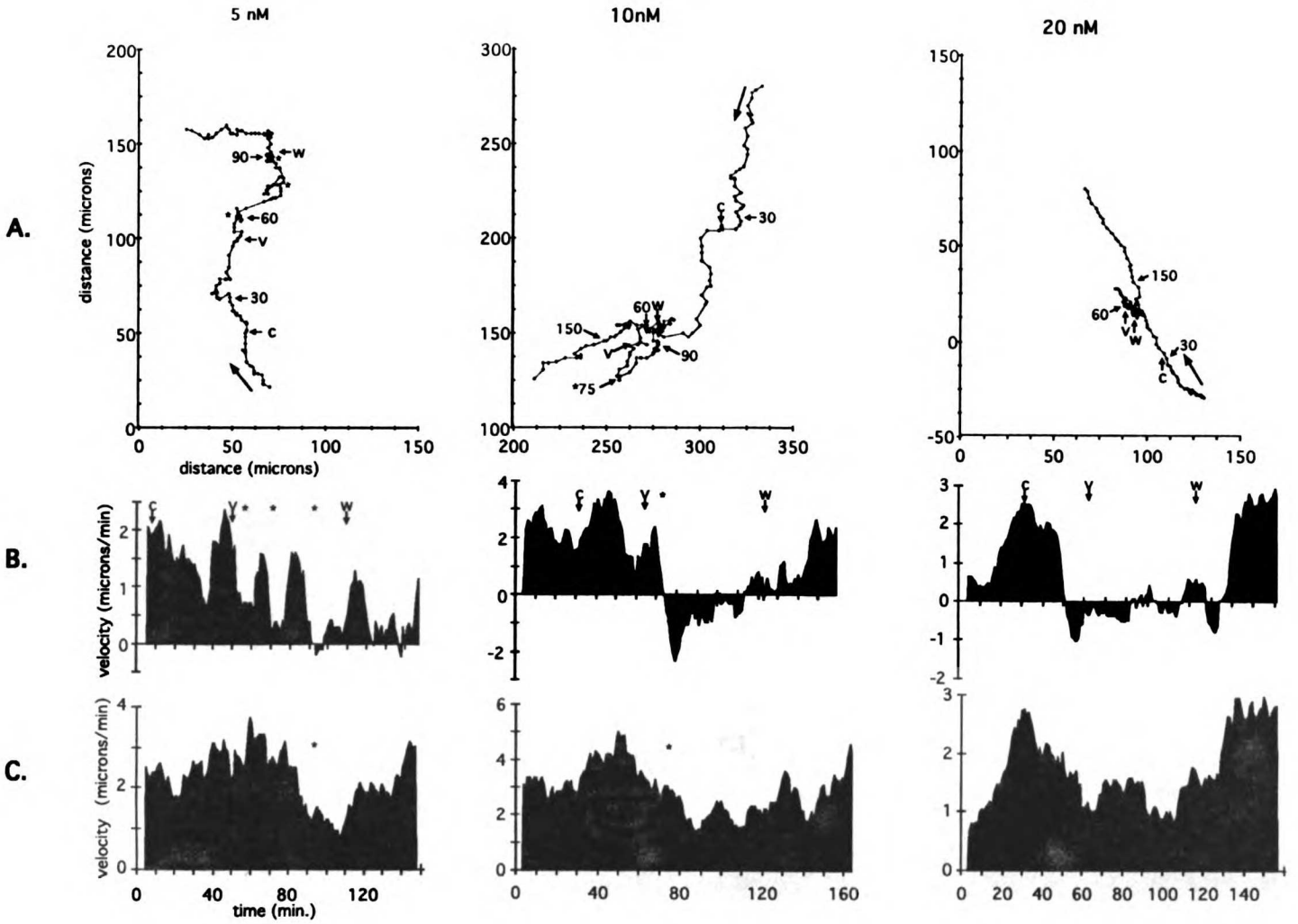
A.
B.
C.
5 nM
10nM
20 nM
distance (microns)
velocity (microns/min)
time (min.)
c
y
w
90
60
v
30
150
75

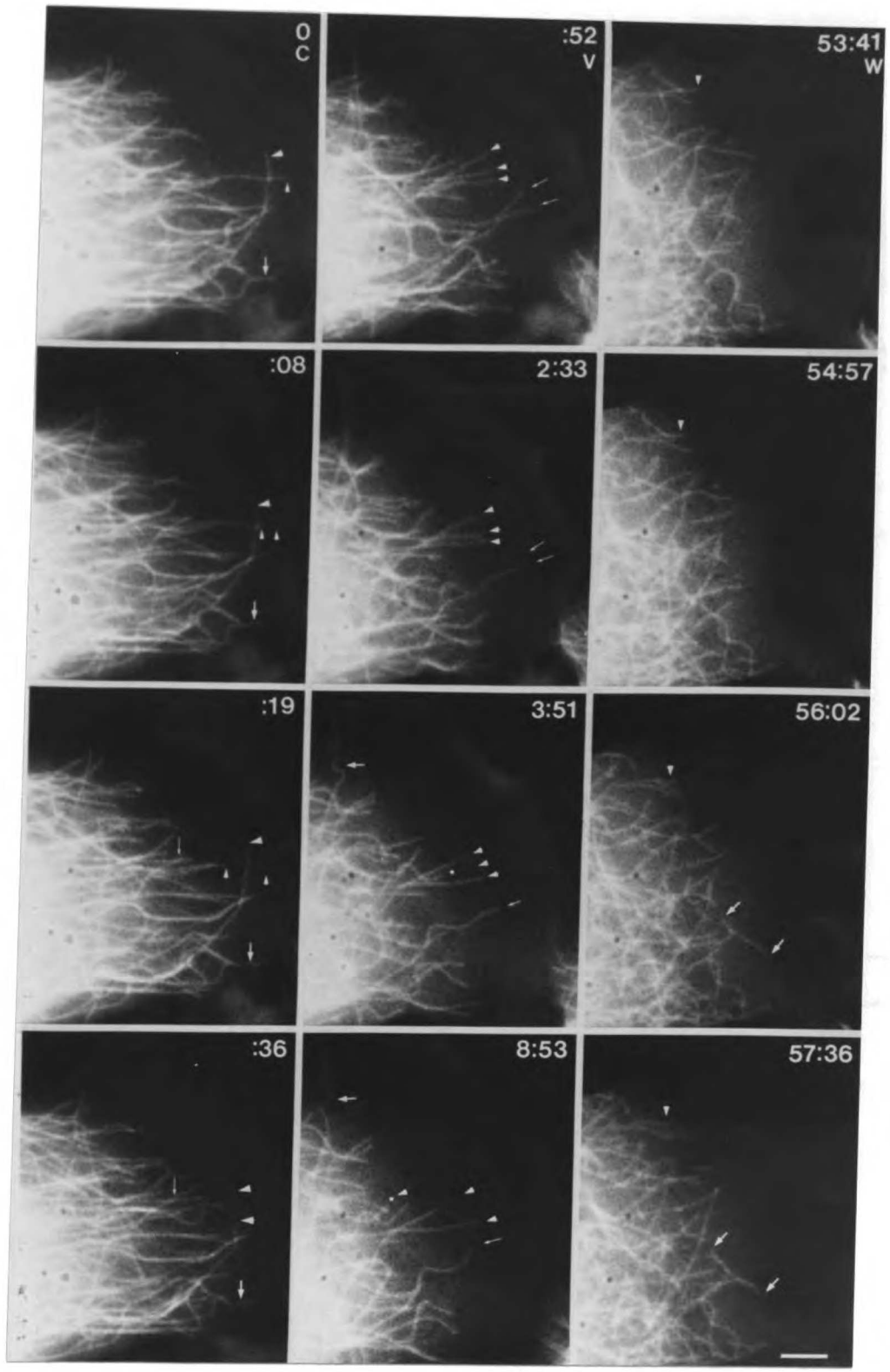
0
C
:52
V
53:41
W
:08
2:33
54:57
:19
3:51
56:02
:36
8:53
57:36

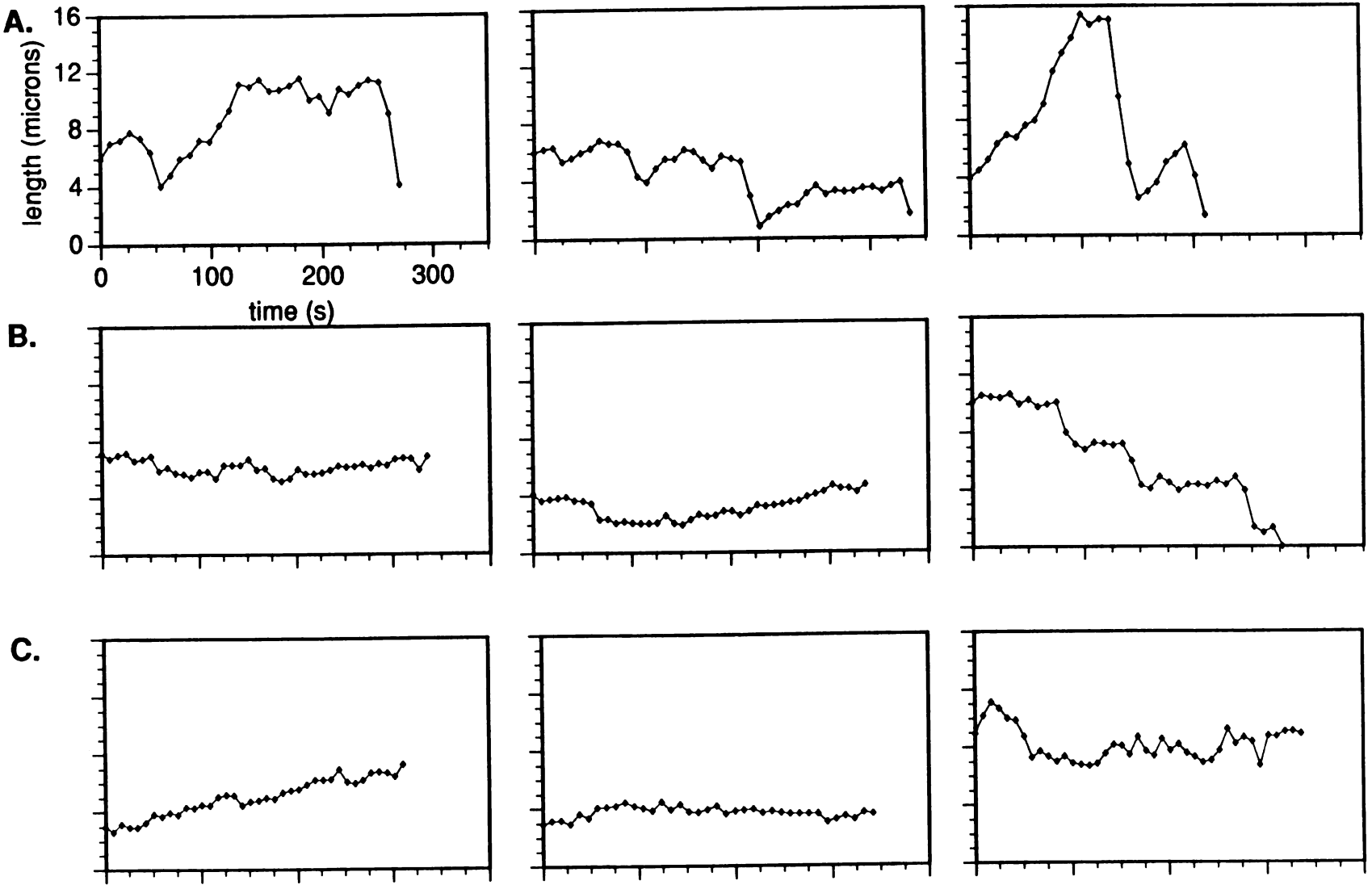
A.
B.
C.
length (microns)
16
12
8
4
0
0
100
200
300
time (s)

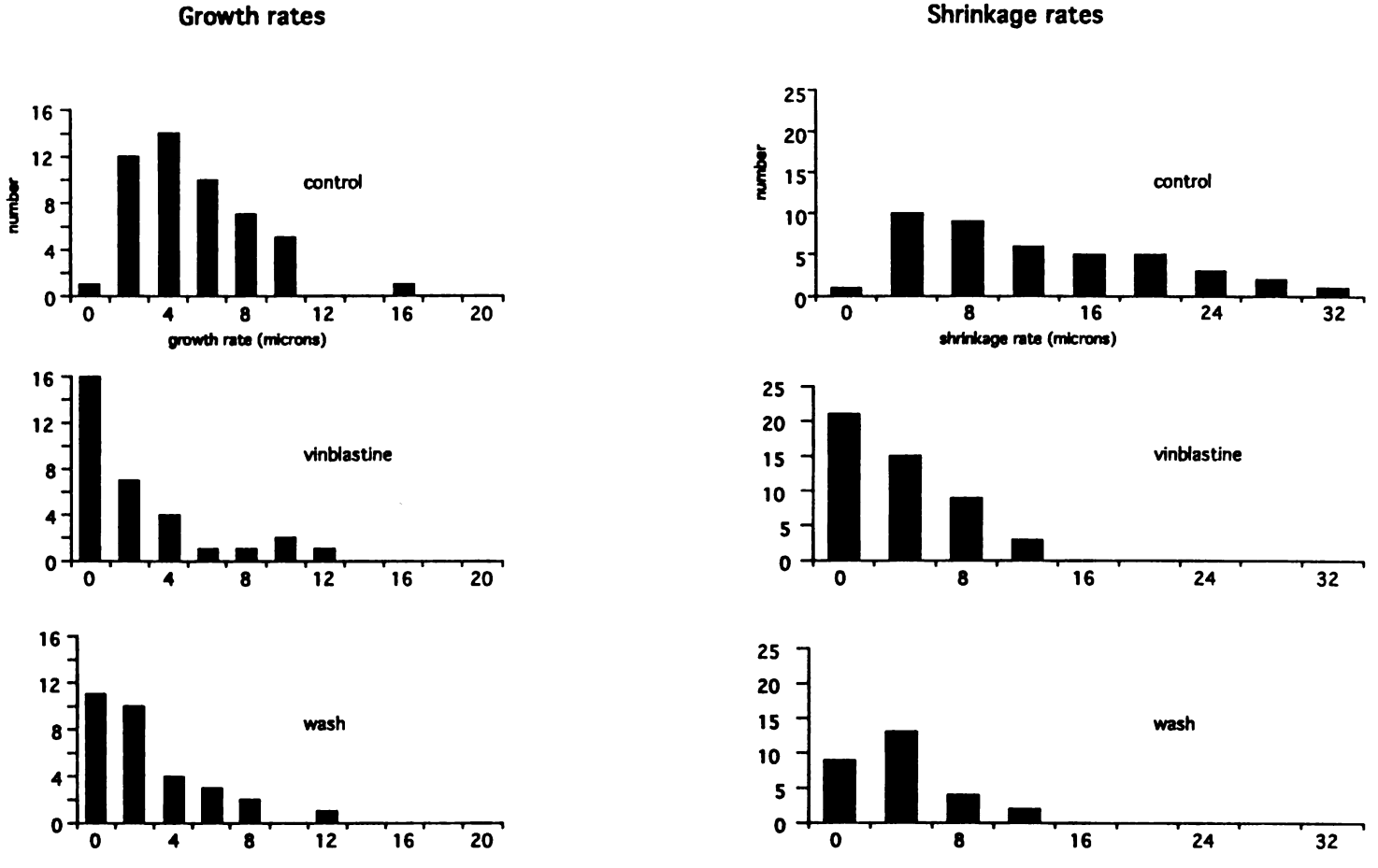
Growth rates
Shrinkage rates
number
control
growth rate (microns)
shrinkage rate (microns)
vinblastine
wash
0
4
8
12
16
20
24
32
5
10
15
20
25

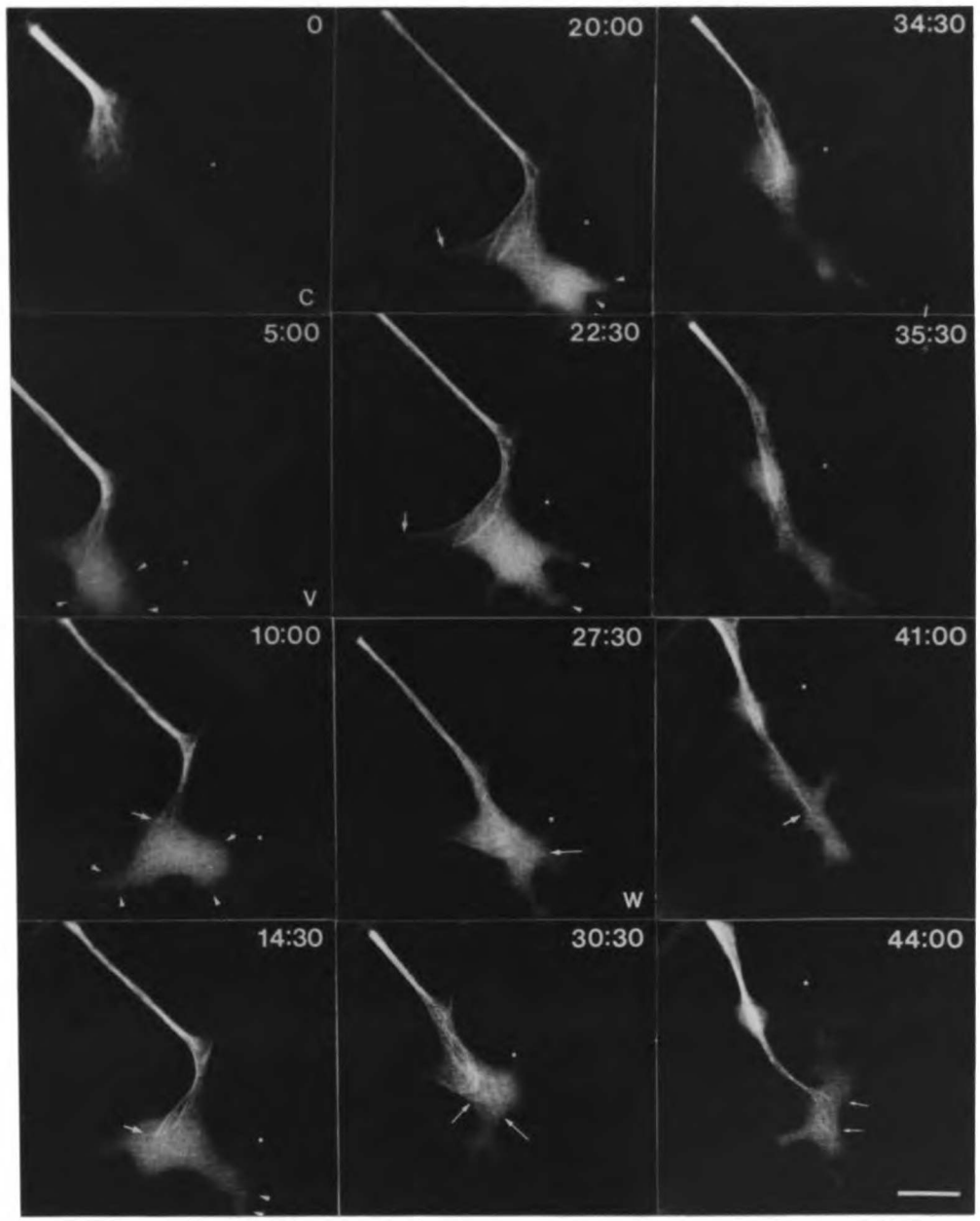
0
20:00
34:30
C
5:00
22:30
35:30
V
10:00
27:30
41:00
W
14:30
30:30
44:00

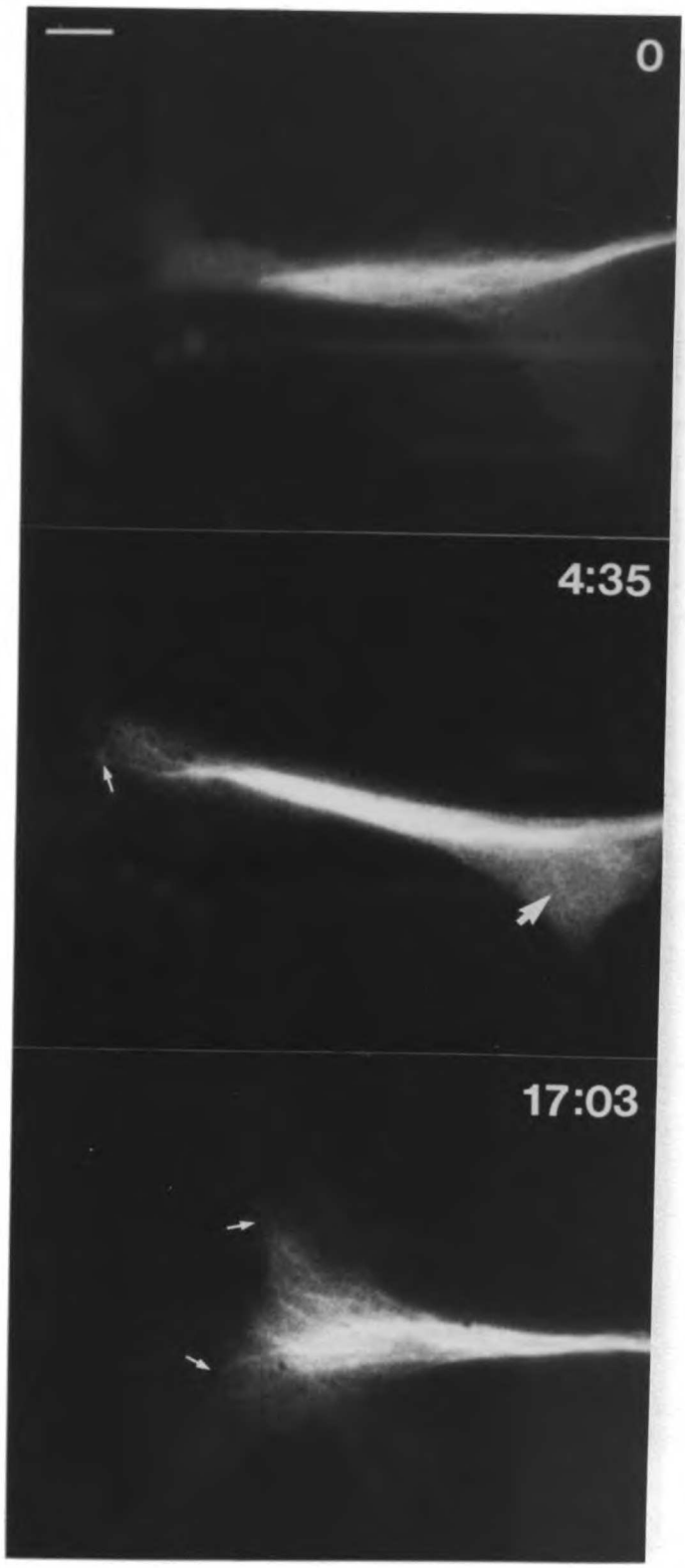
0
4:35
17:03

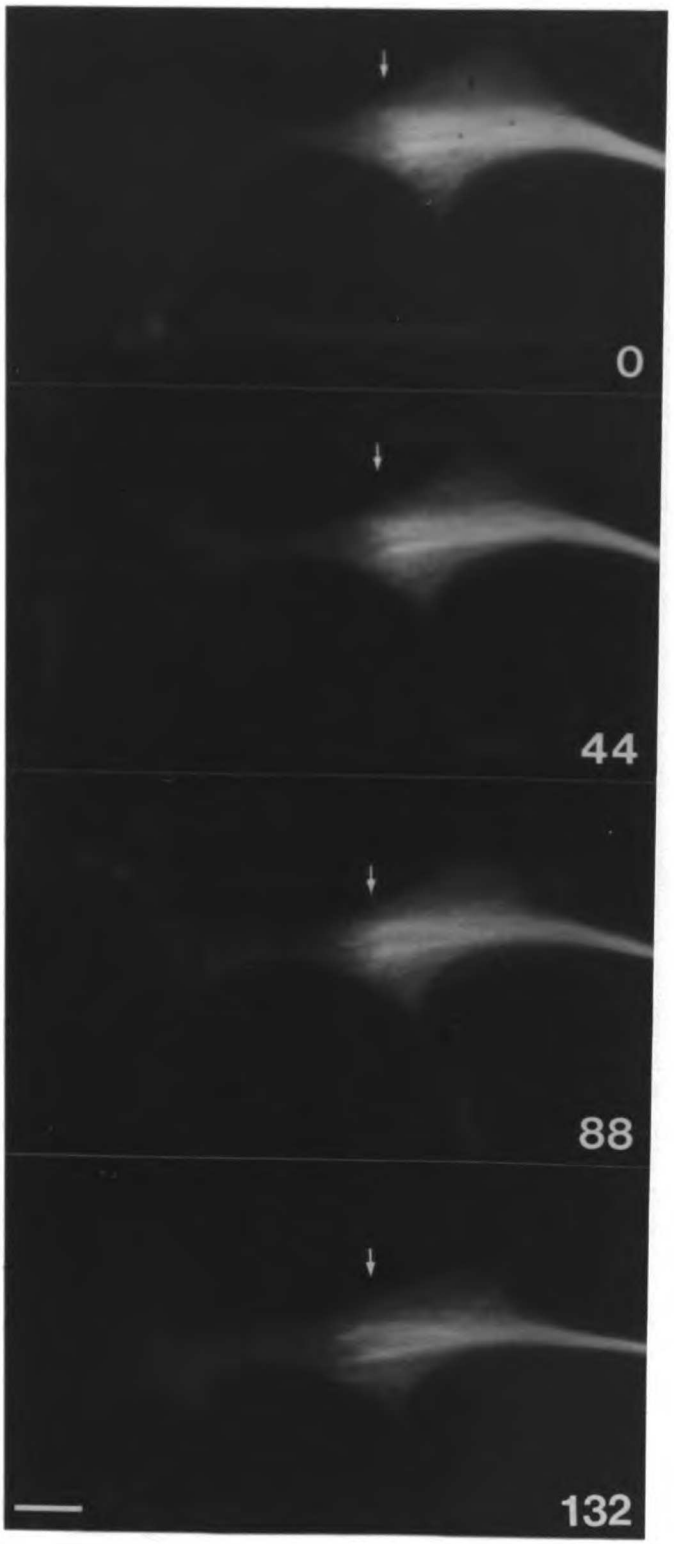
0
44
88
132

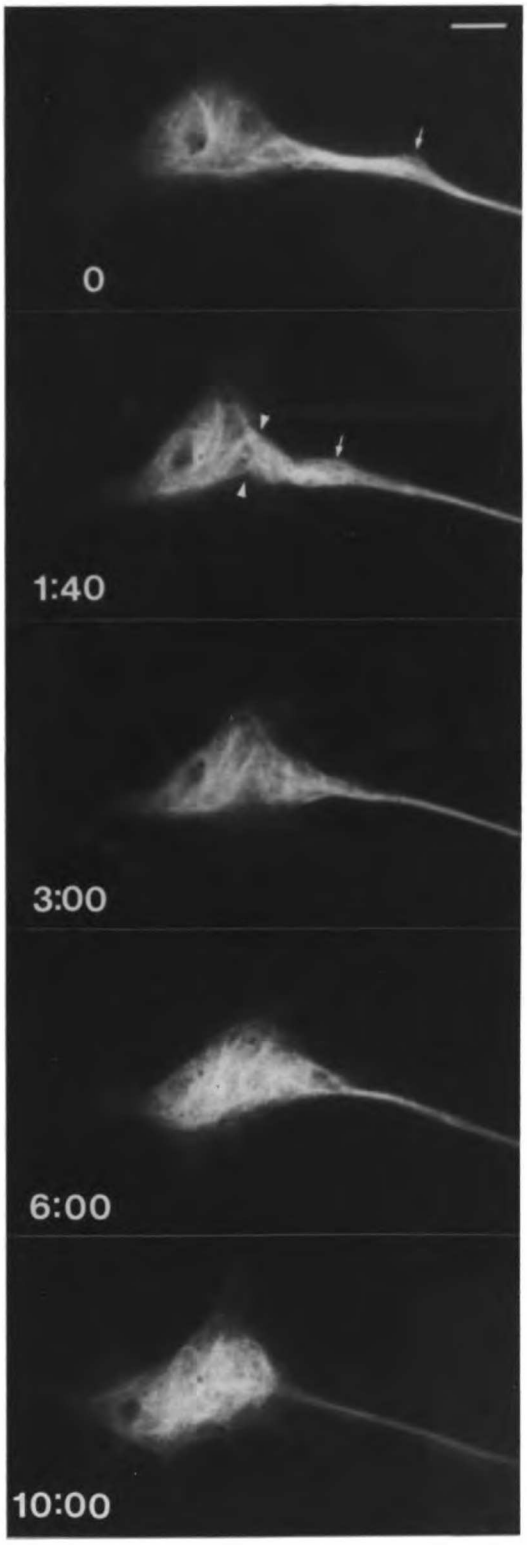
0
1:40
3:00
6:00
10:00

# Chapter 5
# Future Directions

## FUTURE DIRECTIONS

I have characterized individual microtubule behavior in growth cones during axonal elongation and turning to understand how microtubule dynamics and polymer movement are controlled to generate the highly organized microtubule array in neurons. The goal of this work was to identify the activities that modulate microtubules in growth cones as a means for establishing biochemical assays for studying these activities with purified tubulin in vitro.

To follow microtubules in living neurons, I along with Sigrid Reinsch, developed a novel approach to fluorescently label neuronal microtubules by microinjection of Xenopus eggs and culturing the neural tubes (Chapter 2). This approach had several critical advantages over the micro-injection of single neurons. The slow turnover of some axonal microtubules makes it difficult to uniformly label microtubules when differentiated neurons are directly microinjected. In contrast, injecting the egg assured that the all microtubules in the neurons that we observed were labeled. Furthermore, many cells were labeled by one rather simple microinjection. By plating cells by explants, it was very easy to find labeled neurons, whereas with direct microinjection, it is often difficult to re-locate injected cells. For observation, the Xenopus neurons appeared to be particularly resistant to photodamage. This is likely due to culturing at room temperature rather than at 37 C, and to the presence of reducing factors in embryonic cells which can mitigate oxidative damage. This resistance to photodamage was increased further by observing the cells under anoxic conditions.

For fluorescence observations, I established the use of a cooled CCD camera as the optimal means of imaging single microtubules in living cells. Previously, in our laboratory, Silicon Intensified Target (SIT) or intensified

SIT (ISIT) cameras were used to record cellular microtubules [1]. I found that these video cameras did not have sufficiently low noise to cleanly detect microtubules in the Xenopus neurons which were less brightly labeled and thicker than injected fibroblasts. The main advantage of the cooled CCD was its extremely low noise levels given its sensitivity of detection so very short exposures of the cells would yield very clean images. Furthermore, the CCD camera was able to integrate the signal over the length of the exposure because of its low noise characteristics rather than averaging the signal as is done with video cameras.

After developing these technical advances, it became possible to cleanly visualize microtubules in living neurons. I could not analyze neuronal microtubule dynamics in detail because most microtubules would become incorporated in microtubule bundles where, due to the resolution limits of the light microscope, I could not follow single microtubules. I found, however, that the organization and localization of microtubules during axonal growth and guidance relies heavily on translocating microtubule polymer within the growth cone and by microtubule bundling. In the following sections I will describe the various behaviors of growth cone microtubules and their role in axonal growth and guidance as well as the likely biochemical activities responsible for the behaviors.

**The role of microtubule dynamics in growth and guidance**

I compared the dynamics of microtubules in growth cones to the dynamics of pure tubulin at steady state or microtubules in non-growing cells such as fibroblasts expecting to find that one of the dynamic parameters (growth rate, shrinkage rate, catastrophe and rescue frequencies) might be different, accounting for the stabilization and net growth of polymer in

neurons (chapter 2). While I found that growth cone microtubules were dynamic, I could not directly detect a difference in dynamic instability parameters that accounted for the net growth of the microtubule array. This failure does no suggest that microtubule dynamics are not modulated, but rather is related to the difficulty in following microtubules over long periods of time (chapter 2).

To establish whether elongation of the microtubule array occurs by polymerization and stabilization of growth cone microtubules, it will be necessary to do high-resolution photoactivation of microtubules in the growth cone and neck combined with fluorescence imaging of total microtubules. With this approach it will be possible to determine how many microtubules are sliding forward, and whether this forward sliding accounts for the elongation of the microtubule array. Until now, this approach has been unfeasible primarily because the hydrophobic characteristics of caged fluorescein (Tim Mitchison, personal communication) yielded very poor labeling of tubulin, so enough photoactivated signal could not be generated for imaging single microtubules. The development of caged-rhodamine (Tim Mitchison, personal communication) and also the development of more sensitive CCD cameras holds promise that this experiment will become feasible in the future. Neurons could be co-injected with caged rhodamine and fluorescein-tubulin so total microtubules could be followed in fluorescein and microtubule movement and turnover could be monitored in rhodamine. This would require development of efficient double dichroic mirrors for high output fluorescence of both rhodamine and fluorescein signals using filter wheels. Alternatively, it may be possible to inject rhodamine-tubulin and caged -rhodamine tubulin, and follow a brighter spot

of photoactivated polymer on a dimmer background of rhodamine tubulin then only one fluorescent channel could be used.

While modulation of microtubule dynamics must occur in neurons, it will be very difficult to study in living neurons. In vitro studies examining the effect of the neuronal MAP, tau, on microtubule dynamics showed that tau affects all measurable dynamic instability parameters resulting in longer, more stable microtubules. Phosphorylation of tau with MAP kinase inhibited its function by reducing its affinity for microtubules [2]. Given this data, it would be interesting to determine if phosphorylation of tau is localized within the neuron.

While Xenopus neurons are not the optimal cell in which to study regulation of microtubule dynamics, the non-neuronal cells in the explant cultures may present a good opportunity to do so. Dynamics of individual microtubules could readily be followed in the lamella of spread cells under various conditions (Chapter 4). Observations of these cells would have the same benefits as for the neurons, namely, ease of labeling and resistance to photodamage. It would be interesting to examine the effect of cell-cell contact on microtubule dynamics as work on cell-cell contact of Aplysia growth cones suggests that microtubule behavior is modified by such signals. Immunohistochemical studies suggest that phosphatase inhibitors destabilize microtubules in cultured cells [3]. It should be easy with this system to directly determine the effect of activating signaling pathways such as receptor tyrosine kinases, or G-proteins on microtubule dynamics using RTK ligands, or kinase activators and inhibitors. It may also be possible to determine the effect of various proteins on microtubule dynamics either by injecting RNA or protein directly into the plated cells, or into the Xenopus egg.

To test the role of dynamics in neurite outgrowth I inhibited dynamics with low doses of vinblastine. These experiments indicate that microtubule dynamics are crucial for persistent axonal elongation (Chapter 4). The immediate response of the growth cone to the drug suggests that growth cone microtubules are the primary target. My observations of microtubules indicate that the requirement for dynamics may not be for supplying polymer for growth, but for allowing polymerization of microtubules into lamella, which may then guide invasion and bundling of microtubules into the lamella. This may be testable using the local inactivation of colcemid by ultraviolet light. Neurons could be treated with low doses of colcemid or pulses of colcemid that would inhibit microtubule polymerization [4,5]. Local inactivation of the colcemid with a spot of ultraviolet light would allow polymerization in the area, and if such dynamic microtubules nucleated bundling of other microtubules, one could see sliding of pre-existing microtubules along the newly polymerized microtubules. Alternatively, it may be possible to locally ablate microtubules using techniques such as CALI [6]

**Translocation of microtubules through the cytoplasm**

Static images of growth cone microtubules as well as models that ascribe a role for microtubules as structural supports for the axon may give the impression that microtubules are stiff unmoving rods in the cytoplasm. I found, however, that microtubules undergo tremendous movements and bending in the growth cone cytoplasm. Considering that microtubules are relatively stiff, they must be subject to large forces in the growth cone [7]. The movement of microtubules is a major means of supplying polymer to growth cones, of forming bundles during axon formation and of localizing

microtubules within the growth cone during turning . My observations indicate that microtubule bending comes both from the translocation of microtubules down the axon generating compressive forces on the microtubule ends in the growth cone and also from the interaction of microtubules with other cytoskeletal components leading to their lateral movement within the growth cone (Chapters 2 and 3). Molecular motors attached to cortical actin may provide the force to move microtubules laterally with the growth cone. I attempted to characterize microtubule movement through the cytoplasm by injecting both Xenopus eggs and PC12 cells with microtubule seeds. These seeds (GMPCPP seeds(), EGS seeds() and tau-coated GMPCPP seeds), which are stable for days in vitro, are quickly destabilized in vivo (<1 minute) making this experiment impossible. this indicates that a powerful microtubule depolymerizing or severing activity exists in interphase cells. Fortunately, I found that Xenopus fibroblast-like cells treated with vinblastine generate small fragments of microtubules that translocate rapidly (0.5 μm/sec) through the lamella indicating that microtubules can interact with elements in lamella that may capture microtubules and pull on them (data not shown). Filamentous actin is the best candidate for the lamellipodia structures that may capture microtubules since the edges of moving cells generate high levels of actin. It would therefore be of great interest to identify motors that move microtubules along actin filaments. It is likely that such an activity exists in other cells, such as in the cleavage furrow of dividing cells to position the microtubule spindle properly, and in the Xenopus egg to generate cortical rotation. Therefore, frog egg cytoplasm might be a good source for identifying and characterizing such an activity.

**Microtubule bundling**

Both during axon elongation and growth cone turning microtubule bundling is an early and probably important step in the formation of new axon. Our calculations of microtubule rescue frequencies suggest that microtubule bundling may be an important means of stabilizing microtubules in the axon (Chapter 2). During axon formation microtubule bundling preceded the collapse of membrane around it suggesting that microtubule bundling may organize actin redistribution. When microtubules are induced to bundle in non-neuronal cells by the expression of MAPs such as tau, in some cases, processes form where the cell cortex is closely associated with the bundle, further supporting the notion that bundles may organize the cortical membrane [8,9].

It may be possible to test the role of microtubule bundling in axonogenesis by constructing inducible bundling factors. Such factors could be constructed by attaching an inducible dimerization domain on a microtubule binding domain. Thus, the protein would normal be bound to the sides of microtubules, but when dimerization was induced, proteins on different microtubules might dimerize and cause bundling. The repeat domain of tau could be used for microtubule binding, and the FK506-based dimerization system could be used to induce binding. It may be necessary to provide a long linker arm to encourage inter-microtubule cross linking [10].

The microtubule bundling was not a constant, continuous process, but rather, occurred in spurts. As described in Chapter 3 and 4, some bundling may occur by the coalescence and sliding of microtubules along the newly polymerized microtubules in the growth cone. These observations indicate that a regulated bundling protein may normally be inactive in growth cones and occasionally turned on during formation of new axon and maintained in

an active state in the axon. Because I observed what appeared to be microtubule sliding during bundle formation, the bundling protein may be may be a motor that slides parallel microtubules along each other. Kinesin-like proteins which slide microtubules in an anti-parallel fashion have previously been described [11]. Most likely, there will be multiple bundling proteins which all contribute to the generation of the axonal microtubule bundle.

**Conclusion**

In summary, by observing microtubules in growth cones, I have described many of the important microtubule behaviors required for axonal elongation and for growth cone response to guidance cues. This work should allow for the characterization of biochemical activities in neurons that are important for these processes. The predominance of microtubule translocation suggests that microtubule motor proteins play an important role the organization of neuronal microtubules. The recent identification of a very large family of kinesin-like proteins as well as the recent cloning of cytoplasmic dynein has generated many useful reagents through which this hypothesis can be investigated [12]; Walker, 1993 #921; Mikami, 1993 #927; Koonce, 1992 #930. Identification of microtubule bundling factors may also further our understanding of axonal growth. Most important with the bundling proteins will be to understand their regulation by signal transduction molecules such as kinases, as this regulation may be important in determining the spatial segregation of dynamic microtubules to the growth cone and bundled, stable microtubules in axons. By studying motor proteins and bundling factors in vitro, it may then be possible to go back to observing cells and more precisely test the role of the identified proteins in neuronal growth and guidance.

1.Schulze, E. and Kirschner, M. 1988. New features of microtubule behaviour observed in vivo. 334: 356-359.

2.Drechsel, D. N., Hyman, A. A., Cobb, M. H. and Kirschner, M. W. 1992. Modulation of the dynamic instability of tubulin assembly by the microtubule-associated protein tau. . Mol Biol Cell 3: 1141-54.

3.Gurland, G. and Gundersen, G. G. 1993. Protein phosphatase inhibitors induce the selective breakdown of stable microtubules in fibroblasts and epithelial cells. PNAS 90: 8827-8831.

4.Sluder, G. and Rieder, C. L. 1985. Experimental separation of pronuclei in fertilized sea urchin eggs: chromosomes do not organize a spindle in the absence of centrosomes. . J Cell Biol 100: 897-903.

5.Sluder, G., Miller, F. J. and Spanjian, K. 1986. The role of spindle microtubules in the timing of the cell cycle in echinoderm eggs. . J Exp Zool 238: 325-36.

6.Linden, K. G., Liao, J. C. and Jay, D. G. 1992. Spatial specificity of chromophore assisted laser inactivation of protein function. Biophysical Journal 61: 956-962.

7.Gittes, F., Mickey, B., Nettleton, J. and Howard, J. 1993. Flexural rigidity of microtubules and actin filaments measured from thermal fluctuations in shape. . J Cell Biol 120: 923-34.

8.Baas, P. W., Pienkowski, T. P. and Kosik, K. S. 1991. Processes induced by tau expression in Sf9 cells have an axon-like microtubule organization. . J Cell Biol 115: 1333-44.

9.LeClerc, N., Kosik, K. S., Cowan, N., Pienkowski, T. P. and Baas, P. W. 1993. Process formation in Sf9 cells induced by the expression of a microtubule-associated protein 2C-like construct. . Proc Natl Acad Sci U S A 90: 6223-7.

10.Spencer, D. M., Wandless, T. J., Schreiber, S. L. and Crabtree, G. R. 1993. Controlling signal transduction with synthetic ligands. Science 262: 1019-1024.

11.Nislow, C., Lombillo, V. A., Kuriyama, R. and McIntosh, J. R. 1992. A plus-end-directed motor enzyme that moves antiparallel microtubules in vitro localizes to the interzone of mitotic spindles.

12.Walker, R. A., Salmon, E. D. and Endow, S. A. 1990. The Drosophila claret segregation protein is a minus-end directed motor molecule. Nature 347: 780-782.